#### **CHAPTER 1**

#### INTRODUCTION

### 1.0 Background

The reintroduction of Zimbabwe into the international trading community after Independence in 1980 was accompanied by the phenomenal expansion of the horticultural industry in the mid-1980s (Davies, 2000). During this period, it became one of the country's fastest growing export sectors. Of major concern in the study is the floricultural sector which by 2000, was the second largest exporter of cut-flowers in Africa, after Kenya and the third largest supplier of roses to the European Union with a production of 24 million stems in 1995 (Davies, 2000; Sguazzin, 2001). The floricultural industry has contributed significantly to the country's foreign currency earnings and with a projected annual growth of 20%, the sector will continue to make significant contributions to Zimbabwe's Gross Domestic Product (Bafana, 2003).

Roses constitute about 70% of the total cut flowers exported from Zimbabwe. The rest comes from other cut-flowers such as asters, chrysanthemums and proteas. The production of cut-flowers in Zimbabwe tends to be higher during September to May to coincide with the northern hemisphere winter. This ensures that the floricultural farmers get higher returns from their exports because of the shortage of fresh flowers in the northern hemisphere as a result of the adverse winter conditions. The bulk of these flowers are exported to the Netherlands as well as the United Kingdom, Germany, Italy, Sweden, United States, Scandinavia and Australia (Davies, 2000).

# 1.1 Requirements of Floricultural Production

Floricultural production, with particular reference to roses, is very capital intensive with the estimated annual operating costs for a hectare having been approximately US \$823 in 2001 (Sguazzin, 2001). These expenses are incurred because of the requirements of a well-developed infrastructure, the payment of royalties and an efficient marketing system. The short shelf life of cut-flowers demands a well-developed infrastructure for quick and reliable transportation to the export markets. Most of the production of roses occurs in areas near Harare such as Banket/Trelawney, Concession/Glendale, Bindura, Goromonzi and Ruwa because of the established road network and therefore easy access to Harare International Airport (EFGAZ, 1998).

The rose varieties grown in the country are from international breeders such as Interplant, Schreurs, Kordes and Meilland. A royalty payment of 80 US cents a plant is required prior to their use. With an average plant population of 70000 per hectare a substantial amount of capital is therefore required (EFGAZ, 1998; Omniflora, 2005; Sguazzin, 2001).

Floricultural production is the one of the most technologically advanced industries in the country using some of the latest innovations in the world in the form of greenhouses, pack sheds and storage facilities. Greenhouse structures are mainly used for rose production because weather is the major inhibiting factor towards open production. This refers to both seasons; summer (September to April) and winter (May to August). The summer season experiences extremely high temperatures and humidity levels, conditions favourable for pest and disease outbreaks. Fungal diseases particularly the mildews; powdery (causal agent *Sphaerotheca pannosa* var *rosae*) and downy (causal agent *Peronospora sparsa*) are the major diseases in roses. The high temperatures also increase populations of spider mite (*Tetranychus urticae*) and whitefly (*Trialeurodes vaporariorum*). The cool, dry winter season is associated with high evaporative losses and relatively cold nights, conditions that again negatively affect crop productivity (Mhizha, 2003). The crop will therefore experience water stress whilst the low night temperatures compromise crop quality.

Greenhouse production is generally associated with both high production output and quality because of the greenhouse structures providing conditions favourable for crop growth and development (Critten and Bailey, 2002). The greenhouse microclimate is mainly a result of the greenhouse cover, which controls the exchanges of heat and mass between the outside air and the greenhouse environment. This promotes both temperature and humidity levels that are always conducive for crop production throughout the year. The greenhouse structures used in Zimbabwe are mainly of two types, greenhouses and the walk-in tunnels (Mashonjowa, 2001). The greenhouses are mostly of the multi span Dutch Venlo type with plastic covering as the latter tends to be both less fragile and expensive compared to glass. The climate regulation in these greenhouse structures has become automated where a computer monitors the temperature and humidity levels such that it triggers the climate control mechanisms (ventilation and misting) on/off once the pre-determined levels have been reached. This requires continuous measurements of the greenhouse air temperature and relative humidity using wet and dry bulb thermometers, which are strategically placed to give representative measurements as gradients of the variables may occur within the greenhouse (Mhizha, 2003). Generally the sensors are placed near the centre of the greenhouse, at the height of the crop canopy and adjusted with crop growth (Nelson, 1991).

The other greenhouse structures, walk-in tunnels are generally circular arcs (steel tubes) over which are stretched a polyethylene sheet. The structures often have manual climate control, which does not achieve optimal climate but only prevents climate extremities.

Since the early 1990s, there has been an increase in the use of locally produced wooden-framed greenhouse structures by floricultural farmers. Escalating costs of the imported state of the art controlled plant production environment systems coupled with inaccessibility to credit facilities has necessitated the use of these cheap greenhouse structures. Because of an inefficient climate regulatory system, locally produced wooden-framed greenhouses have reduced production capacity, product quality and higher crop disease outbreaks. According to preliminary results from an experimental station in Blackfordby, the wooden-framed greenhouses were found to have only a production capacity of 122 rose stems per square metre compared to the higher output of 224 stems per square metre under the imported steel greenhouses (Davies, 2000). Production costs are thus further increased because of the increased pesticide use associated with the wooden-framed greenhouse structures (Davies, 2000). In most cases disease control measures are implemented late resulting in substantial crop loss.

#### 1.2 Constraint of Greenhouse Production

The greenhouse microclimate does not only promote crop productivity but also has an influence on pest and disease development in the greenhouse. According to Larson (1980) and Mashonjowa (2001) the ventilation mechanism may be a contributory factor to disease occurrence in the greenhouse in two ways;

- the closure of ventilators for heat conservation that is done at higher air temperatures is associated with a high water vapour content such that condensation will occur on the leaf surfaces as the air temperature is cooled to dew point. These conditions are favourable for disease development and spread.
- the air movement brought about by the opening of the vents assists in the dispersal of fungal spores, thus increasing disease occurrence within the greenhouse.

Greenhouse production has therefore led to excessive pesticide use. High chemical usage in the production cycle is of major concern because of the effects of these plant protection products to the environment and health of the workers. Floricultural producers are nowadays being called on to reduce the amount of chemicals used in the production cycle for continued access to export markets. This is being done through registration with floricultural labelling programmes to indicate their conformation to environmental and social standards during the production process. Some of these floricultural labelling programmes include the private sector initiated Dutch-based Floricultural Environmental Project (MPS), that of Migros and the German - based Flower Label Programme (Davies, 2000).

The problems highlighted above emphasize the need for an alternative method of greenhouse microclimate regulation if optimal climate levels for high crop productivity and effective pest management are to be achieved. This is of particular importance since disease control forms a major component of the costs incurred in greenhouse production. Previous research projects on greenhouses have focused on the effect of the greenhouse covering on the microclimate. The current research project attempts to provide a cost effective and efficient method of climate regulation. It is proposed that optimal control of the greenhouse microclimate be predicted from simulations using a Greenhouse Climate Model (GCM) based on outside weather variables. This concept has been extensively researched on in European greenhouses with satisfactory results.

In the modelling of the greenhouse microclimate variables, the greenhouse is regarded as a one-dimensional system, which is subdivided into different layers (cover, air, soil and vegetation). The unknown quantities of the different greenhouse layers are then determined from their respective energy and mass balances. The latter are in the form of differential equations, which are solved iteratively to obtain in most cases the temperatures of the different greenhouse layers. The iteration approach is a "trial and error" method based on guesswork, which is refined until its convergence within a defined error tolerance (Gates and Papain, 1971; Zhang *et al.*, 1997; Wang and Boulard, 2000; Pieters, 2002).

Greenhouse Climate Models can use weather forecasts in the simulations making it suitable for farmers who lack the expensive and sophisticated on-site weather monitoring sensors, which dominate most established floricultural units. The achievement of optimal climate control by the GCMs is expected to reduce incidences of disease outbreaks and ultimately pesticide use. This would ultimately result in an improvement in product yield and quality because of the timely preventative measures based on disease forecasts from the microclimate predictions (Zhang *et al.*, 1997). The preventative measures may include misting and ventilation, which are recommended Integrated Pest Management (IPM) strategies. The use of non-chemical methods will thereby limit pesticide use in the greenhouse. The effectiveness of the ventilation mechanism is expected to also improve through increased accuracy in its operations because of the thorough understanding of the energy and mass balances (Critten and Bailey, 2002). This is expected to reduce its contribution to the dispersal of fungal spores within the greenhouse because of prolonged periods between the opening of the ventilators as well as a reduction in the period in which they are opened.

In the current research the Gembloux Dynamic Greenhouse Climate Model (GDGCM) was selected for the prediction of the microclimate in greenhouses for rose production in Zimbabwe. The selection was based on the adaptability of GDGCM to different greenhouse crops and climatic regions as well as its simplicity. These characteristics of the model arise from its simulation programme (TRNSYS), where the heat and mass balances for the different greenhouse are in units, such that changes to

specific units can be made without knowledge of the whole programme (Pieters, 2002). The GDGCM according to Pieters (2002) incorporates many properties, which were previously not, in a single model including:

- being a dynamic model such that variations in state parameters with time are obtained.
- sub-division of the soil into four sub-layers to increase accuracy in the simulation of the soil temperatures.
- comprising eight non-linear heat balance equations (for the cover, air, vegetation, soil surface and four soil layers) and one mass balance equation for the temperature of the respective greenhouse layers and the relative humidity of the air.
- the changes to the heat capacity and radiative properties of the greenhouse cover in the presence of condensation

## 1.3 Aims and Objectives

The overall aim of this project was to adapt and validate the Gembloux Dynamic Greenhouse Climate Model for the prediction and control of the microclimate of an operational greenhouse for roses in Zimbabwe.

Specific objectives were:

- a) To assess the homogeneity of the greenhouse air for the determination of the correct placement of the sensors within the greenhouse
- b) To adapt the GDGCM to relate the greenhouse microclimate to external climate conditions in Zimbabwe
- c) To monitor the microclimate inside and outside a typical Zimbabwean greenhouse for rose production to provide data for calibrating and validating the model in (b) above

### 1.4 Project Layout

The project contains seven chapters. Chapter 1 gives a background to the study as well as outlining the aims and objectives. A detailed literature review on greenhouse microclimate modelling is found in Chapter 2. The description of the Gembloux Dynamic Greenhouse Climate Model used in the study is in Chapter 3. The materials and methodology used in data collection for the calibration and validation of the GDGCM are contained within Chapter 4. The results and their analysis form Chapters 5 and 6 respectively. Finally the conclusion and recommendations including the references are found in Chapter 7.

#### **CHAPTER 2**

#### LITERATURE REVIEW

#### 2.0 Greenhouse Production

"Greenhouse cultivation is the most recently developed specialisation of horticulture. It developed as a result of technological advancement and the rise in demand for luxury (out-of-season, exotic) products related to increasing prosperity of a growing group of citizens. Today, as a result of the large scale of production and product handling, greenhouse products are no longer as exclusive as they were and they provide a wide range of people with fresh food throughout the year, give enjoyment and add luster to daily life." (Bakker and Challa, 1995).

This form of production occurs under enclosures referred to as greenhouses or controlled plant production environment systems. These systems increase crop productivity through the provision of growing conditions that promote rapid leaf formation such that higher photosynthetic rates in the early stages of crop development are achieved. This may lead to early maturity of the greenhouse crop, thereby shortening the production cycle and ensuring that market dates are met. The high biomass production under greenhouses is due to an increase in assimilates diverted to the harvestable organs in determinate crops whilst with indeterminate crops such as roses, there is a continued assimilate supply to the non-harvestable plants to maintain a high production capacity thereby achieving an optimal balance between the growth of the harvestable organs and the rest of the plant (Marcelis and de Koning, 1995).

Another advantage of the greenhouse systems is the provision of a uniform greenhouse environment which promotes homogenous crop growth and development. This has increased the predictability of the production cycle of greenhouse crops enabling harvesting to coincide with periods of increased market demand with reference to such events as Valentine's Day, Mothers' Day, Fathers' Day or Christmas Day (Mastalerz, 1977; Fernandez and Bailey, 1994; Challa, 2002). Floricultural producers benefit from such events because of the maximization of their returns especially for an enterprise that is capital intensive.

#### 2.1 Greenhouse microclimate

The conditions within the greenhouse that promote crop productivity are referred to as the greenhouse microclimate. These can be defined as those climate variables to which the vegetation in the greenhouse will be exposed and include temperature, radiation, carbon dioxide, humidity and wind (Bot, 1983). This is illustrated in Figure 2.1. The exchanges of the energy and mass between the greenhouse structure and the outside air influence its microclimate. These exchanges can be described by the greenhouse energy and mass budgets. An energy budget is a balance between the energy flows into and out of the greenhouse volume whilst the mass budget involves the in- and outflows of mass (water vapour and carbon dioxide). These budgets are influenced by the greenhouse structure and design, the external environment, crop status and management decisions (Popovski, 1996).

#### 2.1.1 Effects of the Greenhouse Cover on the Greenhouse Microclimate

The greenhouse cover plays an important role in influencing the climatic conditions within the greenhouse volume. The greenhouse cover acts as a barrier between the greenhouse environment and the outside environment. It therefore regulates the exchanges of air and radiation between the outside environment and that of the greenhouse because of the reduced turbulence and its optical properties. The greenhouse structure tends to have a thick boundary layer because of its low air velocity (as a result of the barrier to wind movement by the cover). Hence the boundary layer resistance will be high thereby reducing the sensible and latent heat fluxes between the greenhouse volume and the outside. The resultant effect is a gradual build up in the greenhouse temperature and moisture content. Secondly, the cover is opaque to longwave (thermal) radiation whilst transmitting most of the shortwave (direct and diffuse solar) radiation such that the former is trapped within the greenhouse and as with the reduced turbulence, the air is subsequently warmed up resulting in a higher temperature than the outside air (Bot, 1983). According to Lee (1973) the resultant "greenhouse effect" is primarily due to the suppression of convection as in the first case more than the trapping of infrared radiation. Rosenberg *et al* .(1983), who found that only 22 % of the trapped long wave radiation contributed to a temperature increase whilst the rest was intensely reradiated by the glasshouse surface, confirmed this.

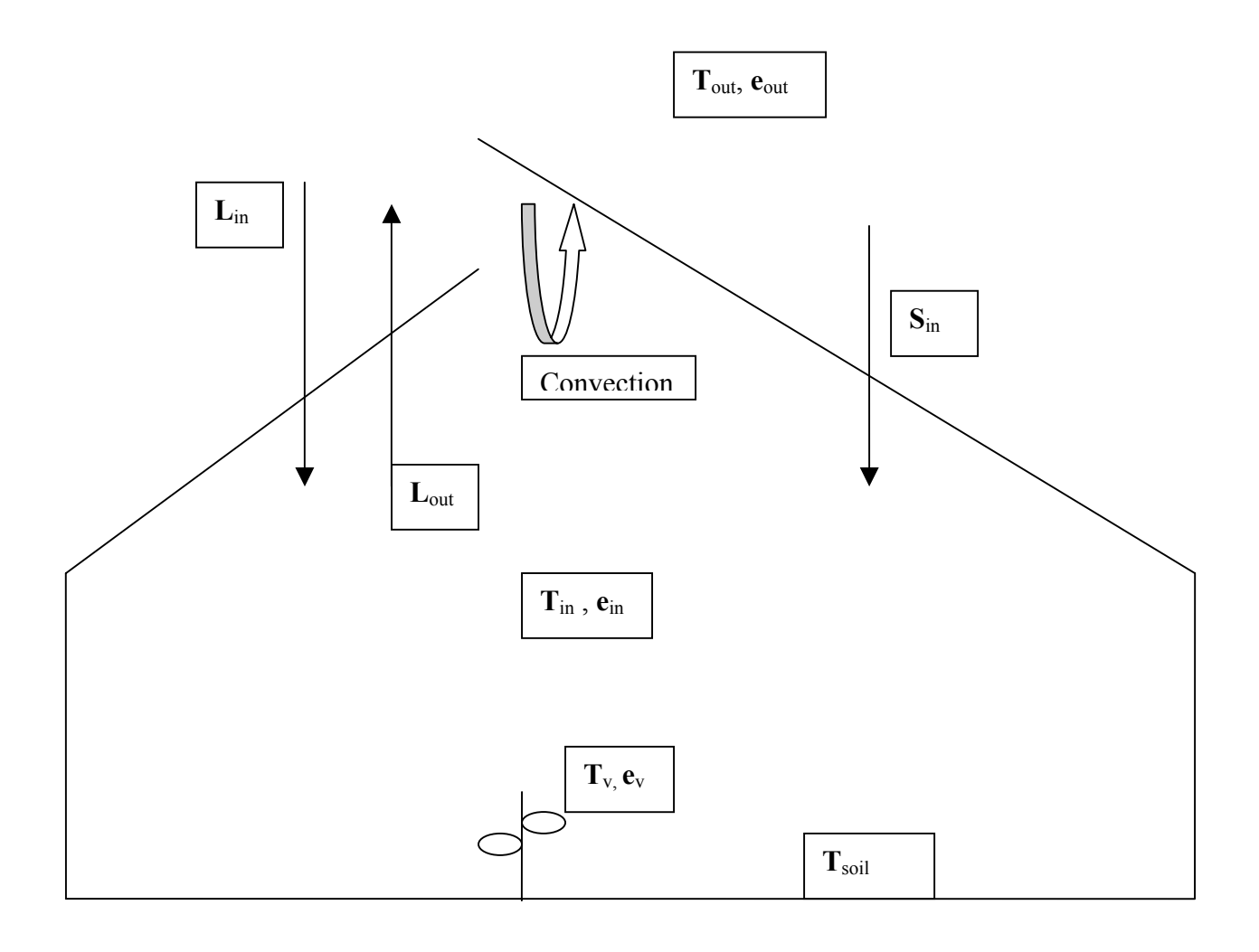


Fig 2.1: Typical microclimate of a ventilated greenhouse:  $L_{in}$  is the downward long wave radiation,  $L_{out}$  is the upward long wave radiation,  $T_{in}$  and  $T_{out}$  represent the inside and outside air temperature respectively,  $S_{in}$  is the incoming solar radiation,  $T_v$  is the vegetation temperature,  $T_{soil}$  is the soil temperature and  $e_{in}$  and  $e_{out}$  are the inside and outside vapour pressure of the air respectively and  $e_v$  is the vegetation vapour pressure.

# 2.2 Effect of Radiation and Temperature on Greenhouse Plant Production

Plant growth is influenced by the interaction of environmental factors, which include the weather variables, soil (moisture and fertility levels) and pest and disease occurrences. These factors are manipulated through good crop husbandry practices to achieve optimal yields. In this section, focus will be mainly on two factors, light and temperature, which are dependent on radiation, an input to the energy budget. It should be noted that under greenhouse production, the crop is well watered and fertilized such that light and temperature tend to be the limiting factors depending on the climatic regions.

The dominant environmental factor in crop production is light because of its influence on the photosynthetic process. Photosynthesis is the process, which provides energy and organic material requirements for plant growth. Roses have high photosynthetically active radiation (PAR) intensity requirements with a maximum of 1200 µmol m<sup>-2</sup> s<sup>-1</sup> (Larson, 1980). According to Mattson and Widner (1971), PAR has been reported to contribute 20 to 50 % to the total yield of a rose crop. However the photoperiod has no effect on the flower initiation of the roses since they are day-neutral plants.

Under adequate sunlight conditions such as is experienced in Zimbabwe, temperature is the most influential environmental factor affecting plant growth and development. Most physiological processes are dependent on temperature because of the requirement of activation energy for their reactions. Hence each physiological process has a temperature range in which it occurs and an optimum temperature where the maximum rate for the reaction is obtained. Any further increase above the optimum temperature will result in a decline in the rates due to other factors becoming limiting and in particular the denaturation of the enzymes, which catalyze the reactions (Mastalerz, 1977; Jones, 1992, Gijzen, 1995).

The growth and development of the rose plants is regulated by the temperature differential between day and night. And it has been found that a daily mean average of 18.6 °C with a combination of 22 °C (day) and 16-18 °C (night) on cloudy days and 24-28 °C (day) and 16-18 °C (night) on sunny days produces very high yield and quality (Madakadze, 2000). Night temperatures tend to have a dominant effect on the stem length and harvesting intervals of roses such that the regulation of the greenhouse temperature for longer periods (14 to 16 hours) at the nighttime level may assist in increasing crop quality and yield (Mastalerz, 1977; FAO, 1990). This is because the lower night temperatures promote increased stem length whilst shortening the harvesting intervals.

However it this microclimatic variable (air temperature), which is the main constraint in greenhouse rose production in Zimbabwe during both the winter and summer periods. During the winter season, night temperatures as low as 10 °C may be recorded whilst the summer season, with particular reference to the months of September to December, experiences high temperatures because of the high radiation load. According to Mashonjowa (2001) daytime temperature can reach up to 45 °C combined with low humidity levels of 30 %. A combination of the high temperatures and low humidity will assist in the dispersal of powdery mildew spores thereby increasing its occurrence within the greenhouse.

Low nighttime temperatures (<15 °C) affect crop quality because of the increased incidences of bullheads and blind shoots. Bullheads are malformed flowers with an increased number of petals and petaloids, which tend to be broader and shortened whilst blind shoots are aborted buds (vonk Noordegraff and Welles, 1995; Madakadze, 2000).

The domination of the respiration process at higher temperatures negatively affects crop productivity because of the reduced accumulation of dry matter. At such temperatures the photosynthetic process is usually inhibited. Another factor that lowers crop productivity is the stress experienced by the plants because of the increase in tissue temperature and the resultant increase in the transpiration rates to counter these temperatures. Reduced product quality also occurs as a result of uneven ripening, sunscald or necrosis and increase in the number of small-sized flowers, which have few petals. Generally the flowers exposed to high temperatures have a short shelf life because of soft growth, where the stem is not firm (Larson, 1980; vonk Noordegraff and Welles, 1995; Madakadze, 2000).

### 2.2.1 Control of temperature within the greenhouse

In greenhouse production, the occurrence of temperature extremes can be prevented in one of three ways: shading, misting or ventilation. Shading involves the application of material such as shade cloths, screens or paints on the greenhouse roofs or walls as a means of reducing the radiation load into the greenhouse and the subsequent increase in the air temperatures. In Zimbabwe, greenhouse covers are usually whitened once prior to the summer season (Mhizha, 2003). In the case of the side screens, their opening increases air circulation within the greenhouse thereby reducing the air temperatures because of the continuous mixing of the air. The use of shade cloths has been reported to successfully reduce light intensity by 50% (Tibbits and Langhans, 1993). This was found to cause reductions both in the PAR transmission and calculated daily crop photosynthesis of 9% and 3.5% respectively when all radiation above 700 W m<sup>-2</sup> was cut off according to Challa *et al.*, 1995. However, the reduction in the photosynthetic process was mainly attributed to other factors such as the subsequent increase in the humidity level due to the shading, which affected the overall crop performance and dominated the effects on photosynthesis (Challa *et al.*, 1995). The latter was supported by Hall and Rao, 1999 who found that the reduction in PAR transmission had no significant effect on the photosynthetic process.

Misting is the other method of lowering air temperatures within the greenhouse. Misting involves the cooling of the greenhouse air through the evaporation of water. Here the fine droplets produced during misting are evaporated using the heat (about 2260 kJ kg<sup>-1</sup> water) withdrawn from the surrounding greenhouse air, which in turn cools down resulting in a lowering of the air temperatures (Breuer and Knies, 1995). The effectiveness of misting is dependent on adequate air circulation otherwise either high temperature gradients may be created within the greenhouse or the moist conditions will lead to a build up of fungal diseases (Mashonjowa, 2001).

The third temperature regulation mechanism is ventilation, which is the most utilized in Zimbabwean greenhouses. Ventilation is the renewal of the greenhouse air, which can take place naturally or by forced means. With forced ventilation, outside air can be sucked into the greenhouse or the inside air out using fans which can be thermostatically controlled. This type of ventilation is not extensively used in Zimbabwean greenhouses because of the high cost of equipment and electricity needed to drive the fans (Mashonjowa, 2001).

The second form of ventilation, which is more relevant to Zimbabwean greenhouses, is natural ventilation. Natural ventilation involves the movement of air between the greenhouse structure and the outside environment through ventilators on its roof or sides. The side openings are mounted on rollers and are manually operated whilst the roof vents are either fixed or controllable openings (Mashonjowa, 2001).

### 2.3 Greenhouse Physical Processes

The state of important greenhouse variables such as the air temperature and its relative humidity as well as the vegetation temperature are determined by energy and mass balances of the respective layers within the greenhouse structure (Bot and van de Braak, 1995). Energy and mass (water vapour and carbon dioxide) exchanges among the greenhouse layers (cover, inside air, vegetation and soil) and with the outside air and the sky occur through a combination of different transfer processes that include radiation, convection, conduction and phase change due to respective temperature and mass gradients.

The energy and mass exchanges for the different greenhouse layers are as follows;

- 1. The greenhouse cover absorbs, reflects and transmits solar radiation from the sky and sun and it in turn exchanges longwave (thermal/infrared) radiation with the sky and other greenhouse layers (air, soil and vegetation). Convective exchanges occur between it and the air both inside and outside of the greenhouse. The cover also exchanges energy (latent heat) with the inside air through condensation.
- 2. The greenhouse air absorbs solar radiation from the sky and sun and it in turn exchanges energy with the cover, crop, soil and outside air by convection. The exchange of energy and mass between this greenhouse layer and the outside air occurs through ventilation.
- 3. The crop absorbs solar radiation from the sky and sun and in turn exchanges longwave radiation with the cover and soil. Convective exchange occurs with the air.

4. The soil absorbs solar radiation from the sky and sun and in turn exchanges longwave radiation with the cover and soil. Convective exchange occurs with the air whilst conductive heat exchange will take place within the sub layers.

#### 2.3.1 Radiation

Radiation involves heat transfer by electromagnetic waves and forms the main energy input into the greenhouse structure. It comprises of shortwave (solar) radiation (0.3 to 3  $\mu$ m) and longwave (thermal) radiation (3 to 100  $\mu$ m). The shortwave radiation may either be direct solar radiation, which comes from the unobscured sun's disc or diffuse solar radiation, which is scattered by the atmosphere (Bot, 1983; Monteith and Unsworth, 1990; Bot and van de Braak, 1995).

# a) Shortwave (Solar) Radiation

Of importance is the amount of total solar radiation within the greenhouse structure because it determines the fraction available for crop growth and development as well as influencing the energy and mass balances of the greenhouse air, crop and soil. Most of the total solar radiation that is transmitted into the greenhouse contributes to the transpiration process (70%) with only about 10 % being utilized for the photosynthetic process (Wang and Boulard, 2000; Mashonjowa, 2001).

The fraction of total solar radiation transmitted into the greenhouse structure is determined by the greenhouse cover and the optical properties of the latter. The transmission of total solar radiation through the greenhouse structure can be expressed as a transmission coefficient, which is a ratio of the measured radiation intensity beneath the covering material (I) to that measured simultaneously outside (I<sub>o</sub>) in the same waveband, such as total solar radiation or infrared radiation (Mhizha, 2003). The formula for the transmission coefficient is

$$\tau = \frac{I}{I_0} \tag{2.3.1}$$

The transmission of the greenhouse is dependent on factors such as the optical properties of its cover and construction (transmissivity, reflectivity, and absorptivity), its geometry and angle of incidence of the incoming radiation. The angle of incidence tends to strongly affect the transmission of direct solar radiation than diffuse solar radiation (Monteith and Unsworth, 1990; Pieters, 2002). The transmittance of the diffuse solar radiation into the greenhouse is influenced more by the distribution of the radiation intensity over the hemisphere. The angle of incidence for direct solar radiation will vary with the time of day, day of year, latitude in which the greenhouse is located and the orientation and geometry of the

surfaces (Bot and van de Braak, 1995). The transmission of the direct solar radiation into the greenhouse structure will therefore be reduced at high angles of incidence because of the increased reflection and absorption. This is most evident during the winter season and periods such as sunrise and sunset because of the low solar elevations (Pollet, 2002). In terms of the greenhouse orientation, it was observed that an E-W orientation had a higher transmittance compared to an N-S orientation particularly during winter in the northern hemisphere since the latter had a greater obstruction from the greenhouse construction parts (Kozai and Kimura, 1977; Kozai, Goudriaan and Kimura, 1978).

## b) Longwave (Thermal) Radiation

Heat transfer by longwave radiation occurs for all surfaces whose absolute temperature is above 0 K, which in this case includes all the greenhouse layers, the outside air and sky (Bot, 1983; Bot and van de Braak, 1995; Pieters, 2002). Longwave radiation exchange between the inside of the greenhouse and the sky is inhibited because the cover is opaque to the former. The amount of longwave radiation emitted by a body per unit time and per unit area is dependent on its absolute temperature, can be calculated using the Stefan-Boltzmann equation as follows:

$$\phi_{rad} = \varepsilon \sigma T^4 \tag{2.3.2}$$

where  $\phi_{rad}$  is the radiated energy flux density (W m<sup>-2</sup>),  $\varepsilon$  is the emissivity of the surface,  $\sigma$  is the Stefan-Boltzmann constant (5.67 x 10<sup>-8</sup> W m<sup>-2</sup> K<sup>-1</sup>) and T is absolute temperature (K)

Equation 2.3.3 is used to calculate the net radiative heat flux  $Q_{R(1\to 2)}$  exchanged between two surfaces, which are in thermal contact. These surfaces can be either any two of the greenhouse layers or the greenhouse cover and the sky.

$$Q_{R(1\to 2)} = \frac{\sigma.(T_1^4 - T_2^4)}{\frac{\rho_1}{\varepsilon_1.A_1} + \frac{1}{F_{21.}A_2} + \frac{\rho_2}{\varepsilon_2.A_2}}$$
(2.3.3)

where A and T are the surface area of the radiator and its surface temperature respectively,  $F_{21}$  is the view factor of surface 2 to surface 1 and where the subscripts 1 and 2 stand for the respective radiators,  $\rho$  is the reflectivity of the surface and  $\varepsilon$  the emissivity of the surface.

The view factor is a geometric quantity dependent on the shape and relative position of the two radiators. The view factor indicates what fraction of the total radiative energy emitted by surface 2 is intercepted by surface 1.

For the thermal radiative exchange between the greenhouse cover and the sky, an effective sky temperature is used in the equation because the radiation would have to be determined at various heights as a result of the variation in the atmospheric temperature and composition with height. The effective sky temperature ( $T_{sky}$ ) can thus be determined as a function of meteorological parameters such as air temperature, relative humidity and cloudiness (Wartena *et al.*, 1973; Bot, 1983). Although Wartena *et al.* (1973) found a correlation between these parameters, they concluded that the latter's use was restricted to the long term determination of an average sky temperature and regions with similar meteorological characteristics as the region in which the measurements had been taken.

For this study the effective sky temperature was calculated based on the equations by Swinbank (1963). The latter gave three equations that could be used for the determination of the effective sky temperature  $T_{sky}$  (for a horizontal surface) based on the cloud conditions (clear sky, partly cloudy and overcast sky conditions). The equation for the effective sky temperature under a clear sky was expressed as:

$$T_{skv} = 0.0552.T_e^{1.5} (2.3.4)$$

where  $T_{sky}$  is effective sky temperature (K) and  $T_e$  outside air temperature (K).

Under an overcast sky, the equation was expressed as

$$T_{sky} = T_e (2.3.5)$$

The radiative sky temperature for a partially clouded sky was expressed as weighted means of the values for the clear and overcast conditions. The weighing factor is the cloudiness  $p_{cl}$  of the sky. This

is expressed as:

$$T_{sky} = p_{cl} T_e + (1 - p_{cl}) \cdot 0.0552 T_e^{1.5}$$
(2.3.6)

# 2.3.2 Convection

Montieth and Unsworth (1990) define convection as transfer of heat and mass by moving air. According to Stanghellini (1987) convection is a more efficient energy transfer mechanism than conduction since it transfers heat over longer distances even in low air velocities. Convective heat transfer from a surface can be described by the following equation:

$$C = k \frac{(T_s - T)}{\delta} \tag{2.3.7}$$

k is the thermal conductivity of the fluid,  $T_s$  the surface temperature, T is fluid temperature and  $\delta$  is an equivalent laminar boundary layer of uniform thickness (Montieth and Unsworth, 1990).

A laminar boundary layer is that layer of air in contact with the surface where streamlines of airflow are almost parallel to the surface (Montieth and Unsworth, 1990). The effective boundary layer can be substituted by a characteristic dimension, which is measured in the direction of the flow. Equation (2.3.7) then becomes

$$C = \left(\frac{d}{\delta}\right) k \frac{(T_s - T)}{d} \tag{2.3.8}$$

The ratio of  $\frac{d}{\delta}$  is the Nusselt number Nu. Nu is a non-dimensional group enabling the comparison of rates of convective heat loss from similar bodies of different scale exposed to different wind speeds (Monteith and Unsworth, 1990).

There are two types of convective transfer, forced and free convection. Forced convection is transfer through a boundary layer of a surface exposed to an air stream, proceeding at a rate, which depends on the velocity of the flow (Monteith and Unsworth, 1990). The Reynolds number (Re)describes the forced convection. Re defines the boundary layer thickness for momentum and is expressed as the ratio of inertial to viscous forces. The flow is laminar when the viscous forces are larger than the inertial whilst vice versa will give a turbulent flow. Re is calculated by the following equation:

$$Re = \frac{ud}{v}$$
 (2.3.9)

where u is the fluid velocity, d characteristic dimension of a surface and v kinematic viscosity of the fluid

Another way of describing forced convection is by use of Nu, which in this case is dependent on the rate of heat transfer through a boundary layer from a surface, which may be either hotter or cooler than the air passing over it. Nu is thus expressed as a function of Re and the Prandtl number (Pr). Pr is a ratio of the thickness of the thermal boundary layer  $(t_H)$  to that for momentum  $(t_M)$ .

Pr is defined by 
$$\frac{v}{\kappa}$$
 (2.3.10)

where  $\kappa$  is the thermal diffusivity of the air

The equation for Nu under forced convection is:

$$Nu = C_1 \operatorname{Re}^n \operatorname{Pr}^m \tag{2.3.11}$$

where  $C_1$ , n and m are constants dependent on the geometry of the surface and the type of convection (Montieth and Unsworth, 1990; Pieters, 2002).

With free or natural convection, the airflow within the greenhouse occurs as a result of density differences brought about by a temperature differential (Stanghellini, 1983: Pieters, 2002). Free convection can be described by the Grashof number (Gr) or Nu as a function of Gr and Pr. Gr is a non-dimensional group and is dependent on the ratio of the product of the buoyancy and inertial forces to the square of the viscous forces (Pieters, 2002). It also expresses the boundary layer thickness for momentum. Forced convection is calculated from the following equation:

$$Gr = \frac{agd^{3}(T_{s} - T)}{v^{2}}$$
 (2.3.12)

where a is the coefficient of thermal expansion of the fluid g is the acceleration of gravity and  $T_s - T$  is the temperature difference between the object and the surrounding fluid (Monteith and Unsworth, 1990).

The other equation for free convection involving Nu is as follows:

$$Nu = C_2 (Gr \operatorname{Pr})^m \tag{2.3.13}$$

where  $C_2$  is a constant dependent on the geometry of the surface and the type of convection.

Pr is assumed to have a constant value of 0.71 in air and therefore equations 2.3.11 and 2.3.13 can be simplified to;

$$Nu = C_3 \operatorname{Re}^n$$
 and  $Nu = C_4 Gr^m$  (Monteith and Unsworth, 1990). (2.3.14)

In terms of convective mass transfer, forced and natural convection are described by a non-dimensional group, the Sherwood number Sh. Sh is defined as the ratio of the actual mass transfer F to the rate of transfer that would occur if the same concentration difference were established across a layer of still air of thickness d (Montieth and Unsworth, 1990). This is expressed in the equation

$$Sh = \frac{F}{D(\chi_s - \chi)/d}$$
 (2.3.15)

where F is the mass flux of the gas per unit surface area (g m<sup>-1</sup> s<sup>-1</sup>),  $\chi_s$  and  $\chi$  are the mean concentration at the surface and in the free atmosphere (g m<sup>-1</sup>) respectively and D the molecular diffusivity of the gas in the air (m<sup>2</sup> s<sup>-1</sup>). The equation for F is:

$$F = \frac{ShD(\chi_s - \chi)}{d} \tag{2.3.16}$$

Under forced convection, Sh is derived from Re and Schmidt (Sc) numbers. Sc is a ratio of the thickness of the mass boundary layer to that of the momentum boundary layer. The formula is expressed as:

$$Sh = C_1 \operatorname{Re}^n Sc^m \tag{2.3.17}$$

Mass transfer under free convection is expressed by the formula:

$$Sh = C_2 (Gr \operatorname{Pr})^m \tag{2.3.18}$$

In the calculation of Gr,  $T_s - T$  is replaced by that for virtual temperature at which the density of dry air is equal to that of moist air at actual temperature. This is expressed as:

$$T_{vo} - T_v = T_o \left( 1 + \frac{0.38e_o}{p} \right) - T \left( 1 + \frac{0.38e}{p} \right)$$
 (2.3.19)

where  $e_o$  and e are the vapour pressure at the surface and in the air respectively, p partial pressure (Monteith and Unsworth, 1990).

Convective transfer is dominated by an upward flux, which occurs under a warmer-than-air regime (T<sub>surface</sub> is greater than T<sub>air</sub>). The latter has an unstable lapse rate within the boundary layer which increases the heat transfer from the warmed surface into the air whilst a cooler-than-air regime because of a stable lapse rate has restricted transfer due to increased boundary resistance (Zhang and Lemeur, 1992). According to Kreith, 1965 the heat transfer for a cooler-than-air surface is only half as efficient as the warmer-than-air surface and the relationship can be described by the following equation:

$$Nu = 0.26(Gr \,\text{Pr})^{0.25} \tag{2.3.20}$$

Another feature of most greenhouse structures is that the convective regime can best be described as mixed because of the influence of fans and ventilators. The dominant convective type in the mixed regime is found by comparing Gr to  $Re^2$ . Free convection will dominate where Gr is much bigger than  $Re^2$  because the buoyancy forces will be much larger than the inertial forces and where Gr is much greater than  $Re^2$ , the buoyancy forces will be negligible and forced convection will be the

dominant convective type (Monteith and Unsworth, 1990). Under a mixed regime, the Nu values are compared for the two convective types with the larger of the values being used.

## a) Ventilation

The convective transfer of energy and mass between the greenhouse air and the outside air is mainly by ventilation, which has been introduced in §2.2.1. The driving force of the ventilation process is the pressure differences between the two environments, which are a result of either an external airflow (wind effect) or temperature-dependent density differences (thermal effects) (Bot and Braak, 1995, Boulard *et al.*, 1999). It has been found that under active ventilation (open greenhouse), the temperature differences are reduced such that the external airflow is the dominant effect whilst the reverse is observed with a low airflow (closed greenhouse). According to Boulard *et al.*, 1999, the airflow caused by the temperature differences is characterized by a convective loop, with high velocities along the walls and floor. The cool air entering through the roof openings thus moves down along the adjacent wall and is heated by the warm ground as it moves across and becomes less dense to rise up along the opposite wall.

Ventilation is normally described as an effective airflow from the inside of the greenhouse to the outside or vice versa because the pressure differences fluctuate as a result of the fluctuations in the external airflow (Bot and Braak, 1995). Effective ventilation can be described either by the ventilation rate or the ventilation flux. The ventilation rate is defined as the air replacement rate within the greenhouse volume  $(h^{-1})$  or the ventilation flux expressed in relation to the area of the greenhouse opening (Bot, 1983). The ventilation air flux can be used for the comparison of different greenhouses with similar types of openings (Bot, 1983; Pieters, 2002). The ventilation volumetric flux was found to be linearly dependent on two factors: the area of the ventilation opening for any opening angle  $(\alpha)$  and the outside wind speed (Boulard and Wang, 2000). The ventilation volumetric flux  $(\phi_v)$  in m<sup>-3</sup> s<sup>-1</sup> can be calculated by the equation of Boullard and Baille, 1995:

$$\phi_V = \frac{A_o}{2} C_d C^{0.5} u \tag{2.3.21}$$

where C is a wind related efficiency coefficient (with a value of 0.09),  $C_d$  an average vent discharge coefficient (with a value of 0.644) and  $A_o$  area of the ventilation opening  $(m^2)$ .

## 2.3.3. Phase change

Phase change is another energy and mass transfer mode that takes place between either the greenhouse cover and the air or the crop and air. Phase change involves the conversion of liquid water into water

vapour (evapotranspiration) or vice versa during condensation. (Pieters, 2002). The transfer of water vapour from an evaporating surface can be described by the following equation:

$$\phi_m = k_m (c_{m,s} - c_{m,a}) \tag{2.3.22}$$

where  $\phi_m$  is the evaporative water vapour flux density (kg m<sup>-2</sup> s<sup>-1</sup>),  $c_{m,s}$  is concentration of the mass at the evaporating surface (kg m<sup>-3</sup>) and  $c_{m,i}$  concentration of the mass in the greenhouse air (kg m<sup>-3</sup>).

## a) Evapotranspiration

In this study the phase change through evapotranspiration will be dealt with in more detail because the process has a strong influence on both the energy and mass balances of the greenhouse. A lot of research on greenhouse microclimate modelling has been based on the evapotranspiration process. Evapotranspiration is the transfer of water vapour from the crop to the atmosphere. It thus involves the transfer of latent heat through the conversion of water into water vapour. Evapotranspiration occurs due to a difference in vapour pressure between the crop canopy and the surrounding air referred to as a vapour pressure deficit, VPD (Bot and Braak, 1995: Pieters, 2002). The rate of the evapotranspiration process is governed by the interaction of climatic variables such as radiation, wind speed, leaf and air temperatures and carbon dioxide concentration. These climatic factors were found to strongly influence the evapotranspiration rate of a mature cucumber crop than its leaf area because the effect of the latter were reduced by shading as well as the small leaf-air temperature differences (Yang *et al.*, 1990).

The other important factors affecting the evapotranspiration rate are the stomatal and boundary resistances. The boundary (aerodynamic) resistance affects the transfer of heat and water vapour from the evaporating canopy surface into the surrounding air whilst stomatal resistance affects water vapour movement from the evaporating cell walls to the leaf surface (Monteith and Unsworth, 1990; Gijzen, 1992; Jones, 1992; Allen *et al.*, 1998). Under greenhouse structures, there is an increase in the aerodynamic resistance because of the reduced airflow. This results in strong decoupling of the leaf surface and the greenhouse bulk air because of the restriction in the transfers of latent heat and sensible heat. The leaf surface therefore becomes more humid and warmer in comparison to the bulk air.

The stomatal resistance for greenhouse crops also follows a similar trend to the boundary resistance being high in comparison to field crops, varying from 20 to 5000 s m<sup>-1</sup> depending on crop species (Gijzen, 1992). Stomatal resistance is strongly influenced by irradiance, with the other factors not

having as strong a correlation. The stomatal resistance reaches its minimal at irradiances of 200 W m<sup>-2</sup> or 400 μmol m<sup>-2</sup> s<sup>-1</sup> (Monteith and Unsworth, 1990). At this light intensity level maximum stomatal aperture will be achieved. Under high light intensity and at ambient CO<sub>2</sub> concentration (350 μmol mol<sup>-1</sup>), cucumber has been found to have a stomatal resistance of 50 s m<sup>-1</sup> (Bakker, 1991<sup>a</sup>; Nederhoff and De Graff, 1992), and for tomato a range of about 67 s m<sup>-1</sup> to 250 s m<sup>-1</sup> (Bakker, 1991<sup>b</sup>; Nederhoff and De Graff, 1992; Jolliet and Bailey, 1992). Work done on greenhouse roses in Zimbabwe by Mhizha (2003) produced daytime stomatal resistance values of 23 s m<sup>-1</sup> and 142 s m<sup>-1</sup> for the clear and overcast sky conditions respectively. Night time stomatal resistance for the crop can be as high as 2500 s m<sup>-1</sup> according to Seginer, 1984.

Two of the methods used to estimate the evapotranspiration rate are the energy balance of a leaf and the Penman-Monteith equation (Zhang and Lemeur, 1992, Allen *et al.*, 1998).

The energy balance of a leaf is expressed as:

$$E = \frac{\rho_a c_p}{\lambda \gamma} \cdot \frac{\{e_s(T_l) - e_a(T_a)\}}{(r_{lv} - r_{av})}$$
(2.3.23)

where  $\lambda$  is the latent heat of vaporization (J kg<sup>-1</sup>), E is the rate of evapotranspiration (kg m<sup>-2</sup> s<sup>-1</sup>),  $e_s(T_l)$  is the saturation vapour pressure at leaf temperature,  $e_a(T_a)$  is the vapour pressure at air temperature,  $r_{lv}$  is the stomatal resistance to vapour transfer,  $r_{av}$  is the boundary layer resistance to vapour transfer and  $\gamma$  is psychometric constant.

The Penman-Monteith equation is a combination of the energy balance and mass transfer. It is expressed as:

$$E = \frac{\Delta(R_n - G) + \rho_a c_p \frac{\left(e_s(T_l) - e_a(T_a)\right)}{r_a}}{\lambda \left[\Delta + \gamma \left(1 + \frac{r_l}{r_a}\right)\right]}$$

(2.3.24)

where  $R_n$  is the net radiation, G is the ground heat flux,  $e_s(T_l) - e_a(T_a)$  represents the vapour pressure deficit of the air,  $\rho_a$  is the mean air density at constant pressure,  $c_p$  is the specific heat of the air,  $\Delta$  is slope of the saturation vapour pressure to temperature relationship,  $\gamma$  is psychometric constant,  $r_s$  (bulk) surface resistance and  $r_a$  aerodynamic resistance

Where the surface conditions cannot be measured or are unknown, the leaf-air vapour pressure difference in both equations can be substituted with the vapour pressure deficit of the ambient air and a term depending on the temperature difference between the leaf and air such that

$$\{e_s(T_l) - e_a(T_a)\} = \{e_s(T_a) - e_a(T_a)\} - \Delta(T_a - T_l) = \delta e + \Delta(T_l - T_a)$$
 (2.3.25)

where  $e_s(T_a)$  represents the saturation vapour pressure deficit of the ambient air,  $\Delta$  the slope of the curve relating saturation vapour pressure to temperature,  $\delta e$  the vapour pressure deficit of the ambient air

#### 2.3.4 Conduction

The other mode of heat transfer is conduction, which occurs in the soil and greenhouse cover. The exchange of heat by conduction in the soil takes place between its sub-layers. The soil is divided into layers because of the changes in its physical and chemical properties with soil depth. Conduction involves the exchange of kinetic energy among molecules or atoms between two different parts of an object. The conductive heat flux density for a plane parallel plate with thickness l and a temperature gradient perpendicular to its surfaces is expressed using the empirical law of Fourier as:

$$q_D = h_D(T_2 - T_1) (2.3.26)$$

where  $q_D$  is conductive heat flux density (W m<sup>-2</sup>) and  $T_2 - T_1$  temperature gradient  $h_D$  is the conductive heat transfer coefficient and is calculated using the equation below:

$$h_D = \frac{\lambda}{I} \tag{2.3.27}$$

where  $\lambda$  thermal conductivity  $(Wm^{-1}K^{-1})$  (W m<sup>-1</sup> K<sup>-1</sup>) and l thickness (m).  $\lambda$  is influenced by the soil type and its moisture content.

#### 2.3.5 Summary

The heat and mass transfers for the different greenhouse layers (cover, air, vegetation and soil) play an important role in influencing their respective temperatures and relative humidity in the case of the greenhouse air. Heat and mass transfer for the different greenhouse layers can occur through radiation, convection, conduction or phase change. Radiation, convection and phase change are the dominant modes of transfer within the greenhouse structure whilst conduction is mostly restricted to the cover and soil.

## 2.4 Modelling of the Greenhouse Microclimate

#### 2.4.1 Introduction

Unfavourable climatic conditions in the greenhouse can occur under cool winter nights or during high radiation intensity periods as has been mentioned in §2.2. The greenhouse microclimate variables (temperature and relative humidity) are thus continuously monitored using wet and dry bulb thermometers such that at predetermined levels, climate control mechanisms such as ventilation can be triggered to adjust these variables within acceptable limits. The computerization of greenhouse microclimate control has reduced labour costs and improved the regulation of the climatic variables. Because of the costs involved in the installation of the equipment, its use has thus been limited to established commercial floricultural greenhouses (Bot, 1995).

The prediction of greenhouse microclimate variables using weather forecasts offers a more affordable tool for greenhouse microclimate control in Zimbabwean greenhouse rose production. The concept of greenhouse microclimate modelling is increasingly being used in research due to increased complexity in greenhouse processes and the huge costs involved in instrumentation (Pieters, 2002).

Modelling is based on the energy balance of the greenhouse, which was first analysed by Businger (1963). The development of the greenhouse energy budget enabled many authors to simulate the greenhouse microclimate variables based on the exchange processes for respective greenhouse layers (Bot, 1983). The energy and mass balances have been of two types: steady state and dynamic. Dynamic energy and water vapour balances are more representative of the greenhouse processes since they incorporate the time dependence of these processes unlike static models, which assume a steady state system (equilibrium).

With the modelling of the greenhouse microclimate, the greenhouse is introduced as a one-dimensional system divided into the cover, air, vegetation and soil (various layers) whose heat balances and in some cases also a mass balance (air) should be determined. These heat and mass balances are in the form of differential equations, which are then solved iteratively as functions of time with given boundary conditions to determine the unknown temperatures of the different greenhouse layers and the relative humidity of the greenhouse air (Seginer *et al.*, 1994; Bot and van de Braak, 1995; Zhang *et al.*, 1997; Wang and Boulard, 2000).

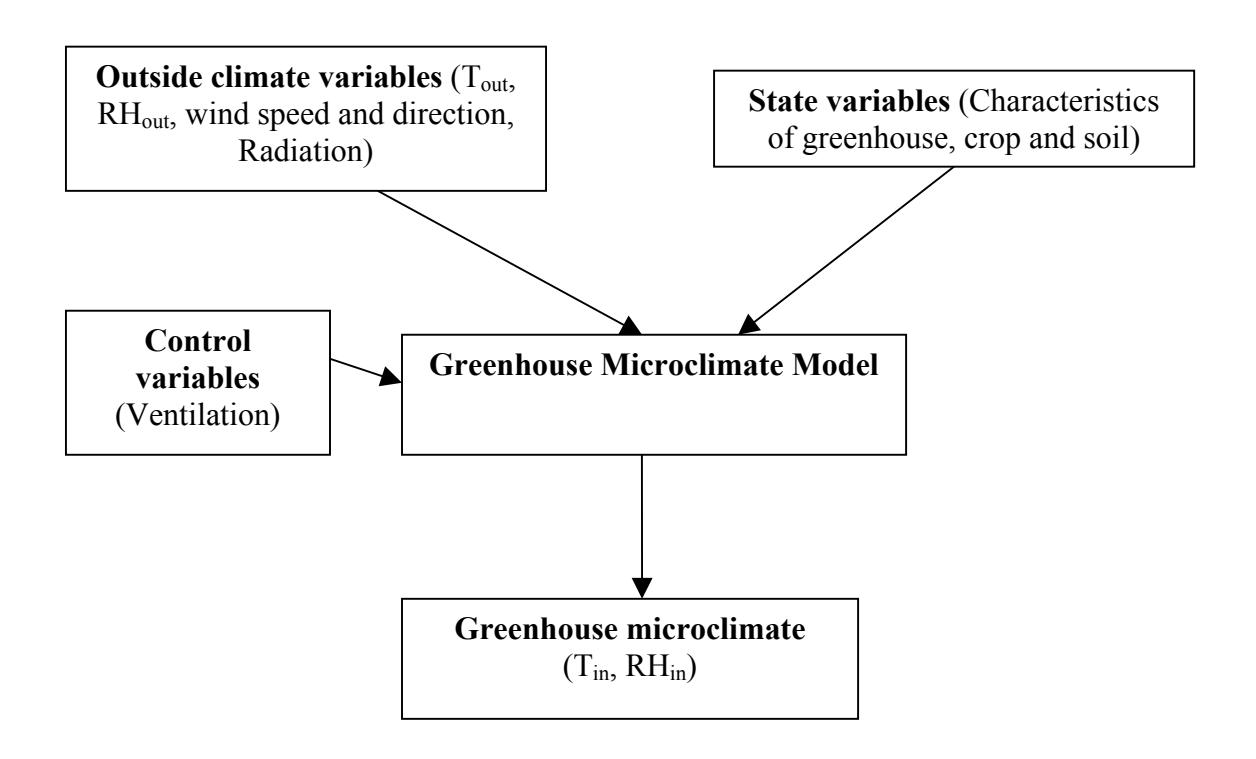


Fig 2.2: The inputs and outputs for a greenhouse microclimate model (Adapted from Bontsema, 1995)

Figure 2.2 shows a simplified method of describing the modelling of the greenhouse microclimate. According to the diagram, the conditions inside a particular greenhouse (outputs) are due to the interactions of three types of variable factors: the external climate variables, control variables (ventilation) and state variables (characteristics of the greenhouse, crop canopy and soil). The variables thereby influence the air temperature and its relative humidity because of their contributions to the heat and mass balances of the air (Seginer *et al.*, 1994; Zhang *et al.*, 1997; Wang and Boulard, 2000).

### 2.4.2 Analysis of the performance of greenhouse microclimate models

The simulation of the greenhouse microclimate variables using the outside climatic conditions is based on the assumption that the two environments are strongly coupled. Under such conditions there has to be an efficient ventilation mechanism, which will assist transfers of heat and mass between the two environments. The efficiency of the ventilation mechanism can be determined either by the ventilation rate or ventilation volumetric flux. On the other hand, it is the same ventilation mechanism and other factors such as heating and the transpiration of a well-developed crop representing the biggest

contribution to the energy balance that increase the difficulties associated with greenhouse microclimate modelling (Seginer, 1997).

However, some greenhouse climate models have produced acceptable predictions despite these constraints. HORTITRANS is one such model which has been able to predict within 8 % of the measured values of the vapour pressure, transpiration and condensation inside a greenhouse for different growth stages of a tomato crop (Jolliet, 1992). HORTITRANS is a single component dynamic model, which only simulates the vapour pressure inside the greenhouse. It is based on a simple water vapour balance because of the linear relationship between the water vapour inside the greenhouse and all the factors affecting it such as ventilation, misting, condensation on the cladding, transpiration and dehumidification.  $E_d$ , the variation in the water stored in the greenhouse air per unit time (mg m<sup>-2</sup> s<sup>-1</sup>) can be described by the equation:

$$E_{d} = E_{t} + E_{ad} - E_{c} - E_{v}$$

$$E_{ad} = E_{ad1} + E_{ad2}$$
(2.4.1)

where  $E_t$  crop transpiration,  $E_{ad1}$  misting,  $E_{ad2}$  dehumidification,  $E_v$  ventilation and  $E_c$  condensation.

The Stanghellini model is considered as the most accurate in the prediction of transpiration compared to other models because it accounts for the variation of the stomatal conductance with solar radiation and the vapour pressure deficit (Jolliet and Bailey, 1992). However unlike the Stanghellini model, HORTITRANS accounts for the feedback effect of the inside humidity on transpiration and condensation by using a correction factor on the calculated condensation for inside air at saturation (Jolliet, 1992).

A transpiration model developed by Boulard and Wang (2000) for simple greenhouse structures in the Mediterranean region was observed to be reliably strong in the summer period due to the activated ventilation, which increased the coupling between the air and external environment. The model performance showed no variation between cloudy and clear days. During the Mediterranean winter, the model performance deteriorated by 20% of the summer value with the contributory factors being the heating and inactive ventilation during the nighttime and the low transpiration rates due to cloudiness during the daytime.

The deterioration in the performance of the model during winter was attributed to the following:

 exclusion of the evapo-condensation process in the water vapour balance although its importance is greater under closed greenhouses.

- larger differences between the internal and external temperatures increased the errors in the derivation of the water vapour pressure deficit of the greenhouse  $\operatorname{air}(VPD_i)$ .  $VPD_i$  is derived as a linear function of outside water vapour deficit and temperature,  $VPD_o$  and  $T_o$ . This is only verified when  $e_s(T_i) e_s(T_o) \cong \delta(T_o) \Delta T$ .
- contribution of the buoyancy forces particularly at high temperatures to ventilation is ignored. This is done to linearise the ventilation process.
- exclusion of a leakage component in the description of the air exchange rate (Boulard and Wang, 2000).

However the errors associated with the prediction during the winter period are considered insignificant since they occur under closed greenhouses when the transpiration fluxes are generally weak, (Boulard and Wang, 2000).

Another model to be considered is that of Avissar and Mahrer (1982), which had reasonable predictions of greenhouse microclimate variables under an unheated commercial greenhouse for tomatoes as observed by Zhang et al. (1997). The model produced root mean square errors (RMSE) of 1.2 °C and 1.8 °C and 5.8% between the predicted and measured air and leaf temperatures and relative humidity respectively. The model performance was particularly better at nighttime because of the simple heat and mass exchange processes due to the absence of solar radiation (Zhang et al., 1997). The increased accuracy of the model during the nighttime was important since it coincided with the prediction of the leaf wetness duration (LWD). Therefore the higher accuracy in the predicted LWD (RMSE 1.9 h d<sup>-1</sup>) ensured effective disease management. Nowadays, it is being advocated that the plant surface microclimate variables be used for disease forecast since they produce improved predictions of the vegetation microclimate thereby optimizing the benefits of Integrated Pest Management (Zhang et al., 1998). This is referred to as the "speaking plant" concept. The model similarly to the Gembloux Dynamic Greenhouse Climate Model (GDGCM) in the following paragraph can be used for long-term greenhouse microclimate predictions because of its inclusion of time-dependent factors such as leaf area index (LAI), rooting density distribution (RD) and the irrigation scheduling.

The GDGCM (Deltour *et al.*, 1995) is another of the models that have also produced reasonable estimates of the greenhouse microclimate variables: the soil temperature, interior air temperature and relative humidity (Wang and Boulard, 2000). The work was done in a ventilated Mediterranean greenhouse where the ventilation was calculated using a linear non-dimensional function from Boulard and Baille, 1995 (refer to §2.3) and standard deviations of 0.5 °C, 0.8 °C and 4.3 % were obtained between the predicted and measured soil temperature, air temperature and relative humidity respectively. However, according to the authors, the model performance deteriorates at sunrise and

sunset periods because of the small volumetric heat capacity assigned to the greenhouse structure such that its air was generally cooler in comparison to the measurements (Wang and Boulard, 2000). The other factor is that the volumetric heat capacity is incorrectly calculated because of the exclusion of the contributions by the greenhouse construction parts. The latter have a large outside surface area such that they have a considerable amount of energy, which is quickly exchanged with the other greenhouse components (Bot, 1983).

### 2.4.3 Selection of a greenhouse climate model

The selection of a GCM for use in greenhouse microclimate prediction depends on the model attributes, which will make it relevant to the situation intended for use. Some of these attributes include the composition of the boundary layers, greenhouse layers and the respective heat and mass balances. Greenhouse microclimate prediction now uses mostly dynamic models, which include those of Takakura *et al.* (1971), Avissar and Mahrer (1982), Bot (1983) and Stanghellini (1986). In the case of the GDGCM, which is used in the study, it incorporates many properties that were not previously found in a single model such as its dynamism and the ability of the sub-models of transpiration and ventilation, to cater for different crop species and ventilation systems respectively (Pieters, 2002). The presence of modules in the simulation programme, TRNSYS enables flexibility in the use of the model as well as increasing its simplicity. This is because changes can be made to specific modules, without having to change the whole programme. It is on this basis, that the model can be adapted for different greenhouse crops and climatic conditions thereby increasing its suitability to use for microclimate prediction in Zimbabwe. Since the model has already been successfully used in the Mediterranean region, with a different climate and under a ventilated greenhouse, this further increased the possibility that the GDGCM could also be adapted for a subtropical climate.

### **CHAPTER 3**

#### MODEL DESCRIPTION

#### 3.0 Introduction

This section of the thesis describes the Gembloux Dynamic Greenhouse Climate Model (GDGCM) in terms of its simulation of the state variables for the different greenhouse layers. The model was originally developed for the microclimate prediction of a greenhouse tomato crop in the temperate region (Pieters, 2002). The GDGCM is a multiple component dynamic model which calculates eight heat balances for the following greenhouse layers: cover, air, vegetation, soil surface and four soil sublayers (Pieters, 2002). It also includes a mass balance for the simulation of the relative humidity of the greenhouse air (refer to Figure 3.1).

The GDGCM uses the TRNSYS software for the simulation and analysis of the heat and mass transfer processes. TRNSYS is a transient simulation programme developed at the Solar Energy Laboratory of the University of Wisconsin-Madison. TRNSYS is a suite of programs designed to simulate transient energy systems. With the current version of TRNSYS (Version 13) users create a text file describing the system being simulated and then launch a FORTRAN program to run it. According to Pieters (2002) the TRNSYS programme runs the simulation using the deck file. The deck file consists of several modules, which are described in separate units. A unit refers to a component of the greenhouse system to be simulated such as the air or vegetation. The types in the deck file are FORTRAN subroutines, which can be used for the description of several units. Therefore a type can be used more than once in a simulation in relation to different units. The deck file should be prepared carefully as in-built control procedures will detect errors in it and prevent simulation runs (Pieters, 2002).

Figure 2.2 describes the overall simulation with inputs (ventilation, outside climate variables, characteristics of the greenhouse, crop and soil) and outputs (inside climate variables). The inputs are read into the programme by means of specific data files (Pieters, 2002). These files normally have a .DAT extension such as the CHARACT.DAT or CLIMAT.DAT files used in the present version of the GDGCM. CHARACT.DAT contains data stored in COMMON blocks such that they can be used anywhere in the programme. Each block contains characteristics of a specific element within the greenhouse. The blocks used in the GDGMM include;

CHRSOIL block containing some of the soil characteristics
CHRCONSTR block containing the construction characteristics

CHRAIR block containing the air characteristics

CHRVEG block containing the vegetation characteristics

COND block containing the characteristics that are influenced by the

processes of condensation and evaporation.

The data from the CHARACT.DAT file is read into the model using Type 60 (the greenhouse construction data reader).

CLIMAT.DAT contains the external weather data (air temperature, relative humidity, wind speed, total solar radiation and cloud cover). The data from the CLIMAT.DAT file is read by Type 9.

## 3.1 **Boundary Conditions**

The model has two components: boundary conditions and the greenhouse system. Boundary conditions will be dealt with first before the greenhouse system. Boundary conditions are found at the limits of the greenhouse system and are referred to as being independent of the greenhouse environment. Boundary conditions include the sky, outside air and the greenhouse subsoil. The sky forms the upper boundary condition with the lower boundary condition being the subsoil. The subsoil tends to have a constant temperature, whose value is assumed to be equivalent to that at the soil depth where there is little temperature variation for small greenhouses whilst with infinitely large greenhouses; it is given as the yearly mean value of the outside air temperature.

As previously mentioned in §2.3, the sky interacts with the greenhouse environment through the exchange of radiation. The exchanges of total solar radiation between the sky and greenhouse system can be simulated using the subroutine, Type 16 (solar radiation processor). The simulation of the radiation data is done using the curve for extraterrestrial radiation. Solar radiation should not be simulated linearly because this introduces errors particularly at sunset and sunrise. The simulation of insolation requires two radiation data sets, which in most cases are the global solar radiation and diffuse solar radiation such that the direct solar radiation is obtained as their difference. However, where only the global radiation measurement is available, Type 16 has the provision of simulating the distribution of the solar radiation over beam and diffuse radiation. The selection of the radiation mode to be used in Type 16 is thus dependent on the set of radiation data that is available as input data.

The longwave (far infrared) radiation from the sky is described using its radiative properties and temperature. In the present version of the model, the radiative properties of the sky are constants whilst the radiative sky temperature, determined by the equation of Swinbank (1963) (refer to § 2.3) is

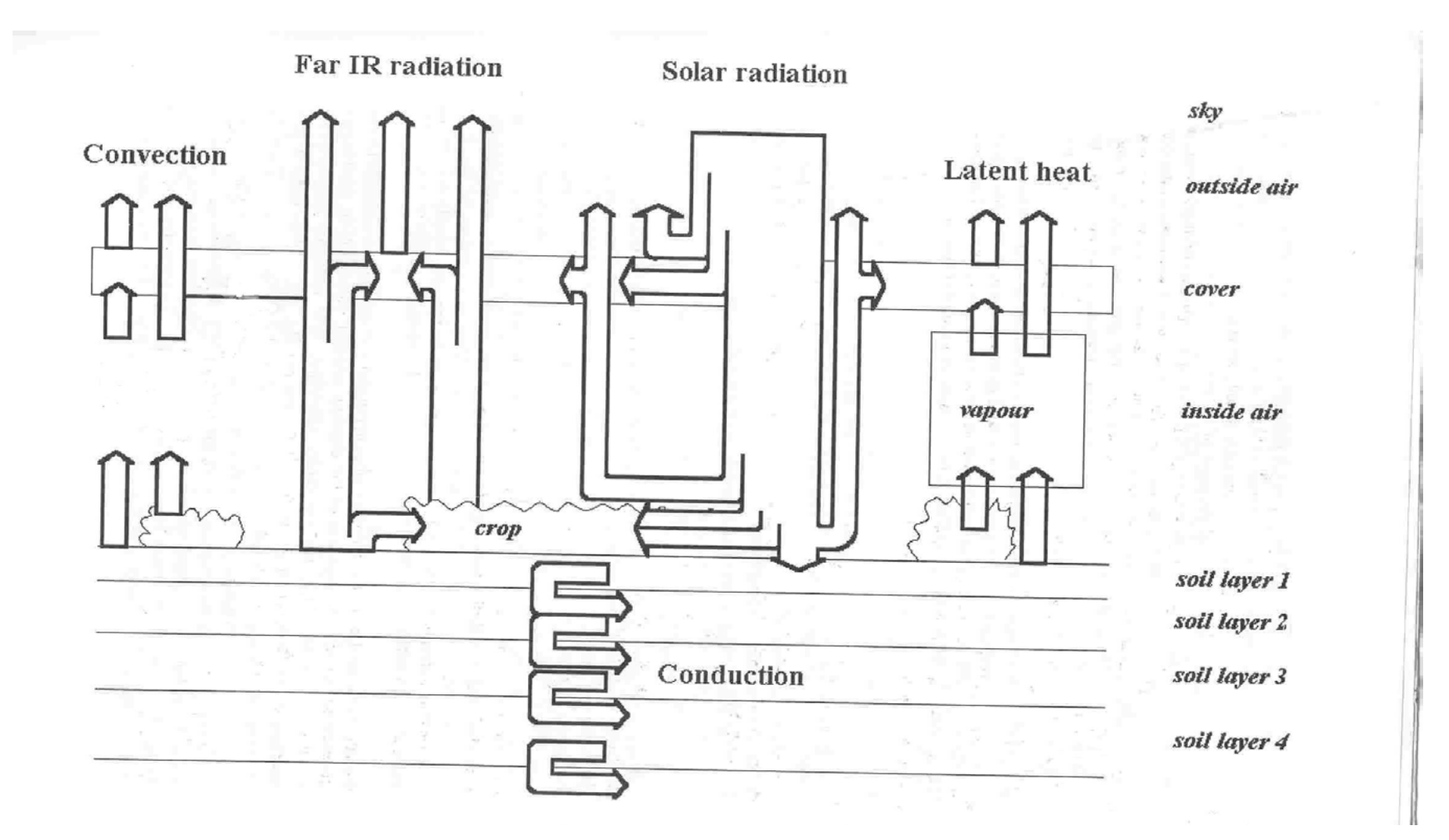


Fig 3.1: Scheme of the Gembloux Dynamic Greenhouse Climate Model (Adapted from Pieters, 2002)

simulated using Type 61. Type 61 not only simulates the radiative sky temperature but other variables related to the position of the sun such as the beam radiation flux density and the day length (Pieters, 2002).

The other boundary conditions, the outside air and subsoil do not require specific treatment since the characteristics of the air are all measurements and those of the subsoil are constants, determined once off by calibration or measurement (Pieters, 2002).

### 3.2 Greenhouse Layers

These refer to the components of the greenhouse system which include the cover, air, vegetation and the soil with its sub-layers. The state variables of individual layers can be simulated from their respective heat balances and the mass balance in the case of the greenhouse air. These heat and mass balances are derived in different units. There is an interlinking of these units because the output in one unit may become input in other units. The heat and mass balances for the greenhouse layers will therefore be described in this section (Pieters, 2002).

#### **3.2.1** Cover

In the modelling of the cover temperature:

- o the cover is assumed to have the same temperature on both its inner and outer cover because of its low conducive resistance, which is given a Bi critical value of 0.1.
  Bi is calculated as the ratio of the conductive resistance to the combined convective resistance and radiative heat resistance.
- the radiative properties of the cover for diffuse solar radiation and thermal radiation are constants whilst those for direct solar radiation are influenced by the angle of incidence.
- o radiation is the only method of heat transfer between the sky and the cover or vice versa. Heat transfer through phase change (evaporation of rainfall) has not yet been incorporated in the model.
- Condensation is regarded as a rare phenomenon on the outer cover according to Pieters (1995) and therefore only occurs inside the cover.

In the model, the subroutine that calculates the heat balance equation for the cover is Type 62. The heat balance for the greenhouse cover is expressed as:

$$c_c' \cdot \frac{dT_c}{dt} = \frac{A_{gr}}{A_c} \cdot \left( q_{V(i,c)} - q_{V(c,e)} + q_{P(i,c)} + q_{R(s,c)} + q_{R(v,c)} - q_{R(c,sky)} + q_{S(c)} \right)$$
(3.2.1)

where  $A_{gr}$  is surface area of the greenhouse,  $A_c$  surface area of the greenhouse cover,  $q_{V(i,c)}$  convective heat flux density from the inside air to the cover (W m<sup>-2</sup>),  $q_{V(c,e)}$  convective heat flux density from the cover to the outside air (W m<sup>-2</sup>),  $q_{P(i,c)}$  heat transfer by phase change (condensation),  $q_{R(s,c)}$  radiative heat flux density from the soil to the cover (W m<sup>-2</sup>),  $q_{R(v,c)}$  radiative heat flux density from the crop to the cover (W m<sup>-2</sup>),  $q_{R(c,sky)}$  radiative heat flux density from the cover to the sky (W m<sup>-2</sup>) and  $q_{R(s,ky,c)}$  solar radiative heat flux density from the sky to the cover (W m<sup>-2</sup>).

Heat exchange between the cover with the sky, vegetation and soil by radiation is mainly influenced by the radiative properties (absorptivity ( $\alpha$ ), reflectivity ( $\rho$ ) and transmissivity( $\tau$ )) of the respective model components. It should be noted that for diffuse solar radiation, the radiative properties tend to be constant with those for direct solar radiation being dependent on the angle of incident (Pieters, 2002).

In the model, heat exchange between the cover with the greenhouse air and outside air occurs by convection. Heat exchange by convection is influenced by the characteristics of the air such as its temperature and velocity. It is assumed that air velocity inside the cover is constant and for the study was given a value of 0.3 m s<sup>-1</sup> (Pieters, 2002). The greenhouse cover and the inside air also exchange heat by phase change where water vapour condenses onto the cool greenhouse cover. Condensation is defined in the model by the following equation:

$$p_{cf} = \frac{L_{cf}}{L_{cf,\text{max}}} \tag{3.2.2}$$

where  $p_{cf}$  is the equivalent water-covered surface factor (wetted fraction of the cover),  $L_{cf}$  is the condensate film thickness and  $L_{cf, \max}$  is the maximum condensate film thickness.

The presence of condensate increases both the heat capacity and opaqueness of the cover to thermal (infrared) radiation, such that more is trapped within the greenhouse. Where condensation has occurred the thermal (infrared) radiative properties of the covering material are replaced with those of water ( $\alpha = 0.93$ ;  $\rho = 0.07$ ;  $\tau = 0$ ).

### 3.2.2 Vegetation

In the determination of heat and mass transfer between the vegetation and other layers of the model, information on the fraction of the greenhouse surface area covered by the vegetation  $(p_v)$ , vegetation mass density  $(m_v)$  and the leaf area index (LAI) is required. In the study,  $p_v$  was calculated for a fully developed crop. Figure 3.2 shows two methods of calculating  $p_v$  for (a) a fully developed crop and (b) a young and sparse crop (Pieters, 2002). In both cases  $p_v$  is determined as the total projected area of the vegetation on the soil surface and related to the total greenhouse area (sum of white and gray surfaces as in Figure 3.2). The LAI is calculated as a ratio of the total leaf area to the total ground surface area. Similarly the vegetation mass density is also expressed with respect to the total greenhouse surface area (Pieters, 2002).

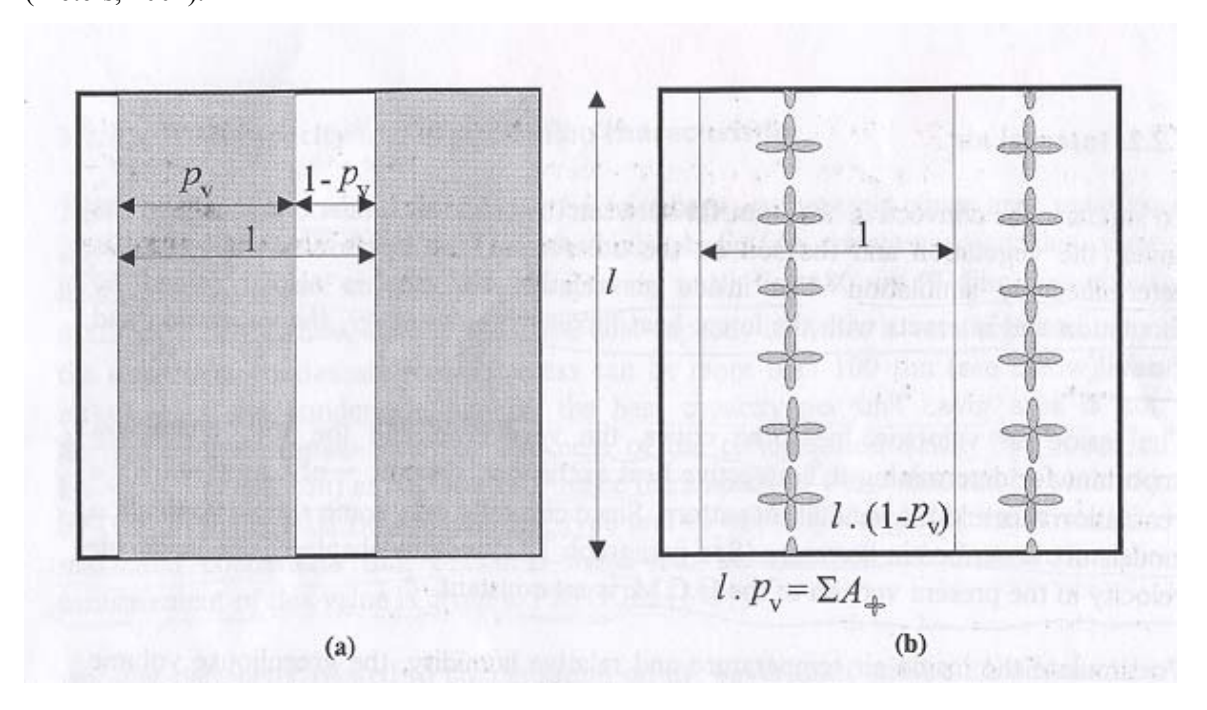


Fig 3.2: Determination of  $p_{\nu}$  for (a) a fully developed crop and for (b) a sparse crop (Source: Pieters, 2002)

The vegetation covered fraction of the soil, LAI and vegetation mass surface density increase during the growing season until their maximum values are reached. Although these time-dependent changes are not linear, the use of forcing functions (Type 14) by the model forces the time-dependent changes to assume a linear pattern (Pieters, 2002).

The FORTRAN subroutine Type 64 is used for the simulation of the vegetation microclimate variables based on the following equation:

$$c_{v}.m_{v}^{'}.\frac{dT_{v}}{dt} = -q_{V(v,i)} - q_{P(v,i)} - q_{R(v,c)} - q_{R(v,sky)} + q_{R(s,v)} + q_{S(v)}$$
(3.2.3)

According to equation 3.2.3 heat exchange by radiation occurs between the vegetation with the cover, soil and sky. The vegetation receives solar radiation from the sky and longwave radiation from the soil whilst in turn losing longwave radiation to the sky and cover. The amount of solar radiation absorbed by the crop will depend on the crop's radiative properties as has been previously mentioned. Here the crop's reflectance  $\rho_{Sv}$  is assumed to be constant and its value corresponds to that for the soil. The transmittance  $\tau_{Sv}$  of the crop will vary depending on the position within the canopy and is described based on Beer's Law as:

$$\tau_{SV} = (1 - \rho_{SV})e^{-k_{v}.LAI} \tag{3.2.4}$$

where  $\rho_{Sv}$  is the reflectance for solar radiation and  $k_v$  canopy attenuation coefficient (Monteith and Unsworth, 1990).

Heat energy by convection is assumed to occur on both surfaces of the leaves within the canopy to the inside air (Pieters, 2005). Differences in the orientations of the upper and leaf surfaces result in differences in their convective transfer coefficients. In the study, the sine function model (transpiration model 0) was used to simulate the stomatal resistance of the greenhouse rose crop. Other sub-models available for use include that of Jolliet and Bailey (1994) and Stanghellini (1987), which are specifically for a greenhouse tomato crop whilst the sine function model is independent of both plant species and climate conditions. The sine function model simulates only the daytime stomatal resistance whilst the nighttime value is considered to be constant. The nighttime stomatal resistance is thus given a maximum value, which is almost constant whilst the daytime values are lower with the minimal stomatal resistance achieved at solar noon.

The mathematical expressions for the sine function model are

for 
$$q_{Sg} = 0$$
  $r_{st} = r_{st \text{ max}}$  (3.2.5)

for 
$$q_{Sg} > 0$$
  $r_{st} - r_{st \max} - (r_{st \max} - r_{st \min}) \cdot \cos \left( \pi \cdot \frac{H - 12}{H_{sset} - H_{srise}} \right)$  (3.2.6)

for 
$$q_{Sg} = \max r_{st} = r_{st \min}$$
 (3.2.7)

where H is hour of the day (hr),  $H_{srise}$  hour of sunrise (hr),  $H_{sset}$  hour of sunset (hr),  $q_{Sg}$  actual global solar radiation (W m<sup>-2</sup>),  $r_{st}$  actual value of the stomatal resistance (s m<sup>-1</sup>),  $r_{stmax}$  maximum (nocturnal) value of the stomatal resistance (s m<sup>-1</sup>),  $r_{stmin}$  minimum (nocturnal) value of the stomatal resistance (s m<sup>-1</sup>).

### 3.2.3 Soil surface layer

The soil surface is assumed to form a barrier to the exchange of water vapour and water with the greenhouse air due to the presence of a covering. The assumption is on the basis that most greenhouse floors are covered with a plastic film, concrete or quarry stones to increase the reflectance of solar radiation towards the vegetation. The concrete and quarry stones are mostly common in commercial Zimbabwean greenhouses.

The soil surface has the following properties:

- it receives mostly diffuse solar radiation and will only have one reflectance  $(\rho_{ss})$  value that for diffuse solar radiation.
- there is no transmission of radiation in the soil such that the far infrared radiative exchange between the soil surface and other components of the greenhouse are influenced by its emittance and reflectance properties.
- the characteristic length for the convective exchanges between the soil surface and other greenhouse components is taken as the distance between subsequent rows.
- since it assumed that all the water vapour that condenses on the soil surface evaporates, the condensate film thickness has no maximum value as in the case of the greenhouse cover.

The heat balance for the simulation of the temperature of the greenhouse soil surface (using Type 65) is as follows:

$$\rho_{s}'.c_{s}.l_{s}.\frac{dT_{s}}{dt} = -q_{V(s,i)} - q_{P(s,i)} - q_{R(s,c)} - q_{R(s,sky)} - q_{R(s,v)} + q_{S(s)} - q_{D(s1)} = 0$$

(3.2.8)

where c is the heat capacity (J kg<sup>-1</sup> K<sup>-1</sup>), l thickness (m) and  $\rho$ ' density (kg m<sup>-3</sup>) and all other terms are as defined in §3.2.1 above.

### 3.2.4 Soil sub-layers

In the model, the soil is divided into four sub-layers to increase the accuracy in the simulation of the conductive heat transfer in the soil. The temperature variations within the soil sub layers are still sinusoidal but associated with a time delay that increases with depth and amplitude that decreases exponentially with depth. Because of the latter, the thickness of the lower soil layers should be greater such that they cover the same temperature difference between the upper and lower edges. Each soil layer is thus assumed to be homogeneous with respect to its thermal conductivity, heat capacity and density.

The temperature of a soil sub layer is simulated at its interface with an underlying slayer. In order to determine the soil temperature, the thermal properties for the interface are calculated as weighted mean values of these characteristics for the two sub layers involved. The weighing factors used in the calculations are the relative thicknesses of the two adjacent layers. The following equations are used for the calculation of the thermal properties at the interface of two soil layers:

$$\rho'_{s23} = \frac{l_{s2} \cdot \rho'_{s2} + l_{s3} \cdot \rho'_{s3}}{l_{s2} + l_{s3}}$$
(3.2.9)

$$c_{s23} = \frac{l_{s2}.c_{s2} + l_{s3}.c_{s3}}{l_{s2} + l_{s3}}$$
(3.2.10)

$$l_{s23} = \frac{l_{s2} + l_{s3}}{2} \tag{3.2.11}$$

The conductive heat flux density at the interface of two soil sub layers (i.e. 2 and 3) is simulated using equation 3.2.12.

$$\rho'_{s23}.c_{s23}.l_{s23}.\frac{dT_{s23}}{dt} = q_{D(s2)} - q_{D(s3)}$$
(3.2.12)

This simulation of the soil layer temperature uses FOTRAN subroutine Type 66 of the present version of the model.

### 3.2.5 Inside air

The simulation of the air temperature and relative humidity inside the greenhouse is done by FORTRAN subroutine Type 63. The respective heat and mass balance equations involved in the simulation of these state variables are expressed as follows:

$$\rho_a' \cdot c_i \cdot \frac{V}{A_{or}} \cdot \frac{dT_i}{dt} = q_{V(s,i)} + q_{V(v,i)} - q_{V(v,i)} - q_{V(i,e)} + q_{HS}$$
(3.2.13)

$$h_{fg} \cdot \frac{V}{A_{gr}} \cdot \frac{dC_i}{dt} = q_{P(s,i)} + q_{P(v,i)} - q_{P(i,c)} + q_{L(i,e)}$$
(3.2.14)

where V is the greenhouse volume  $(m^3)$  and  $C_i$  is the water vapour concentration of the inside air  $(kgm^{-3})$ .

## 3.2.6 Ventilation system

Ventilation was the only control procedure implemented in the greenhouse. In the study, the ventilation was modelled as a P-controlled ventilation system referred to as operation mode 2. "With this ventilation mode the air renewal rate is assumed to be proportional to the difference  $\Delta T_{vent}$  between the actual inside air temperature and the desired (ventilation) inside air temperature, at least for temperature differences between a minimum value  $\Delta T_{vent,min}$  (mostly 0) and a maximum value  $\Delta T_{vent,max}$ , which is selected without any restrictions" (Pieters, 2002). The equations for the actual air renewal rate are as follows for the different conditions:

for 
$$\Delta T_{vent} \le \Delta T_{vent,min}$$
  $R_a = R_{a,min}$  (3.2.15)

for 
$$\Delta T_{vent, min} < \Delta T_{vent} > \Delta T_{vent, max}$$
 
$$R_a = R_{a, min} + \frac{R_{a, max} - R_{a, min}}{\Delta T_{vent, max} - \Delta T_{vent, min}} \Delta T_{vent}$$
 (3.2.16)

for 
$$\Delta T_{vent} \ge \Delta T_{vent \, max}$$
  $R_a = R_{a \, min} + R_{a \, max}$  (3.2.17)

The temperatures for the periods, which govern the ventilation rate during the course of the day, are calculated under Type 70. These ventilation set point temperatures are determined for four periods of the day, which are related to the sunrise and sunset periods. These periods are defined as

$$H_{p1} = H_{srise} + \Delta t_{p1} \tag{3.2.18}$$

$$H_{p2} = H_{srise} + \Delta t_{p2} \tag{3.2.19}$$

$$H_{p3} = H_{sset} + \Delta t_{p3} \tag{3.2.20}$$

$$H_{p4} = H_{sset} + \Delta t_{p4} \tag{3.2.21}$$

where H is the hour of the day (hr),  $\Delta t$  is the time interval between the beginning of the period and the moment of sunrise or sunset (hr) and the subscripts p1, p2, p3 and p4 represent the four ventilation periods with srise and sset representing sunrise and sunset respectively.

# 3.3 Running a Simulation using the Gembloux Dynamic Greenhouse Climate Model

The simulation is run for 168 hours (one week) with a time step of one minute (Pieters, 2002). This means that for  $t_0 = 0$  the weather data for the previous day (2400) is used.

The simulation produces four output files (Units 20, 23, 24 and 25). Unit 20 was the most important in the study because it gives the temperatures of the greenhouse layers (cover, air, vegetation, soil surface and soil interfaces) as well as the relative humidity of the inside air. The output for the study was given at 30 minute intervals (Pieters, 2002).

To use the GDGCM, the following files should be copied to a separate directory on the hard disk of a PC.

**UDGCM.EXE** 

CLIMAT.DAT

CHARACT.DAT

REPET.DAT

#### EXAMPLE1.DEK

To run the simulation, the following steps were carried out after adjustments to the climate, character and deck files:

Step 1: Run the program UDGCM.EXE

**Step 2:** The following question appears:

HAS YOUR TRNSYS DECK ALREADY BEEN PROCESSED? (Y, N)

Type N →

**Step 3:** The following question appears:

WHICH FILE FOR SIMULATION DECK?

Type ???????.DEK (The name of the deck file). For the study this was Floraline.DEK

**Step 4:** The following question appears:

NAME OF FILE CONTAINING MODEL CHARACTERISTICS:

Type CHARACT.DAT ↓

# **CHAPTER 4**

#### **MATERIALS AND METHODS**

#### 4.0 Introduction

The study was divided into three parts. The first part involved investigating the homogeneity of the greenhouse environment where measurements of temperature and humidity were carried out simultaneously at different positions within the greenhouse and then in the central position of the greenhouse to enable a comparison with the results for the spatial arrangement. This was done in the month of November 2004 and the period 8-11 February 2005 respectively.

The second part of the study involved comparison of the greenhouse microclimate with that of the outside. Measurements of the climate variables were carried out inside and outside a greenhouse during the months of November 2004 to February 2005.

The third part of the study was the calibration and validation of the Gembloux Greenhouse Dynamic Climate Model using the climate data collected in Part 2. The calibration also required measurements of the greenhouse and soil characteristics.

# **4.1** Site

The measurement of weather parameters was done at Floraline Private Limited, which is located in Harare, 31.04° E and 17.4° S, altitude 1502 m. The company specialized in the provision of propagation material for greenhouse rose production. The greenhouse used for the data collection was a test site for rose cultivars from international rose breeders such as InterPlant Roses, Nirp International, Schreurs, Kordes Roses, Meilland and SpekRose Breeding International. The performance of these cultivars is assessed in the test greenhouse prior to their release for commercial production as scion stock. The greenhouse consisted of three spans and covered a total area of approximately 1260 m². The ridges and gutters were at heights of 7.5 m and 4.0 m respectively. The greenhouse cover was a 200  $\mu$ m UVA Rose Diffused polyethylene, which had special ultraviolet – blocking composition for the reduction of incidences of blackening of red rose petals, pest and diseases (Politiv, 1999). The roses were grown in a vermiculite substrate in troughs, each 0.4 m x 20.0 m in size with a depth of 0.15 m. These troughs were placed in drainage trays on raised beds of soil. The drainage trays

were not placed directly on the bed of soil but on a layer of quarry stones which separated the two. A similar layer of quarry stones was also placed in the trough prior to adding the vermiculite substrate. The sides of the soil were covered with a plastic with the paths in between the beds covered with quarry stones to increase the reflectivity of solar radiation from the soil to the rose crop. Vermiculite was used as the substrate because of its high drainage capacity and low fertility such that there are no incidences of water logging and the fertility levels could be easily adapted to suit the crop being grown. The rose plants were watered using a drip irrigation system with two lateral lines for each trough. During the daytime the paths were watered periodically to lower the greenhouse air temperature through evaporative cooling.

#### 4.1.1 Climate

Harare has a mean annual rainfall of 820 mm with the mean maximum and minimum monthly temperatures of 28 °C and 7 °C respectively.

# 4.2 Experimental Design

For parts 2 and 3 of the study, two automatic weather stations (AWS) were set up at Floraline Private Limited to take measurements of weather parameters inside and outside the greenhouse. The sensors for the measurement of the weather variables were connected to Delta-T<sup>1</sup> DL2e loggers. The two Delta-T data loggers were programmed to take measurements at 5-second intervals, which were then averaged over 30 minutes. A laptop computer was used to download data at regular intervals.

The outside AWS was set up in an open place a distance of more than 20 m from any obstructions to the sensors (see Figure 4.1). The following weather parameters were measured: air temperature and relative humidity at 1.2 m above ground, global solar radiation, photosynthetically active radiation (PAR), wind direction, wind speed and soil temperature at two depths (5 cm and 20 cm).

As it was impossible to locate the weather station at the centre of the greenhouse because of the presence of a concrete path, all inside weather data were measured about 17 m from the nearest wall of the greenhouse. The inside AWS measured the following climatic variables: air temperature and relative humidity at 1.2 m above ground, global solar radiation, PAR and

<sup>&</sup>lt;sup>1</sup> Manufactured by Delta-T Devices Ltd., 128 Low Road, Burwell, Cambridge CB5 OEJ, England

soil temperature (see Figure 4.2). The only physiological data collected was that of leaf temperature of the rose crop. Leaf temperature was measured on both the upper and lower leaf surface of a rose plant using radiation thermometers.

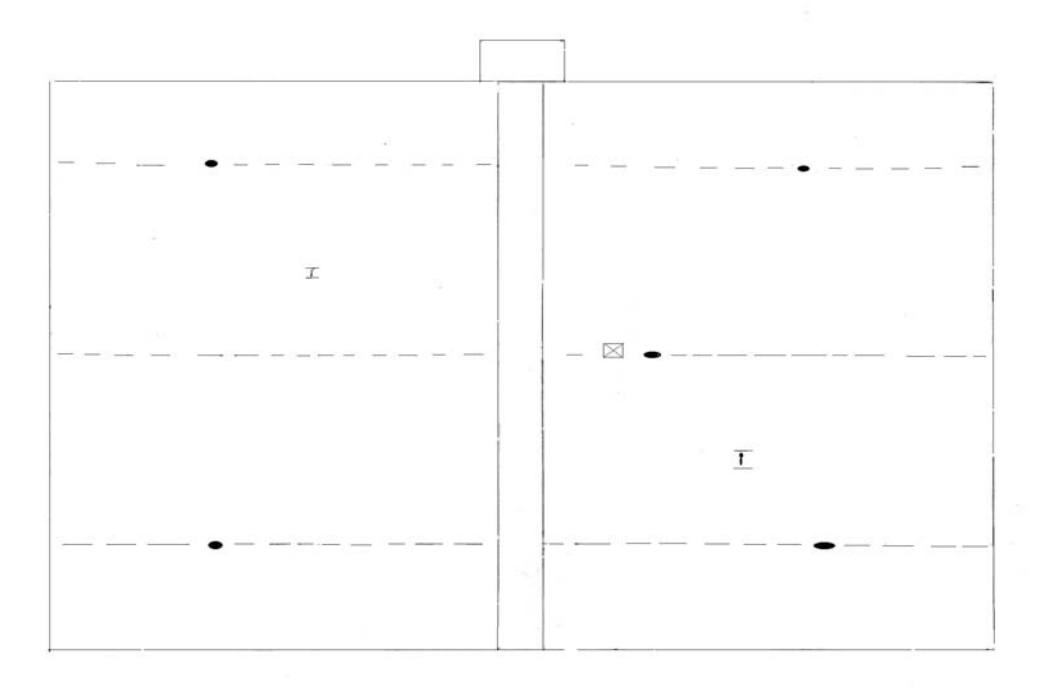


Fig 4.1: Outside Automatic Weather Station at Floraline Pvt. Ltd



Fig 4.2: Experimental setup inside a commercial greenhouse at Floraline Pvt. Ltd

The investigation of the homogeneity of the greenhouse air was done by taking measurements of air temperature and relative humidity carried out at four other places in the greenhouse besides the central sensor to determine the spatial variation (see Figure 4.3). The air temperature and humidity probes were then placed together on the central mast to enable comparison with the measurements when they were at the initial positions. This also served to check for instrument errors. The temperature and humidity sensors were mounted at heights of 1.2 m above ground on masts and connected to the inside AWS together with the central temperature and humidity sensor. A laptop computer was used to download data at regular intervals.



# Scale 1 cm represents 2m

Key
Station 1: Delta-T Type RHT2nl-02 (s/n 453)
Station 2: HMP45A (s/n U1010026)
Station 3: HMP45A (s/n Y0610052)
Station 4: YA100C (s/n 107902/1)
Station 5: CS500 (s/n T254005)

Automatic Weather Station

Fan
roof vents

Fig 4.3: Diagram of the placement of the temperature and relative humidity sensors within the greenhouse (6 November 2004)

#### 4.3 Field Measurements

#### 4.3.1 Radiation

A pair of LI-COR<sup>1</sup> quantum sensors of type LI-190SZ (serial numbers Q28884 and Q28885) was used for the measurement of photosynthetically active radiation (PAR) in the waveband 0.4 to 0.7  $\mu$ m inside and outside the greenhouse. The PAR received on a plane surface is measured using a silicon photodiode sensor.

The measurement of the total solar radiation was done using a pyranometer outside the greenhouse and a tube solarimeter inside. The LI-COR pyranometer used was a type LI-200SZ (serial number PY32951). The sensor uses a silicon photodiode for the measurement of solar radiation. The LI-COR pyranometer has to be mounted clear of all obstructions to either direct or diffuse radiation for higher accuracy. The tube solarimeter<sup>2</sup> was more applicable inside the greenhouse because of the non uniformity in the distribution of radiation within the structure. The sensor uses a copper-constantan thermopile and radiation is measured in the waveband 0.35 to  $2.5\mu m$ . The tube solarimeter used was reference number TSL 2917.

The quantum and pyranometer were mounted on platforms attached to the mast at height of 2 m. The tube solarimeter was mounted above the crop canopy along the crop row. It was placed in an N-S orientation.

# 4.3.2 Air temperature and relative humidity

The measurement of air temperature and relative humidity was done using four types of sensors: HMP45AC temperature and relative humidity probes<sup>3</sup> (serial numbers Y0610051, Y0610052 and U1010026), CS500<sup>4</sup> (serial number T2540005), YA100C (serial number 107902/1) and Delta-T Type RHT2nl-02 (453)<sup>5</sup> and Delta-T RHA1. Appendix B shows the periods in which the different temperature and humidity sensors were in use during the course of the data collection exercise.

<sup>&</sup>lt;sup>1</sup> Manufactured by LI-COR, inc., 4421 Superior Street, P.O. Box 4425 Licoln, NE 68504 USA

<sup>&</sup>lt;sup>2</sup> Manufactured by Delta-T Devices Ltd., 128 Low Road, Burwell, Cambridge CB5 OEJ, England

<sup>&</sup>lt;sup>3</sup> Manufactured by Campbell Scientific, inc. 815 West 1800 North, Logan, UT 84321-1784, USA

<sup>&</sup>lt;sup>4</sup> Manufactured by Campbell Scientific, inc. 815 West 1800 North, Logan, UT 84321-1784, USA

<sup>&</sup>lt;sup>5</sup> Manufactured by Delta-T Devices Ltd., 128 Low Road, Burwell, Cambridge CB5 OEJ, England

# a) HMP45AC temperature and relative humidity probes

The HMP45AC temperature and relative humidity probes contain a Platinum Resistance Temperature detector (PRT) and a Vaisala HUMICAP 180 capacitive relative humidity sensor. The temperature sensor has a measurement range of -40 °C to +60 °C with its accuracy at manufacture being greatest at 20 °C (0.2 °C) and lowest at 40 °C (0.4 °C). The relative humidity sensor has a measurement range of 0 to 100%. Its accuracy at manufacture and at 20% is 2% RH (0 to 90% Relative Humidity) and 3% RH (90 to 100% Relative Humidity).

# b) CS500 temperature and relative humidity probe

The model CS500 temperature and relative humidity probe uses a 1000  $\Omega$  PRT (type DIN 43760B) for temperature measurement and a Vaisala capacitive humidity sensor (INTERCAP) for the relative humidity measurement. The measurement range for temperature is -40 °C to +60 °C. The temperature sensor has an accuracy range of  $\pm 0.5$  at -40 °C and  $\pm 0.6$  at 60 °C whilst the relative humidity accuracy ranges from  $\pm 2.0$  % at 10% and  $\pm 3.0$  at 90%.

# c) RHT2nl temperature and relative humidity probe

The RHT2nl comprises a relative humidity and air temperature transducer housed in a solar radiation shield. The transducer requires power and gives two output signals for the relative humidity and air temperature. The relative humidity and air temperature sensors are contained in a plug-in module. The module can be replaced at routine maintenance intervals. The air temperature measurements by RHT2nl have an accuracy of  $\pm 0.1\,^{\circ}\text{C}$  with non-linear thermistor.

# d) RHA1 temperature and relative humidity probe

The RHA1 consists of both air temperature and relative humidity sensors housed in a screen. The relative humidity sensor consisting of cracked chromium oxide alters its capacitance in response to the changes in relative humidity. The air temperature is measured with a 2 kOhm hermetically sealed thermistor.

The temperature and humidity sensors were attached onto the inside and outside masts at a height of 1.2m from the ground. They were used with louvered radiation shields to protect them from direct radiation and allow air circulation.

# 4.3.3 Soil temperature

The soil temperature was measured with the use of Delta-T soil temperature probes, Type ST1. The sensor consists of a stainless steel clad thermistor probe with a 5m cable, which is immersed into the soil. The measurement range for the temperature is -20 to +80 °C with an accuracy  $\pm$  0.2 °C over 0 to 70 °C (Delta-T Devices User Manual, 1996).

The probes were immersed into the soil at two depths (5cm and 20cm) outside the greenhouse. The depth of the vermiculite mixture used inside the greenhouse restricted the placement of the soil temperature probe at the two depths (5cm and 20cm). The soil temperature probes were thus placed at estimated depths of 5cm and 15cm.

# 4.3.4 Leaf temperature

The temperature of the upper and lower leaf surfaces were measured using the infrared radiation thermocouples Type K. These were fixed on stands placed within the troughs such that the radiation window faced the leaf surface.

## 4.3.5 Air movement

The direction of the air flow outside the greenhouse was measured using a wind vane type W200P<sup>1</sup> serial number 7879 (with the arm serial number F20 879). A cup anemometer type A100L2, reference number 5526 was used to measure the wind speed. The air flow inside the greenhouse was measured for two weeks using an air velocity transducer<sup>2</sup> (serial number 03110481). The air transducer is a precision instrument designed to measure air velocity in fixed installations or test applications. The transducer indicates velocity at standard conditions of 21.1°C and 101.4 kPa.

These sensors were attached to the mast as shown in Figures 4.1 and 4.2.

 $<sup>^{\</sup>rm 1}$  Manufactured by Vector Instruments, 115 Marsh Road, RHYL Clwyd LL18 2AB

<sup>&</sup>lt;sup>2</sup> TSI Incorporated, 500 Cardigan Road, Soreview, MN 55126 U.S.A.

# 4.4 Equations Used in the Analysis

# 4.4.1 Vapour pressure

The vapour pressure was used in the comparison between the inside and outside greenhouse microclimate instead of the relative humidity. The relative humidity shows increased variation with air temperature compared to the vapour pressure. The vapour pressure e(kPa) was calculated using equation 4.4.1:

$$e = 0.006108 * RH * 10^{\left[\frac{7.5T_a}{237.5 + T_a}\right]}$$
(4.4.1)

where RH is the relative humidity (%) and  $T_a$  is the air temperature in  ${}^{\rm o}{\rm C}$ .

# 4.4.2 Cloudiness Factor

The cloudiness factor (CF) used in the outside climate data for the model was estimated using equation 4.4.2. The method involved plotting the total solar radiation  $S_{actual}$  measured outside the greenhouse for individual days. A curve was then drawn over all the other curves to get the maximum global solar radiation  $S_{\rm max}$ , referred to as the upper envelope for that period. The values of the minimum global solar radiation ( $S_{\rm min}$ ) were calculated as a  ${}^{1}\!\!/4$  of the  $S_{\rm max}$  values and joined together to form the lower curve (envelope). The values for  $S_{\rm max}$  and  $S_{\rm max}$  for the period 0600 to 1800 were then used in equation 4.4.1 to estimate the cloud cover for the individual days during the same period.

$$\frac{S_{\text{max}} - S_{\text{actual}}}{S_{\text{max}} - S_{\text{min}}} \times 100 \tag{4.4.2}$$

Appendix C summarizes the procedure described above. This method was thus only able to calculate cloud cover for 0600 to 1800 as well as on a weekly basis.

#### 4.5 Instrument Calibration

Instruments are always calibrated prior to field measurements. Calibration reduces instrument related measurement errors. This is particularly true in the case where different types of a sensor may be use whose specifications are manufacturer dependent. Calibration of sensors is carried out against an in-house standard and ensures firstly that the deviations from the standard are within the accuracy limits advertised by the manufacturers of the sensors and secondly that adjustments to the measurements can be effected where necessary (Mhizha, 2003).

# 4.5.1 Radiation pyranometers

The pyranometers were calibrated against a type CM11 Kipp & Zonen pyranometer<sup>1</sup> (serial number 997082), designated as the in-house standard. To test the other sensors against the standard, all the sensors were exposed on the roof of the Physics Department building and the mean output over consecutive 5 minute periods were recorded for several days by a data logger. The ratio of the outputs (in W m<sup>-2</sup>) of each sensor to the standard was then calculated. If the mean ratio (test/standard value) at the highest values of solar radiation (those in the interval two hours on either side of midday on days with less cloud cover) deviated from 1 by more than 5%, a new calibration constant (or multiplier) was determined as follows:

• The output of the test sensor in mV was plotted against the output recorded by the standard (in W m<sup>2</sup>). The gradient (or slope) of such a graph was taken as the calibration factor for the sensor. The calibration factors are shown in Table 4.5.1.

Table 4.1: Calibration factors for the radiation sensors

Radiation Sensor	Calibration equation
PY32951	y=75.85x-12.76
KZ986750 <sup>2</sup>	y=197.45x+2.16
TSL2916	y=77.59x-32.4
TSL2917	y=73.78x-35.51
TSL16208	y=39.90x-36.34

<sup>&</sup>lt;sup>1</sup> Manufactured by Kipp & Zonen B.V., P.O. 507, 2600AM, Delft, The Netherlands

<sup>&</sup>lt;sup>2</sup> Manufactured by Kipp & Zonen B.V., P.O. 507, 2600AM, Delft, The Netherlands

# 4.5.2 Quantum sensors

The pair of quantum sensors (serial numbers Q28884 and Q28885) was exposed on the roof of the Physics Department building and measurements were recorded on a data logger, again as 5-minute averages. The sensors were compared against each other by calculating ratios of the outputs in mol m<sup>-2</sup> s<sup>-1</sup>. A standard was not available for the calibrations and therefore the sensors were compared against each other to check that they gave the same output under similar conditions. The two sensors were found to be than less 0.1% different from each other and therefore their original calibration constants were not adjusted.

# 4.5.3 Temperature and relative humidity probes

The calibration of the temperature and relative humidity probes was done using a dew–point mirror measuring system. The dew–point mirror measuring system is considered a reliable method of measuring absolute humidity of a gas. The temperature and relative humidity probes were immersed in the flow chamber of the system and connected to a data logger for the recording of the outputs. YA100C and CS500 were connected to a CR23X data logger, (z13) whilst the probes HMP45AC s/n Y0610051, HMP45AC s/n Y0610052, HMP45AC s/n U101026 andRHT2nl-02 s/n 453 and the output from the dew-point mirror system were connected to a Delta-T datalogger. Varying the dew point and that of the constant waterbath temperatures between 5°C and ambient temperature (25°C) then controlled the temperature and relative humidity of the flow chamber.

The regressions of the outputs of the tested sensor against the dew-point system were plotted. The regression plots were used to obtain the calibration factors for the sensors with a zero intercept. These are given in Table 4.5.2.

**Table 4.2:** Calibration factors for temperature and humidity probes

Tubic iver cumpitation and included the manually proper		
Sensor	Serial Number	Calibration equation
HMP45AC	U1010026	$T_c = -40 + mV/10.365$
		RH = 0 + mV/9.793
HMP45AC	Y0610051	$T_c = -40 + mV/10.110$
		RH = 0 + mV/9.801
HMP45AC	Y0610052	$T_c = -40 + mV/10.271$
		RH = 0 + mV/9.797
YA100C	107902/1	$T_c = 0 + mV/9.880$
		RH = 0 + mV/9.887
CS500	T2540005	$T_c = -40 + mV/10.366$
		RH = 0 + mV/9.695
RHT2nl	453	RH = 0 + mV/9.158

#### 4.6 Model Calibration

The calibration of the GDGCM model involved adjustment of some of the model parameters in the deck and character files and ensuring that it could still work after these changes. The original GGDCM was developed for a glasshouse tomato crop in Netherlands and therefore it had to be adapted for a greenhouse rose crop in Zimbabwe. Zimbabwe, in the southern hemisphere, experiences a subtropical climate in comparison to the temperate climate of Netherlands. The calibration will be explained with respect to the FORTRAN subroutine s(Types).

The dimensions of the greenhouse used in the study are shown in Table 4.6.1. These were included in the CHARACT.DAT file while was read by Type 60.

Table 4.3: Characteristics of the commercial greenhouse used at Floraline Pvt Ltd

Greenhouse characteristic	value
Latitude	17.8 °S
Length	44.0 m
Width	28.5 m
Number of spans	3
Height of eaves (gutters)	4.0 m
Height of ridge	7.5 m

# 4.6.1 Type 9 Card reader for the outside climate data

Type 9 was adjusted to read five weather parameters: global radiation, cloudiness factor, temperature, wind speed and relative humidity. The diffuse solar radiation was not measured

in the study. The global radiation, temperature, relative humidity and wind speed were measured by the respective sensors connected to the external AWS described in §4.3 above. The cloudiness factor was estimated using the equation 4.4.1 (refer to §4.4).

# 4.6.2 Type 14 Forcing functions for LAI ( leaf area index) , $p_v$ (cultivated fraction of the greenhouse floor) and $m_v$ (vegetation mass density)

**Table 4.4:** Forcing functions for LAI,  $p_v$  and  $m_v$ 

Forcing Function	Original value	Adapted Value
LAI	1.7	3 (estimate)
$p_{v}$	0.153	0.23 (calculated)
$m_{\rm v}$	0.571	0.571 (unchanged)

The roses were at different growth stages of development in the greenhouse and an average LAI of 3 was used.

# 4.6.3 Type 16 Radiation data

In Type 16, the radiation mode 5 was used because the global radiation measurements were the only radiation data available. The distribution over direct and diffuse radiation was simulated by means of the correlation proposed by Reindl *et a.l.* (1990).

# 4.6.4 Type 64 Vegetation

The sine function was used for the determination of the stomatal resistance. The  $R_{stmax}$  (maximum stomatal resistance) and  $DR_{st}$  (difference between maximum and minimum stomatal resistance) values used in the study were based on measurements carried out to verify previous work done by Mashonjowa (2001) and Mhizha (2003) with a rose crop. For the study only the daytime stomatal resistance measurements in the rose crop were carried out and an average value of 74 s m<sup>-1</sup> was obtained.

# 4.6.5 Type 73 Heating system

The greenhouse used for the study was not heated thus the heating system was removed from the present version of the model.

# 4.7 Model Runs

The model was run using two data sets 3 to 11 November 2004 and 25 November to 01 December 2004. The first data set was used for the calibration after adjustment of the stomatal resistance values (2000 s m<sup>-1</sup> (maximum) and 200 s m<sup>-1</sup> (minimum) to 1800 s m<sup>-1</sup> and 200 s m<sup>-1</sup> respectively (refer to Appendix D). The evaluation of the model was done using the data set (25 November to 01 December 2004).

# 4.8 Data Analysis

The data collected in the study was analyzed using the Excel Data Analysis ToolPak.

# **CHAPTER 5**

#### **RESULTS**

# **5.1 Transmission Coefficients**

The transmission of the greenhouse cover to total solar radiation and photosynthetically active radiation (PAR) was determined to enable adjustment to the transmission coefficients in the block containing the greenhouse construction characteristics. The transmission of the greenhouse cover determines the amount of PAR and total solar radiation received within the greenhouse structure and therefore influences the photosynthetic process as well as the heat balances of the greenhouse layers respectively.

The transmission coefficients were calculated as means of half-hourly ratios for the period 0800 to 1600 local time. The ratios were of the inside total solar radiation or PAR to that measured outside the greenhouse for each half hour. The classification of the days into clear, partly cloudy and cloudy was based on the estimated cloud cover, which was derived using equation 4.4.1 (refer to §4.4). Table 5.1 shows transmission coefficients for clear days (DOY 308 and 334-3 and 29 November 2004), partly cloudy days (DOY 309, 311 and 337 – 4 and 6 November 2004 and 2 December 2004) and cloudy days (DOY 331, 332, 333, 338, 340 and 341 (26 to 28 November 2004 and 3, 5 and 6 December 2004) observed during the data collection exercise in November 2004. These days were numbered using the Julian calendar, where the first day of the year corresponds to Day Of Year (DOY) 1 and the last day of the year to DOY 365 for an ordinary year and DOY 366 for a leap year. This is shown in Appendix A.

Table 5.1: The daily average transmission coefficients of a greenhouse at Floraline Pvt Ltd calculated from PAR and total solar radiation measurements in November 2004. Error ranges are calculated as standard deviations of the daily total averages from 0800 to 1600 local time

		Transmission coefficients (%)	
Day	Condition	PAR	Total solar
308	Clear	$71.1 \pm 6.9$	70.4 ± 8.4
309	Partly cloudy	$71.4 \pm 9.0$	$70.3 \pm 8.3$
311	Partly cloudy	$69.3 \pm 7.2$	$68.2 \pm 8.6$
331	Cloudy	$71.9 \pm 5.3$	$69.1 \pm 7.0$
332	Cloudy	$74.9 \pm 6.4$	$67.4 \pm 8.5$
333	Cloudy	$70.9 \pm 6.4$	$67.2 \pm 7.2$
334	Clear	$73.5 \pm 6.8$	$71.7 \pm 7.0$
337	Partly cloudy	$73.0 \pm 5.9$	$66.1 \pm 7.6$
338	Cloudy	$74.2 \pm 4.2$	$64.9 \pm 5.1$
340	Cloudy	$72.5 \pm 2.0$	$61.6 \pm 4.3$
341	Cloudy	$74.5 \pm 3.4$	$60.7 \pm 8.3$

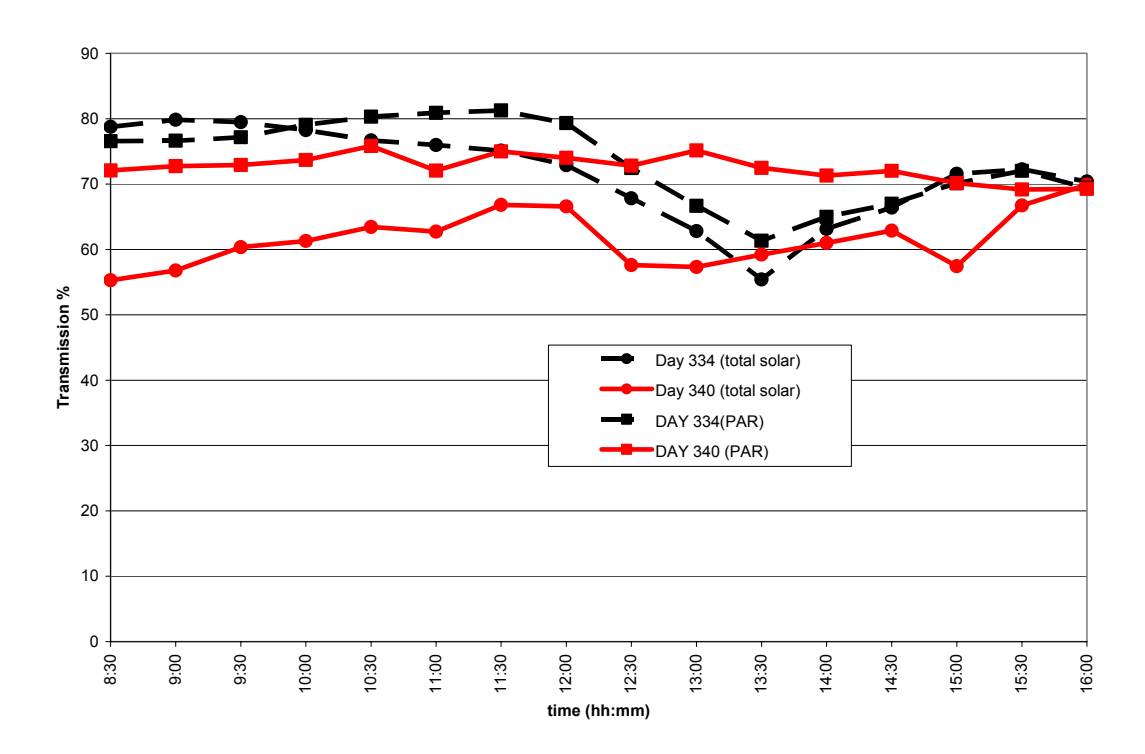


Fig 5.1: Diurnal variation in total solar radiation and PAR transmittance on a clear day (DOY 334) and cloudy day (DOY 340)

The transmission of the PAR does not show much variation under the different cloud conditions (clear, partly cloudy and cloudy) compared to that for total solar radiation.

Differences of 5.6% and 11% were obtained between the minimum and maximum values of the PAR and total solar radiation respectively (refer to Table 5.1). According to Figure 5.1, the transmission of a greenhouse structure is dependent on solar elevation, which affects the angle of incidence. Generally the transmission of the greenhouse cover should increase with an increase in solar elevation and vice versa. At high solar elevation (a low angle of incidence) the transmission increases because of the lower reflectance and absorptance properties of the cover whilst the reverse is observed with low solar elevation (increased angle of incidence). The clear day produced greater variation in the transmission of the greenhouse structure to both PAR and total solar radiation compared to the cloudy day. The former has a higher dependence to the angle of incidence because direct solar radiation is the dominant radiation component unlike under cloudy conditions, which have a higher fraction of diffuse solar radiation. The radiative properties (reflection and transmission) of the diffuse solar radiation are constant for the different angles of incidences thereby resulting in little variation in the transmittances (Mashonjowa, 2001; Pieter, 2002). However there were periods during the daytime where abrupt drops in transmission were observed (at 1330 - refer to Figures 5.1). This was a result of the shadows from the construction parts.

#### **5.2** Greenhouse Microclimate Measurements

# 5.2.1 Temperature and vapour pressure variations within the greenhouse

The homogeneity of the greenhouse air was assessed using data from 6 November 2004 (DOY 311). This was done when the five temperature and humidity sensors were placed at different positions within the greenhouse (refer to §4.3).

# 5.2.1 a) Temperature Variations

Figure 5.2 show the spatial temperature variations within the greenhouse using DOY 311 (6 November 2004) whilst Figure 5.3 shows the regression analysis of the spatial temperature variations within the greenhouse for the same day.

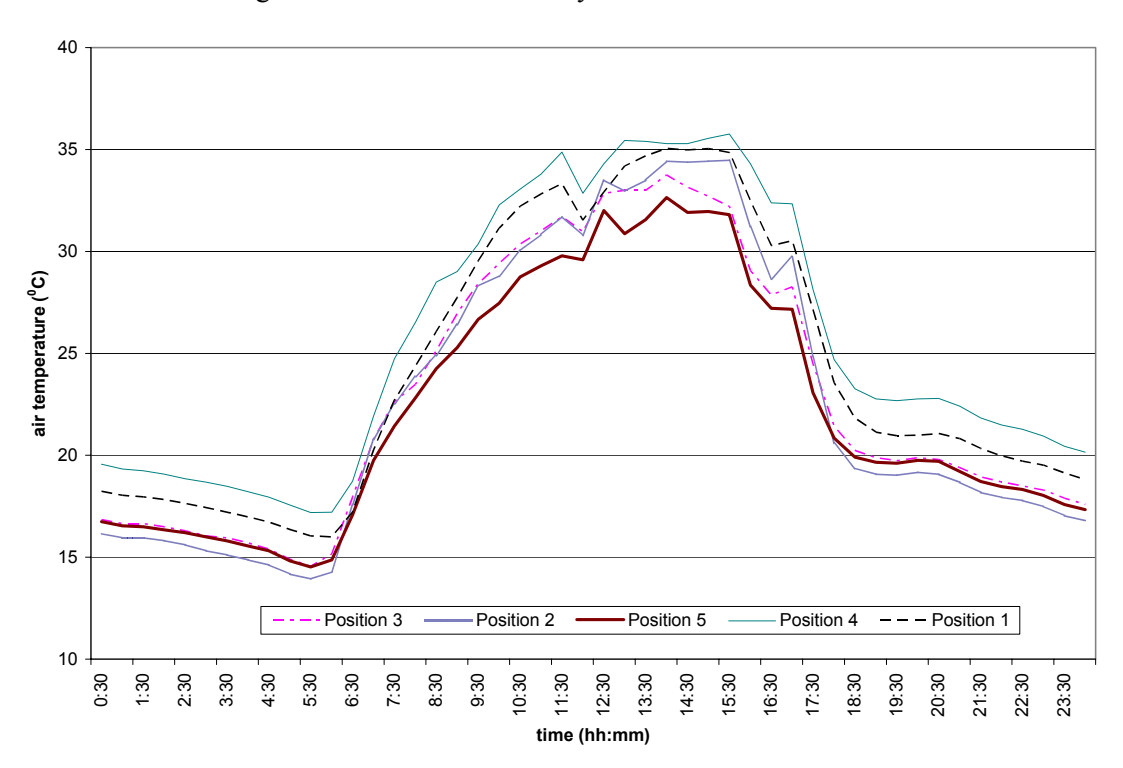


Fig 5.2: Spatial temperature variations inside the greenhouse on DOY 311 (6 November 2004) where Positions 1, 2, 4 and 5 were being compared with Position 3 (the central sensor)

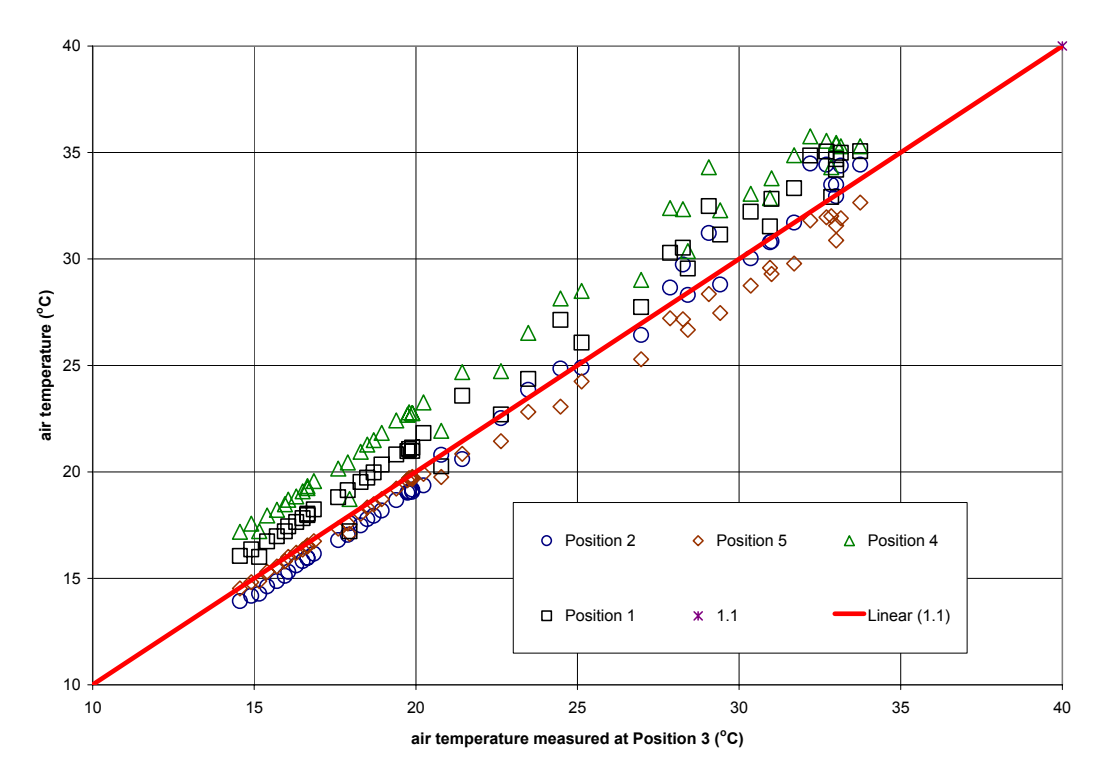


Fig 5.3: Regression analysis of the spatial temperature variations inside the greenhouse on DOY 311 (6 November 2004) where Positions 1, 2, 4 and 5 were being compared with Position 3 (the central sensor)

Figures 5.2 and 5.3 both show that there were spatial temperature variations within the greenhouse. The sensors (Positions 1 and 4) placed further from the central sensor (Position 3) recorded higher temperature differences from the latter compared to those that were near (Positions 2 and 5). The sensor on Position 5 was observed to deviate more from the central sensor (Position 3) with increase in air temperature. Average temperature differences of Positions 1, 2, 4 and 5 from Position 3 were 1.4 °C, 0.2 °C, 2.7 °C and 0.7 °C respectively. Positions 5 and 2 were generally cooler at nighttime and daytime respectively compared to the other positions whilst Position 4 had the highest temperatures throughout the day.

A comparison of the daytime and nighttime deviations from the Position 3 was also carried out. It was found that the sensors at Positions 1, 2, 4 and 5 deviated more from the central sensor (Position 3) during the daytime compared to the nighttime. The greater daytime differences from the reference sensor may have been as a result of the radiation input. There was increased warming of the air during the daytime as a result as of the increased available energy, thereby increasing these differences. Statistically the sensors on Positions 1, 2 and 4 were significantly different from the central sensor (Position 3).

# 5.2.1 b) Vapour Pressure Variations

The spatial vapour pressure variations within the commercial greenhouse at Floraline Pvt Ltd using DOY 311 are shown in Figure 5.4. Figure 5.5 shows the regression analysis of the spatial vapour pressure variations within the commercial greenhouse at Floraline Pvt Ltd using DOY 311.

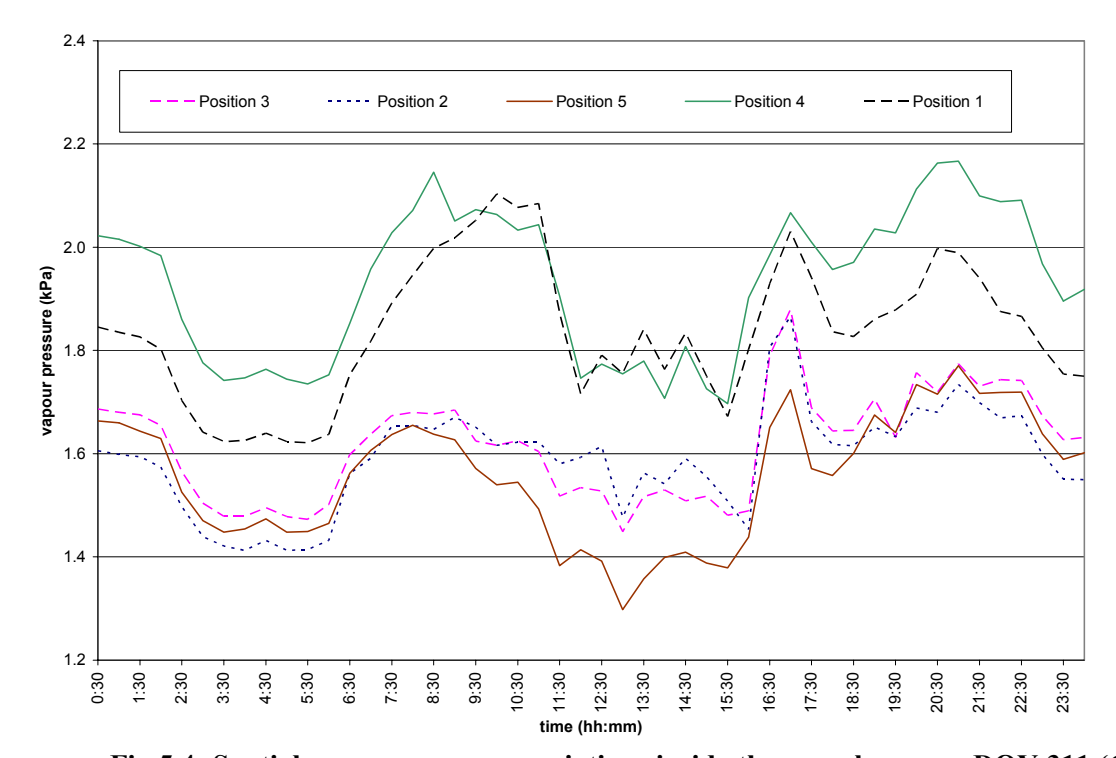


Fig 5.4: Spatial vapour pressure variations inside the greenhouse on DOY 311 (6 November 2004) where Positions 1, 2, 4 and 5 were being compared with Position 3 (the central sensor)

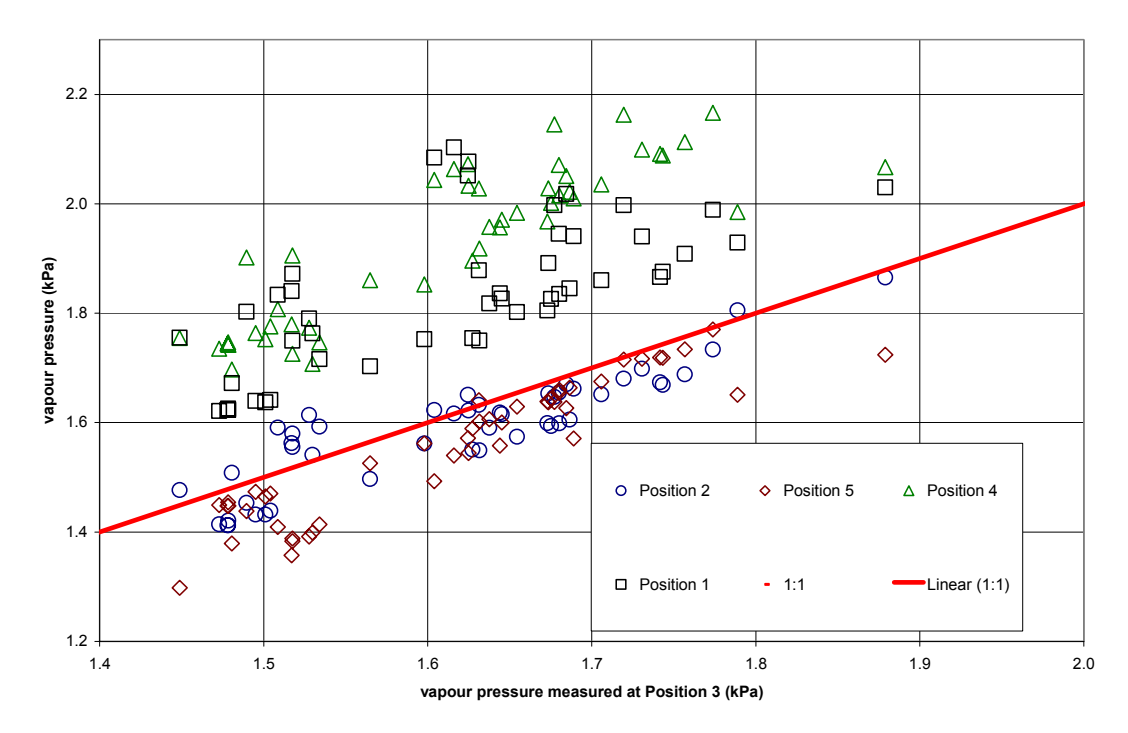


Fig 5.5: Regression analysis of spatial vapour pressure variations inside the greenhouse on DOY 311 (6 November 2004) where Positions 1, 2, 4 and 5 were being compared with Position 3 (the central sensor)

Figures 5.4 and 5.5 both show that there were also spatial vapour pressure differences within the greenhouse. Again sensors on Positions 4 and 1 had the greatest differences from the central sensor (Position 3). Average vapour pressure differences of 0.22 kPa, 0.03 kPa, 0.32 kPa and 0.06 kPa from Position 3 were obtained on Positions 1, 2, 4 and 5 respectively. The sensors on Positions 2 and 5 were observed to have recorded lower vapour pressures whilst those on Positions 1 and 4 had higher vapour pressures compared to the central sensor (Position 3).

Similarly to the temperature, the sensors deviated more from the reference sensor during the daytime hours compared to nighttime.

The air temperature and vapour pressure variations within the greenhouse obtained on day 311 could not be properly verified using measurements from Day 39 (8 February 2005). This was mainly due to only three of the sensors which had been used on Day 311 still being operational on the latter day (Day 39). The operational sensors were for Positions 3 (central sensor), 4 and 5 (refer to Appendix B).

However it was concluded that the greenhouse air was not homogeneous because of the spatial variations of air temperature and vapour pressure within the greenhouse. These differences could have arisen due to differential warming of the air within the greenhouse. According to Boulard *et al.*, 1999 temperature and vapour pressure variations should occur within the greenhouse particularly in the presence of a mature crop. The latter will affect the general airflow thereby creating air pockets, which have different air temperature and vapour pressure. Secondly the transpiration process contributes to the heat and mass balances of the greenhouse air, which strongly influence the air temperature and vapour pressure of the latter.

The temperature and relative humidity measurements for the sensors used in the greenhouse were therefore averaged to obtain a representative of the greenhouse air. These values were then used in the comparison of the greenhouse microclimate with the outside measurements as well as the model calibration and validation.

# 5.2.2 Comparison of the greenhouse microclimate with the outside measurements

A comparative analysis between the measured greenhouse microclimate variables and those outside was done for the quantification of the relationship between the greenhouse and external environment. The comparison was based on the measured microclimate variables, which included air temperature, relative humidity, PAR and total solar radiation. The calculated vapour pressure was used in the comparative analysis instead of the relative humidity because of the increased variation of the relative humidity with the air temperature.

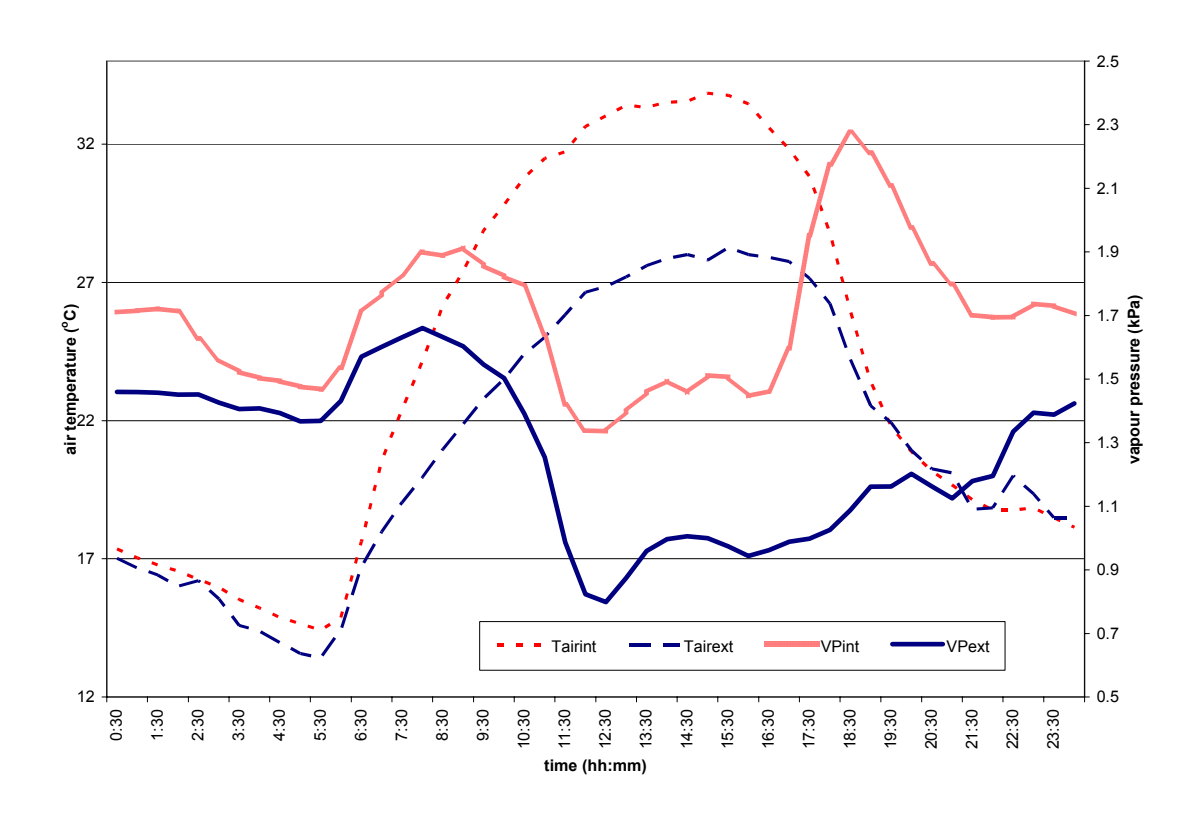


Fig 5.6: Comparison of the temperature and vapour pressure inside and outside the greenhouse at Floraline Pvt Ltd on a clear day (DOY 334 - 29 November 2004)

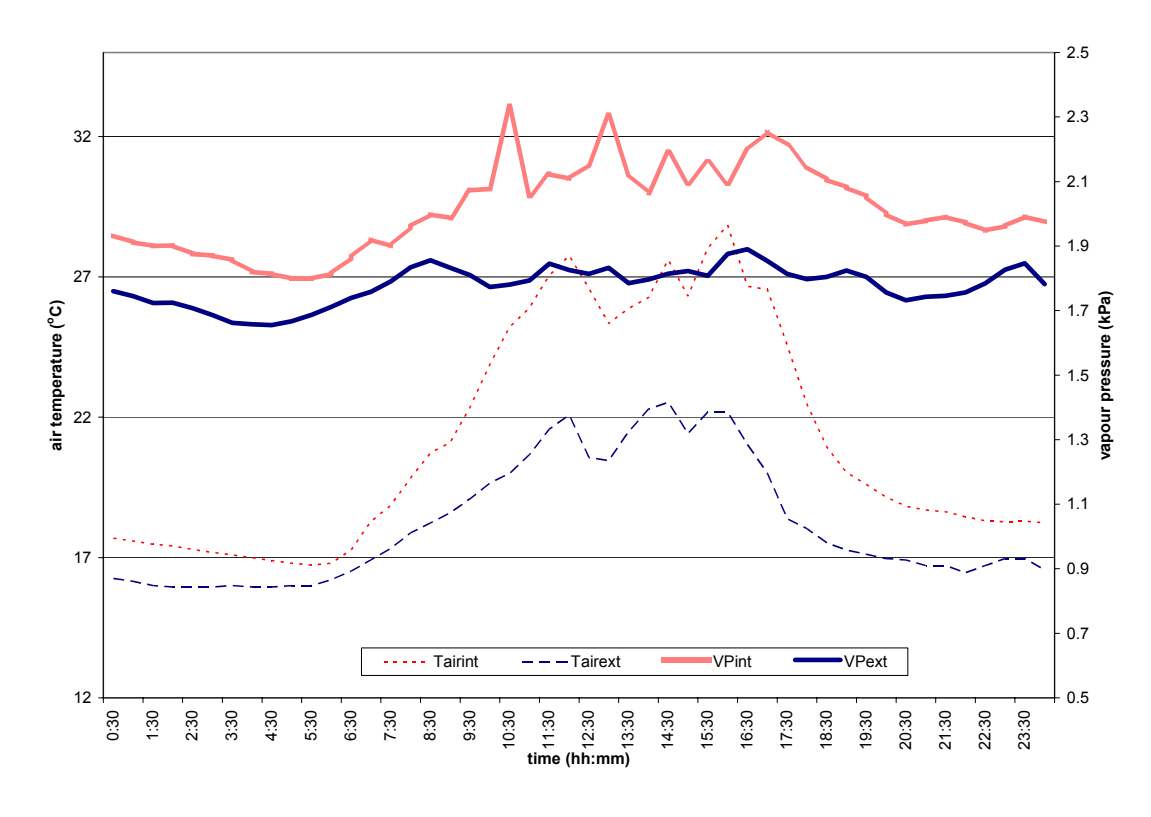


Fig 5.7: Comparison of the temperature and vapour pressure inside and outside the greenhouse at Floraline Pvt Ltd on a cloudy day (DOY 340 - 5 December 2004)

Figures 5.6 and 5.7 both show that the temperature inside the greenhouse was generally higher than that outside for both days. The greenhouse was warmer than outside probably because of its opaqueness to longwave (infrared) radiation and the reduced turbulence within the greenhouse structure, which did not quickly dissipate the heat, as was the case outside the greenhouse. These factors increased the available energy for warming up the greenhouse air. This also led to the inside air temperature reaching its maximum value before the outside on the clear day (refer to Figure 5.6).

The maximum air temperatures for the inside and outside of the greenhouse were 33.8 °C and 28.3 °C respectively on DOY 334 (a clear day) and 28.8 °C and 22.5 °C respectively on DOY 340 (a cloudy day). The clear day had a higher direct solar radiation input, which increased the available energy for heating its air resulting in higher temperatures being recorded. This also caused a higher temperature range being obtained for the clear day in comparison to the cloudy day. On DOY 334 the greenhouse air was slightly lower (<2 °C) than outside during the nighttime because of losses through radiation. The greenhouse cover was cooler than the greenhouse air because of increased longwave radiation loss under a clear sky therefore heat is then radiated from the warmer greenhouse air to the cover and subsequently to the outside air. The "greenhouse effect" on the cloudy day resulted in the inside temperatures being maintained above those of the outside because of the reduced thermal radiation losses from the greenhouse cover to the outside air.

High vapour pressure was recorded inside the greenhouse for both days except for the periods 0330 to 0430 (DOY 334) and 0500 to 0900 (DOY 340). The higher inside vapour pressure was due to both the higher air temperatures and humidity within the greenhouse. The maximum vapour pressure was 2.3 kPa (inside) and 1.7 kPa (outside) for the clear day with 2.3 kPa (inside) and 1.9 kPa (outside) for the cloudy day. The respective minima were 1.3 kPa and 0.8 kPa for the clear day and 1.8 kPa for both inside and outside on the cloudy day. Maximum vapour pressure differences of 1.0 kPa and 0.4 kPa between the inside and outside were recorded for DOY 344 (at 1800 hours) and DOY 340 (at 1030 hours) respectively. The two days did not show any variation in the maximum vapour pressures inside the greenhouse. The inside minimum vapour pressure differed by 28% for the two days.

The vapour pressures both inside and outside the greenhouse declined steeply from 0800 until midday on the clear day whilst the inside vapour pressure was then observed to rise sharply from 1700 to 1830 where it reached its highest value of the day (2.3 kPa) after which it then

declined steeply until 2030. There was a gradual increase in the vapour pressure outside the greenhouse 2100 to 0230 (clear day) and 1900 to 2100 (cloudy day). Generally there was little variation in the vapour pressure outside the greenhouse on a cloudy day whilst the internal vapour showed continuous fluctuations between 1030 and 1700.

The sharp decline in the daytime vapour pressure could have been as a result of increased convection (from the fans and open vents), which brought in a dry air mass thereby lowering its moisture content. The sharp rise in the vapour pressure inside the greenhouse observed in the late afternoon was as a result of management operations (irrigation). This was supported by the fact that a similar pattern was also observed on other days during the same period (1630 to 1830).

# 5.2.2 Vapour Pressure Deficit

A comparison of the vapour pressure deficit between the inside and outside of the greenhouse is shown in Figure 5.8 for DOY 334 (a clear day) and DOY 340 (a cloudy day).

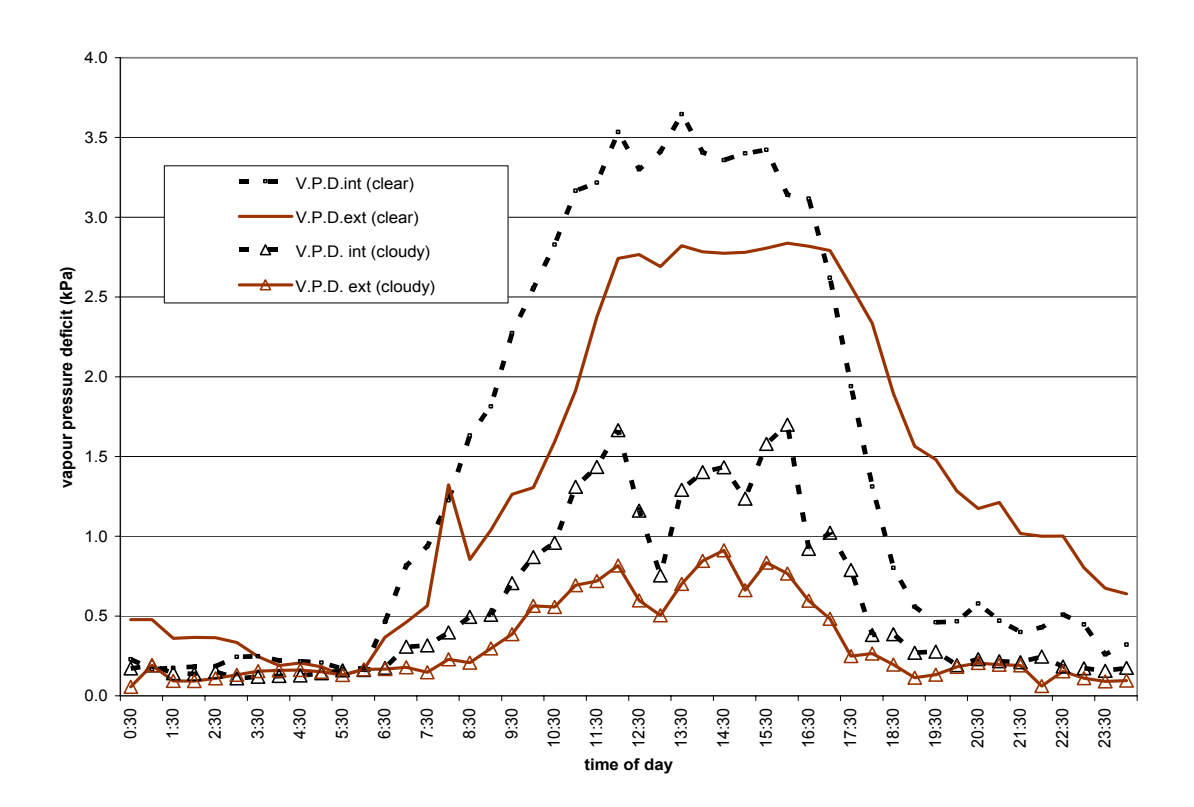


Fig 5.8: Comparison of the vapour pressure deficit inside and outside the greenhouse on a clear day (DOY 334-29 November 2004) and a cloudy day (DOY 340-5 December 2004)

Figure 5.8 shows that the daytime vapour pressure deficit (VPD) was greater inside the greenhouse compared to the outside for both days. The clear day also recorded the highest VPD both inside and outside. The period 1700 to 0330 had a greater VPD outside than inside for the clear day whilst no consistent pattern was observed during the same period for the cloudy day. A comparison of the respective inside and outside VPD between the two days produced differences greater that 100% (112% and 211%).

According to Monteith and Unsworth (1990) the saturation vapour pressure varies exponentially with the air temperature. Hence the warmer air will have a higher saturation vapour pressure thereby increasing its evaporative power (VPD) as shown in Figure 5.8. The high transpiration rates inside the greenhouse are thus attributed to the high evaporative power of the air (VPD). The higher VPD recorded during the nighttime outside the greenhouse on the clear day was due to the lower temperatures inside the greenhouse compared to the outside because of increased long wave radiation exchange between the greenhouse air and cooler cover.

# 5.2.4 Leaf temperatures

Figures 5.9 and 5.10 show a comparison of the upper and lower leaf surface temperatures for DOY 334 (a clear day) and DOY 340 (a cloudy day) respectively.

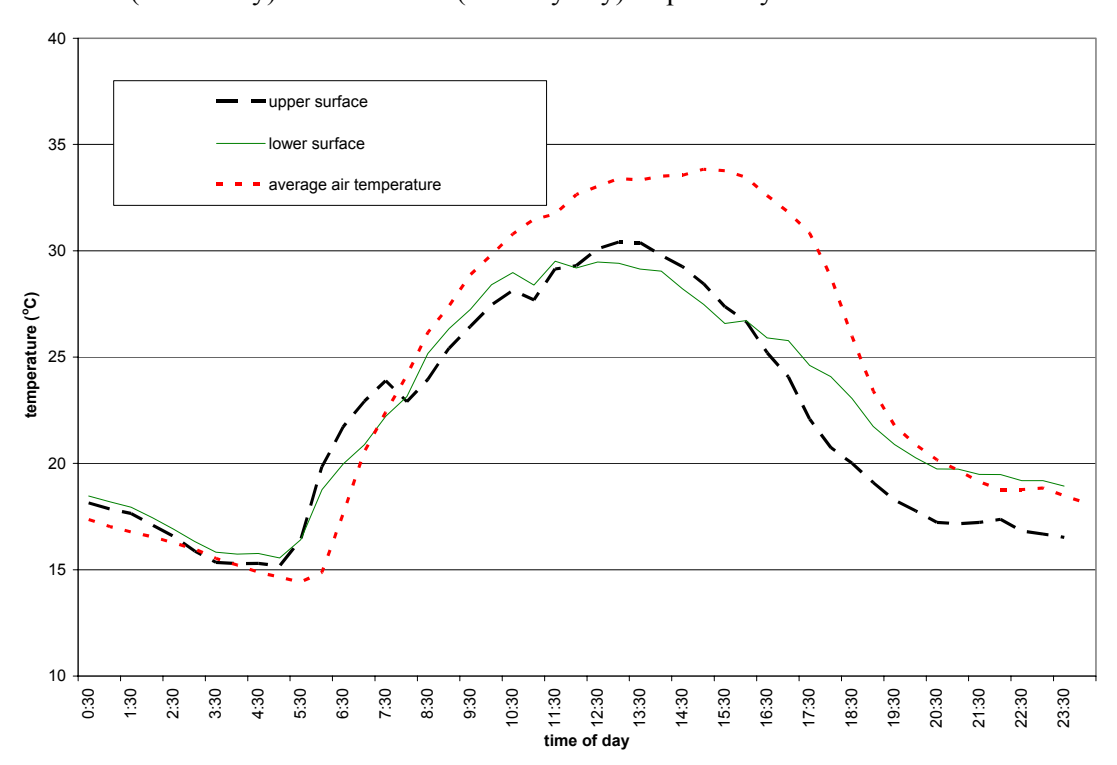


Fig 5.9: Comparison of the temperature between the upper and lower leaf surfaces in a greenhouse on DOY 334 (29 November 2004)

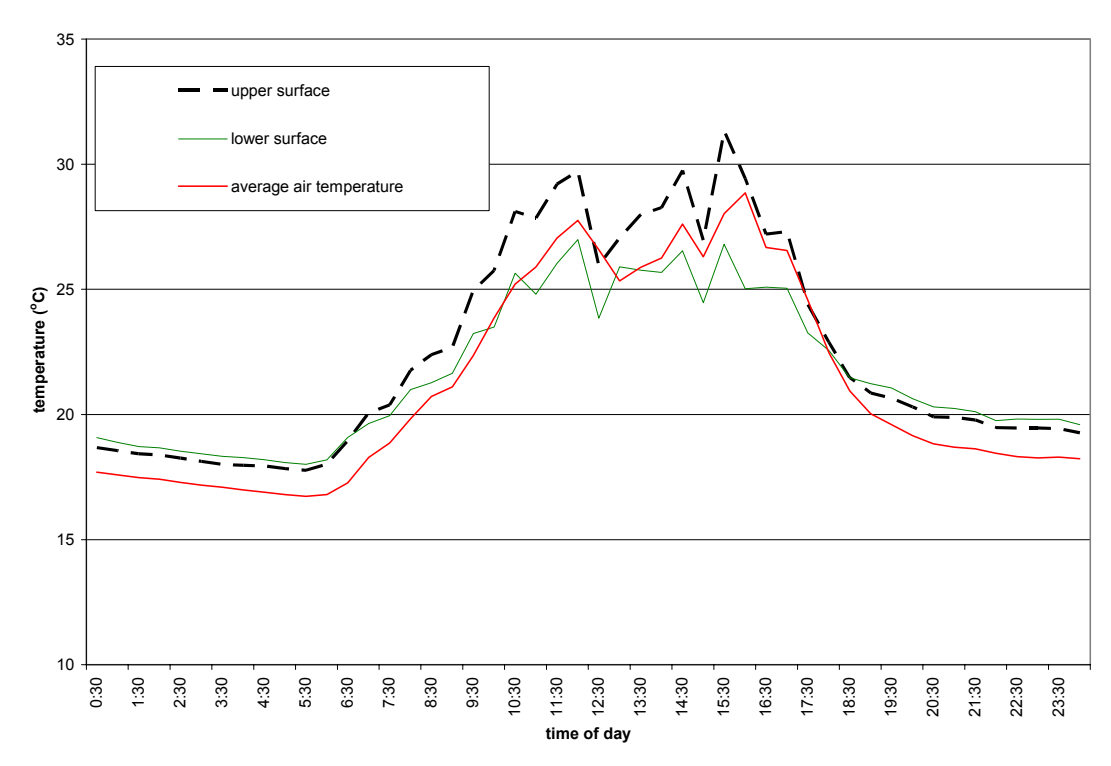


Fig 5.10: Comparison of the temperature between the upper and lower leaf surfaces in a greenhouse on DOY 340 (5 December 2004)

On both days the upper leaf surfaces were warmer than the lower surfaces. The maximum temperatures for the upper leaf surface were 31.3 °C (DOY 340) and 30.4 °C (DOY 334) whilst these were 29.5 °C (DOY 334) and 27 °C (DOY 340) for the lower leaf surface. Temperature differences of greater than 1 °C for DOY 340 were obtained during the daytime (0830 to 1730) whilst the nighttime had minimal differences of less than -0.4 °C. The maximum temperature difference between the two leaf surfaces for the cloudy day was 4.5 °C (at 1530). Unlike DOY 340, the upper leaf surface for DOY 334 did not have a consistently higher temperature than the lower surface for the daytime period. It was cooler than the lower leaf surface between 0830 and 1200 (the differences were less than -1.2 °C) whilst from 1230 to 1600, it became warmer than the lower leaf surface (with differences of less than 1.3 °C) and between 1630 and 2400, its temperature fell below than of the lower leaf surface again (differences being between -2 °C and -3.4 °C).

Generally the upper leaf surface should be warmer than the lower surface because of its exposure to radiation compared to the shaded leaf surfaces. Therefore the upper surface of the leaf should be warmer than the lower surface since the latter does not receive much radiation. However it was observed that the differences between the two surfaces during the daytime tend to be greater on the cloudy day (DOY 340) than the clear day (DOY 334). On DOY 334,

the drop in the temperature of the upper surface during 0830 to 1200 could have been a result of spraying as this was usually done early in the morning. The high nighttime differences on the same day could have been as a result of the positioning of the sensor such that it was also recording temperatures of other objects in its view instead of that for leaf surface only. The day to day operations often left the sensor not properly positioned to measure the leaf surface temperatures. The higher lower surface temperatures during the nighttime may have been a result of increased longwave radiative losses from the upper leaf surface compared to the lower leaf surface. The lower leaf surfaces could also have been warmed by the thermal radiation emitted by the ground thus maintaining its temperatures above those of the upper leaf surfaces. These results are in agreement with Kostyuk *et al.*, 1990 who found temperature differentials of between 5 °C and 9 °C for a greenhouse tomato crop.

According to Stanghellini (1983) temperature differences should occur within the crop canopy because of its heterogeneous nature (differences in leaf size, age, orientation) but since these variations are usually minimal averaging them off does not create huge errors. However other authors have observed that flowers with their closed canopy such as roses should have larger vertical temperature gradients in comparison to other greenhouse crops. In the following section, the leaf temperatures were averaged as it was assumed the temperature differences within the rose canopy were marginal.

#### 5.3 Model Results

The calibration and validation of the Gembloux Dynamic Greenhouse Climate Model was done using two data sets (3 to 9 November 2004 and 25 November to 1 December 2004). The calibration of the model enabled adjustments to the data file, the greenhouse characteristic file and the transpiration sub-model parameters whilst a different data set was then used to evaluate the model performance during the validation. For the study the calibration of the transpiration sub-model was done by finding the maximum and minimum stomatal resistance values that gave the best fit to the measured air temperature. The maximum and minimum stomatal resistance values that were used in the calibration were from previous work done on greenhouse roses as well as daytime measurements that had been carried out during the study. The regression analysis is shown in Appendix D and the stomatal resistance values that gave the best fit were 1800 s m<sup>-1</sup> (maximum) and 200 s m<sup>-1</sup> (minimum) respectively.

The days used to assess the model performance were mixed (clear, partly cloudy and cloudy).

# 5.3.1 Air temperature

Figure 5.11 shows the comparison of average air temperature with the simulated air temperature before and after the calibration of the transpiration sub-model of the GDGCM. Figure 5.12 shows the regression analysis of the simulated against the measured average air temperature inside the greenhouse for the calibration. In Appendix E, the differences between the air temperature inside and outside of the greenhouse are represented by

Tint (measured) - Text and Tint (sim) - Text for the measurements and simulation respectively.

# 5.3.1 a) Calibration

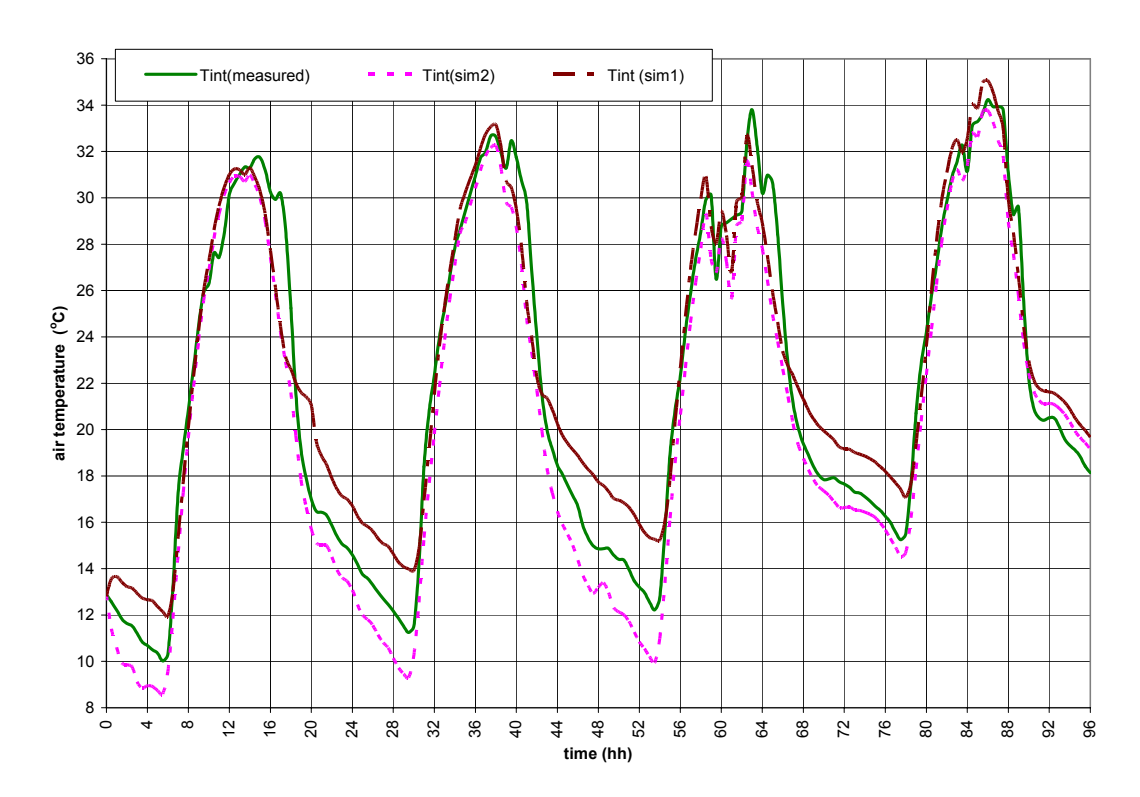


Fig 5.11: Comparison of the simulated and measured average air temperature inside the greenhouse on DOY 308 to DOY 311. Sim1 and Sim2 represent the simulations with the Gembloux Dynamic Greenhouse Climate Model before and after the calibration respectively.

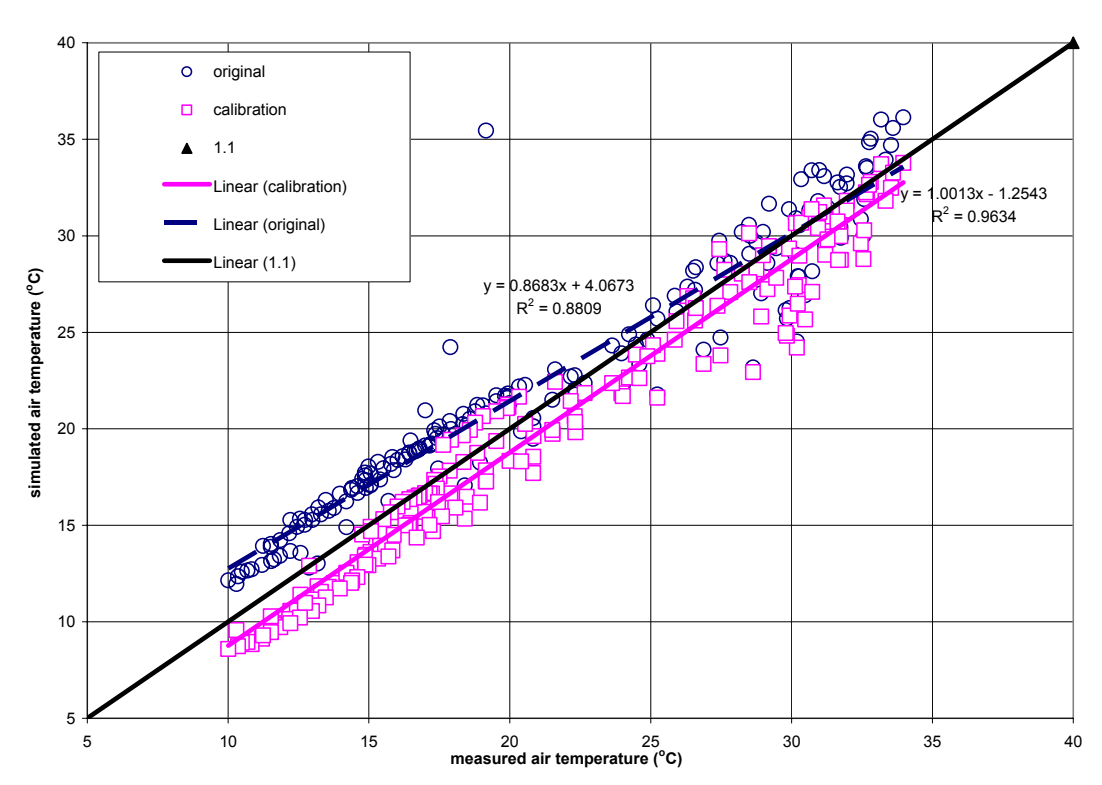


Fig 5.12: Regression analysis for the simulated and measured average air temperature inside the greenhouse on DOY 308 to DOY 311 before and after the calibration of the Gembloux Dynamic Greenhouse Climate Model.

Table 5.2: Root mean square errors (RMSE) of the simulation of the greenhouse air temperature using the Gembloux Dynamic Greenhouse Climate Model for DOY 308 to DOY 311

DOY		<b>RMSE</b>
	Daytime (°C)	Nighttime (°C)
308	1.999	0.293
309	1.319	0.236
310	1.637	0.728
311	0.982	0.761

A comparison of the simulation with the measured average air temperature produced maximum differences of -6  $^{\circ}$ C (DOY 308), -5  $^{\circ}$ C (DOY 309) , - 5.7 (DOY 310) and -3.8 (DOY 311). It was observed that after the calibration of the transpiration sub-model, the model underestimated the nighttime air temperature (1830 to 2400) compared to the original. During this period the calibration had simulated – measured air temperature differences less than -2  $^{\circ}$ C whereas prior to the calibration these differences were as high as -4  $^{\circ}$ C (DOY 309). The regression analysis shows that the calibration had a better correlation compared to the original model ( $r^2$ =0.96 and  $r^2$ =0.88 respectively). This was attributed to the fact that the model simulated the air temperature very well during the nighttime. At lower air

temperatures ( $<20\,^{\circ}$ C) the original model deviated more from the 1:1 line whilst showing less deviation at temperatures greater than 25  $^{\circ}$ C. The calibration line shows a consistent deviation from the 1:1 line for the temperature range 5  $^{\circ}$ C to 40  $^{\circ}$ C.

Based on Table 5.2, the model tended to deviate more from the actual measurements during the daytime (0630 to 1800) compared to the nightime (0030 to 0600 and 1830 to 2400). The percentage differences between the daytime and nighttime RMSE for the four days were 50% (DOY 308), 18% (DOY 309), 45% (DOY 310) and 78% (DOY 311) respectively. The daytime had greater temperature differences (2.0 °C) between the inside and outside as a result of the radiation input, which the model failed to pick up thereby increasing the simulation errors. This was contrary to the nighttime where there was little variation in these temperatures, enabling the model to predict with increased accuracy. Another factor that affected the model performance was the time lag between the increases in the simulated air temperature with that of the actual measurements particularly during the daytime resulting in increased simulation errors. This can be attributed to the different volumetric heat capacities of the simulated and actual greenhouse air such that the model has a delayed response to the temperature changes (Wang and Boulard, 2000). The volumetric heat capacity differences arise from those of pressure; the model had a standard pressure of 1013 hPa compared to 850hPa in Zimbabwe. The smaller nighttime differences obtained in the study were similar to the observations by Zhang et al., 1997 who concluded that the increased accuracy of the model during this period was due the absence of radiation and reduced ventilation, which made modelling easy because of the simple heat and mass balances. The highest daytime and nighttime errors were obtained on DOY 308 (2.0 °C) and DOY 311 (0.8 °C) respectively whilst DOY 311 and DOY 309 had the least daytime and nighttime errors respectively.

# 5.3.1 b) Validation

After the calibration of the GDGCM, a different data set (DOY 331 to DOY 335) was used to evaluate its performance. Figure 5.13 shows the comparison of the simulation with the measurements of the average air temperature within the greenhouse whilst Figure 5.14 shows the regression analysis. The differences between the air temperature inside and outside the greenhouse are given in Appendix E for both the measured and simulated.

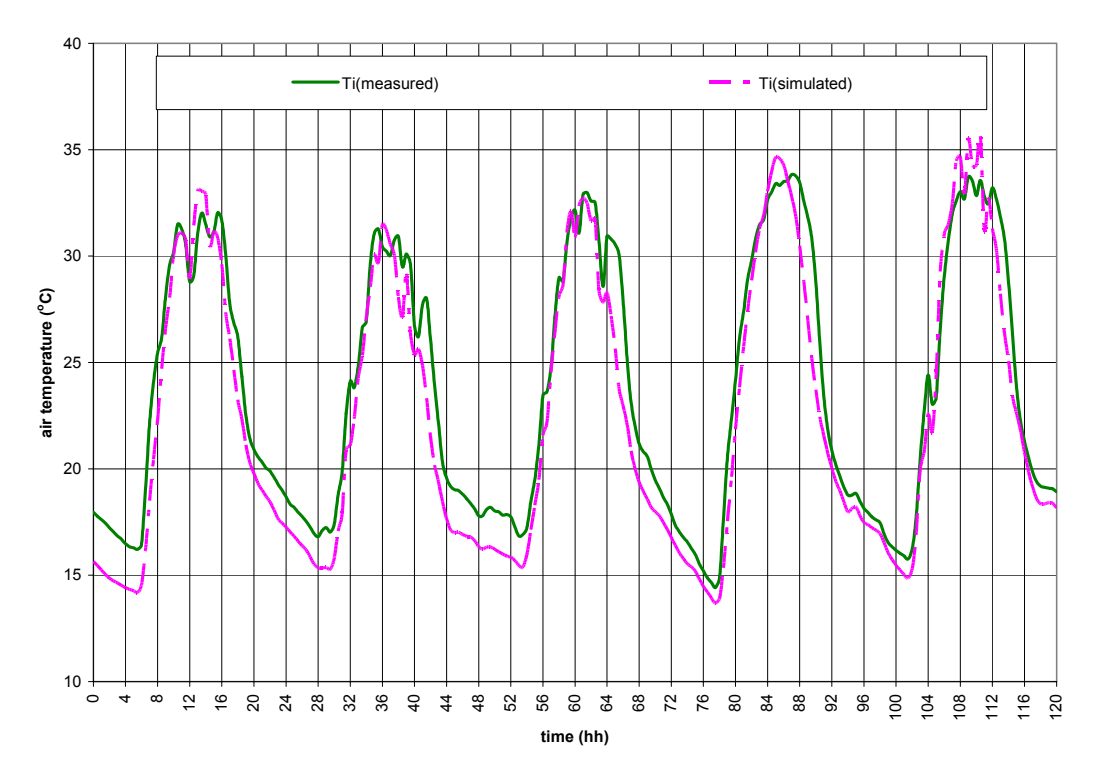


Fig 5.13: Comparison of the simulated and measured average air temperature inside the greenhouse on DOY 331 to DOY 335. The simulation was done with the Gembloux Dynamic Greenhouse Climate Model.

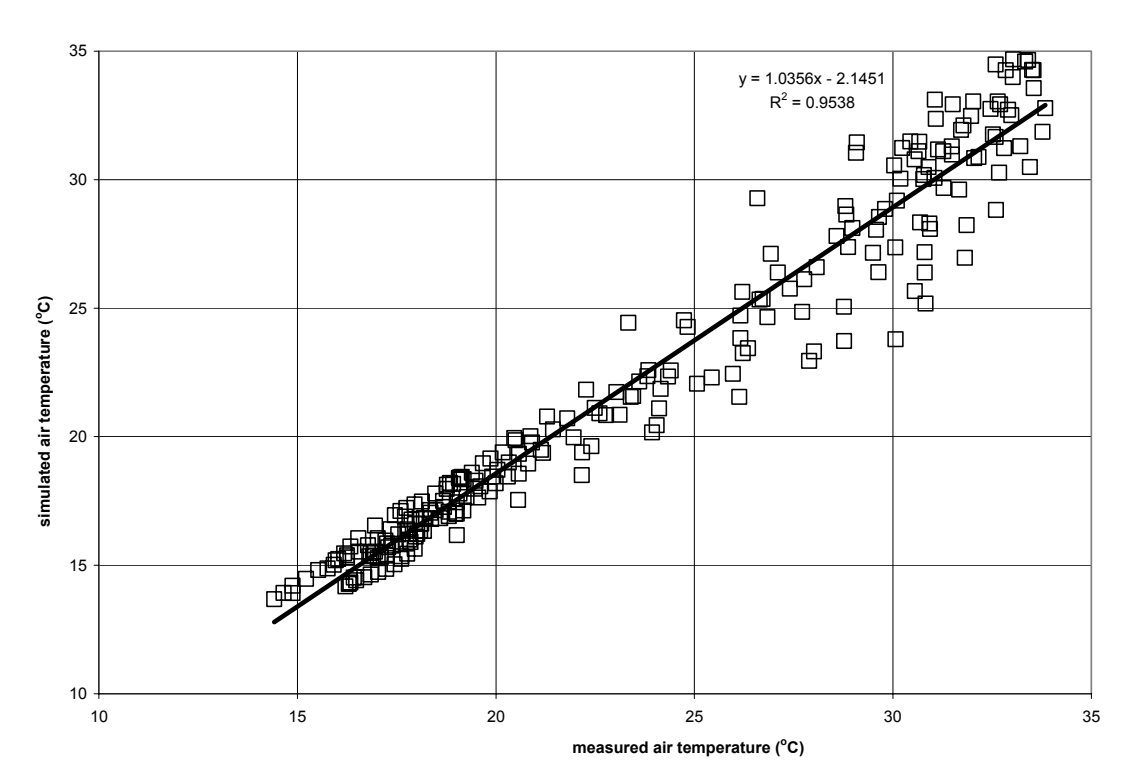


Fig 5.14: Regression analysis for the simulated and measured average air temperature inside the greenhouse on DOY 331 to DOY 335.

Table 5.3: Root mean square of the simulation of the greenhouse air temperature using the Gembloux Dynamic Greenhouse Climate Model for DOY 331 to DOY 335

DOY		RMSE
	Daytime (°C)	Nighttime (°C)
331	1.694	0.424
332	1.478	0.528
333	1.786	0.404
334	1.962	0.589
335	1.998	0.482

The model underestimated the average air temperature inside the greenhouse for DOY 331 to DOY 335. The maximum temperature differences obtained between the simulated and measurements were- 3.6 °C (DOY 331), -4.7 °C (DOY 332), -6.3 °C (DOY 333), -5.6 °C (DOY 334) and -4.4 °C (DOY 335). In comparison with the calibration period, the validation period, had a ~4% reduction in the nighttime differences whilst the daytime differences increased by ~20% (Tables 5.2 and 5.3). DOY 332 and DOY 333 had the least errors for the daytime and nighttime (1.478 °C and 0.404 °C respectively) whilst DOY 335 and 334 had the greatest daytime and nighttime errors respectively.

The regression analysis (Figure 5.14) for the validation period had a value of  $r^2$ =0.95, which was lower than for the calibration ( $r^2$ =0.96). The validation therefore had a slightly lower correlation of the simulated with the measured average air temperature. A strong correlation was observed at lower temperature (< 20 °C), whilst above that the simulated and measured showed greater deviations.

Overall, there were differences in the model performance for the two periods, with the validation period tending to give a better nighttime simulation than that for the calibration and vice versa.

# 5.3.2 Humidity

### 5.3.2 a) Calibration

A comparison of the simulated and measured relative humidity or vapour pressure was also done to analyze the model performance after the calibration. This is shown in Figures 5.15 and 5.16 whilst Figure 5.17 shows the regression analysis between the simulated and measured average vapour pressure. The differences between the simulated and measured vapour pressure inside the greenhouse to that measured outside respectively are shown in Appendix F. The calculated RMSE for the calibration period are given in Table 5.4.

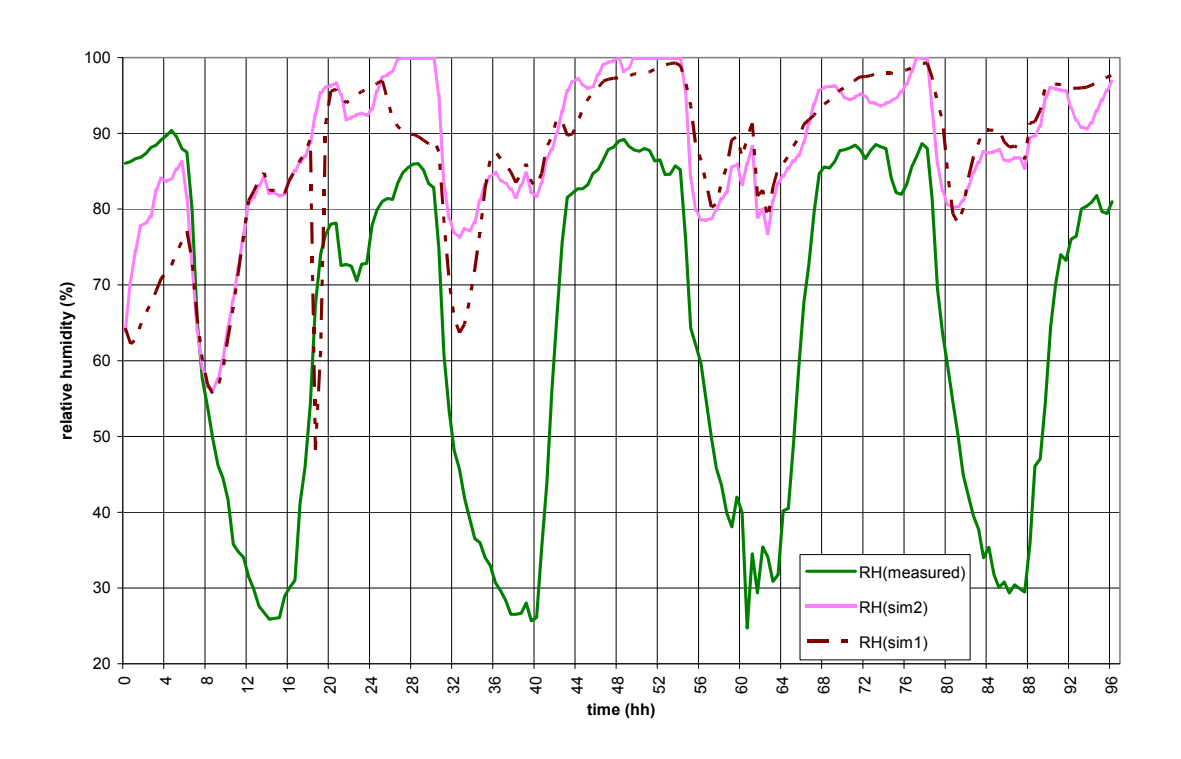


Fig 5.15: Comparison of the simulated and measured average relative humidity within the greenhouse on DOY 308 to DOY 311. Sim1 and Sim2 represent the simulations with the Gembloux Dynamic Greenhouse Climate Model before and after the calibration respectively.

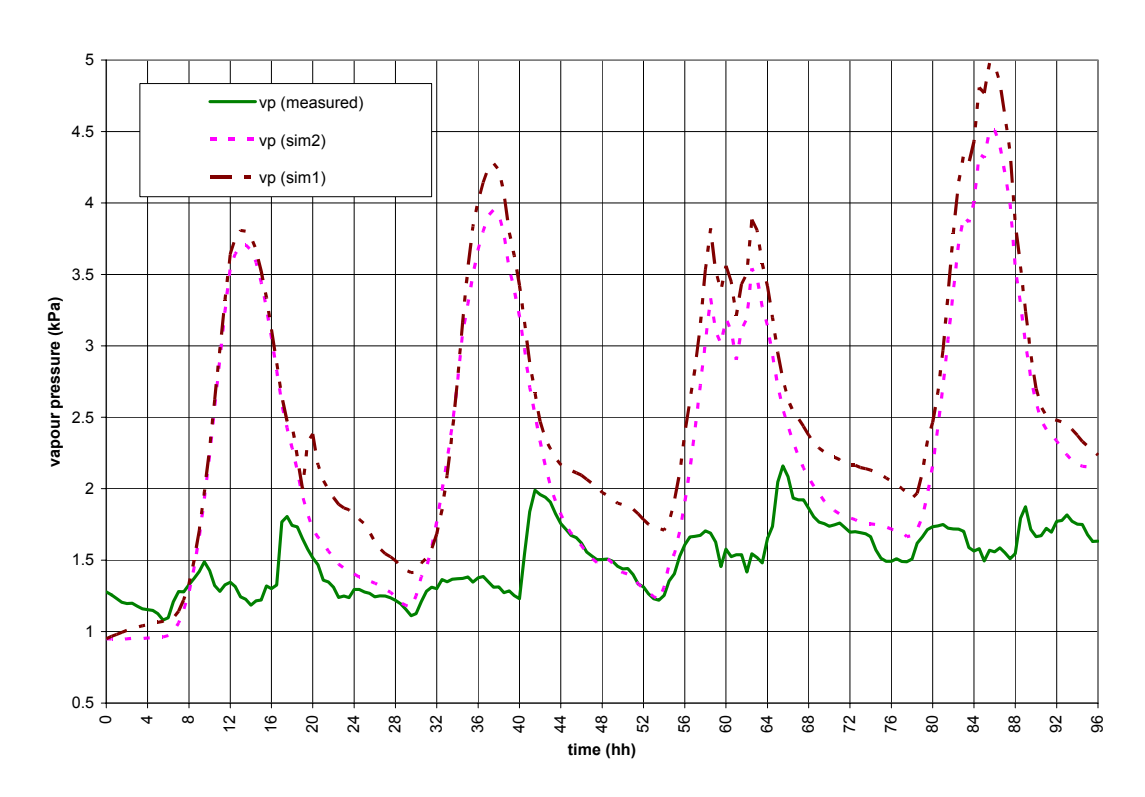


Fig 5.16: Comparison of the simulated and measured average vapour pressure within the greenhouse on DOY 308 to DOY 311. Sim1 and sim2 represent the simulations with the Gembloux Dynamic Greenhouse Climate Model before and after the calibration.

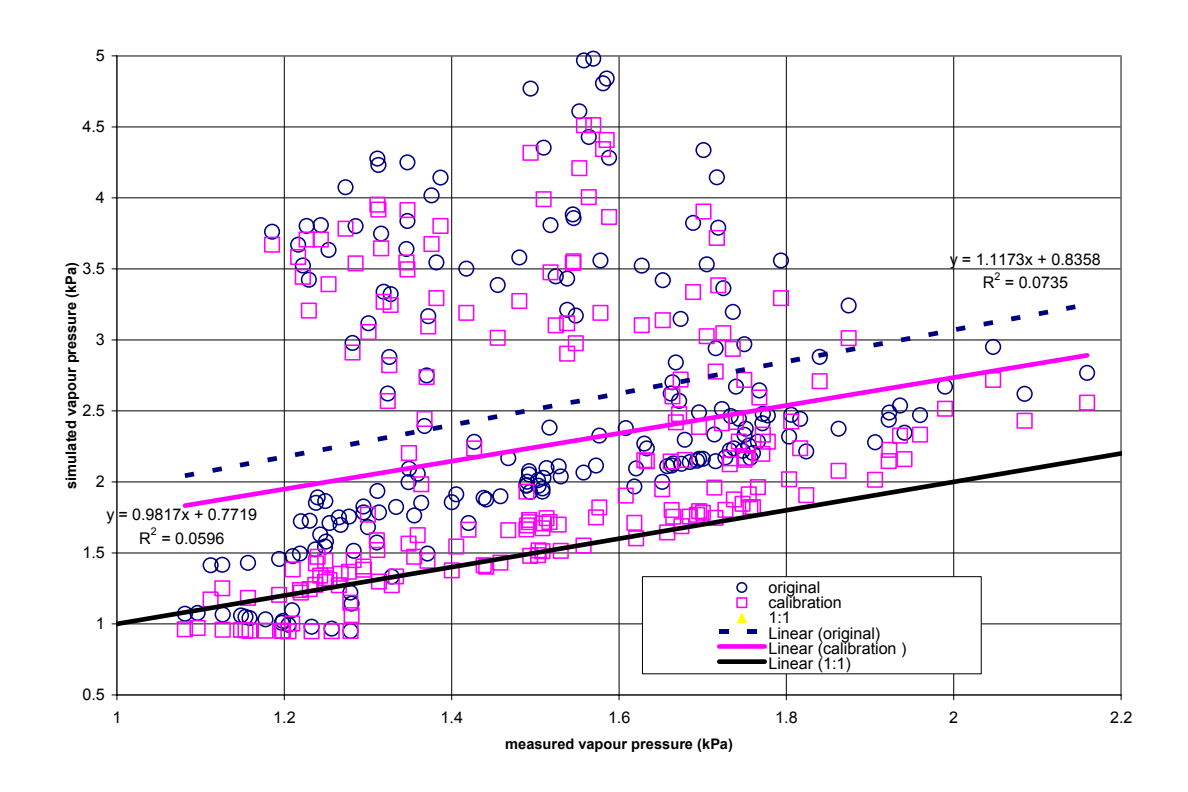


Fig 5.17: Regression analysis for the simulated and measured average vapour pressure inside the greenhouse on DOY 308 to DOY 311 before and after the calibration of the Gembloux Dynamic Greenhouse Climate Model.

Table 5.4: Root mean square errors (RMSE) of the simulation of the greenhouse vapour pressure using the Gembloux Dynamic Greenhouse Climate Model for DOY 308 to DOY 311

DOY		RMSE
	Daytime (kPa)	Nighttime (kPa)
308	0.962	0.229
309	0.883	0.055
310	0.623	0.111
311	0.945	0.213

Figure 5.15 shows that there were great deviations of the simulated relative humidity from the measured average relative humidity. The maximum differences obtained between the simulated and measured were 59% and 26% for the daytime and nightime respectively. However the early morning hours (0030 to 0630) had differences less than 20%, which at some periods even fell to below 10% (DOY 308, 310 and 311). There was very little variation in the simulated relative humidity during the day compared to the actual measurements where there was a big drop at midday to achieve the minimum values then increasing at nighttime to

reach the maximum values. The high daytime differences were also observed by comparing the simulated and measured average vapour pressure in Figure 5.16. The maximum difference in the daytime vapour pressure between the simulated and measured was 2.95 kPa compared to 0.69 kPa for the nighttime.

There was observed to be very little relationship between the simulated and measured average vapour pressure according to Figure 5.17. This was confirmed by the low  $r^2$  values of 0.08 and 0.06 for the original (simulation 1) and calibration (simulation 2) respectively.

Based on the RMSE values in Table 5.4, the DOY 310 had a better simulation of the daytime vapour pressure of the greenhouse with DOY 309 having a better nighttime simulation. DOY 308 had the worst overall simulation with daytime and nighttime RMSE values of 0.229 kPa and 0.962 kPa respectively. The cloud cover may have had some effects on the model performance because the clear day (DOY 308) had the greatest errors compared to the other days which were partly cloudy to cloudy. Similarly to the air temperature, the clear day had greater vapour pressure differences between the inside and outside of the greenhouse which the model could not simulate. Again, the daytime showed greater deviations from the measured average vapour pressure as was the case with the air temperature. The overestimation of the relative humidity by the model may have been due to a lower simulated ventilation rate, which caused a build up in the moisture content of the greenhouse. The ventilation system in the model did not relate well to that in the greenhouse because of the partial calibration of the ventilation sub-model parameters. The partial calibration was done because the model did not run successfully after some of the adjustments.

# 5.3.2 b) Validation

The model performance was then assessed using a different data set for the period of DOY 331 to 335. A comparison of the simulated and measured average relative humidity or vapour pressure is shown in Figures 5.18 and 5.19 respectively. The differences between the simulated and measured vapour inside the greenhouse to that measured outside respectively are shown in Appendix F. Figure 5.20 shows the regression analysis for the simulation whilst the RMSE values are in Table 5.5.

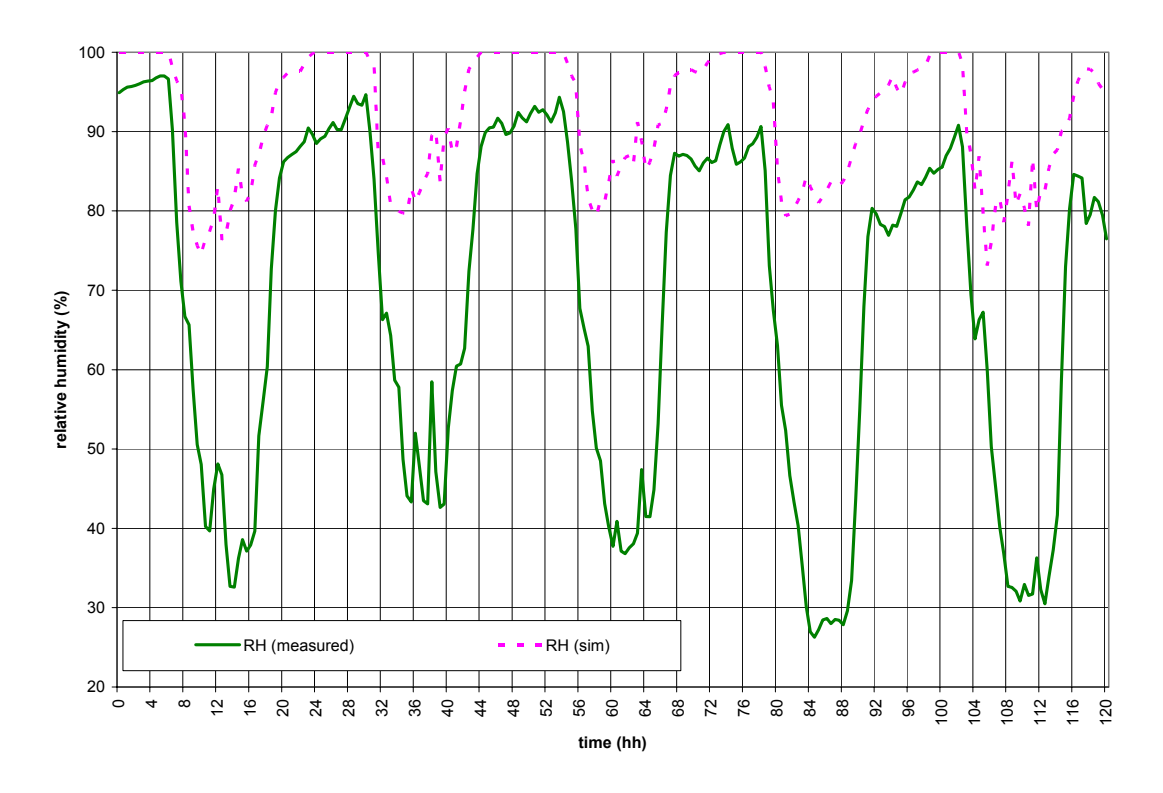


Fig 5.18: Comparison of the simulated and measured average relative humidity within the greenhouse on DOY 331 to DOY 335

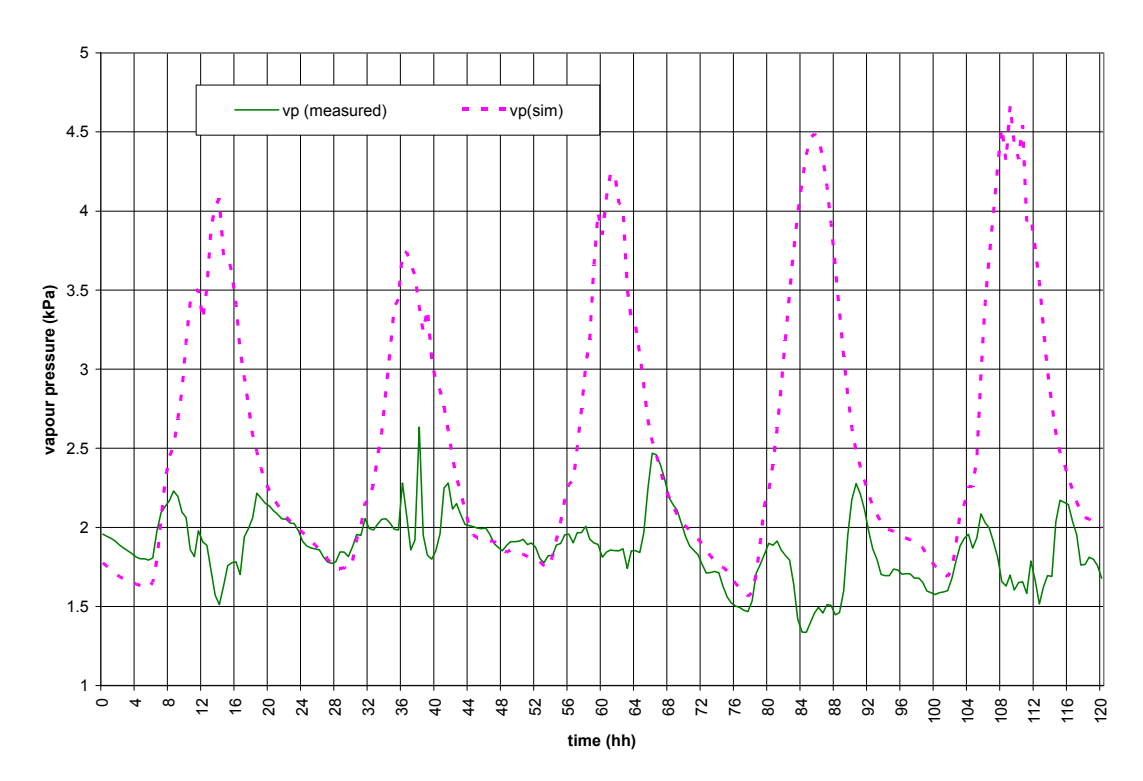


Fig 5.19: Comparison of the simulated and measured average vapour pressure within the greenhouse on DOY 331 to DOY 335

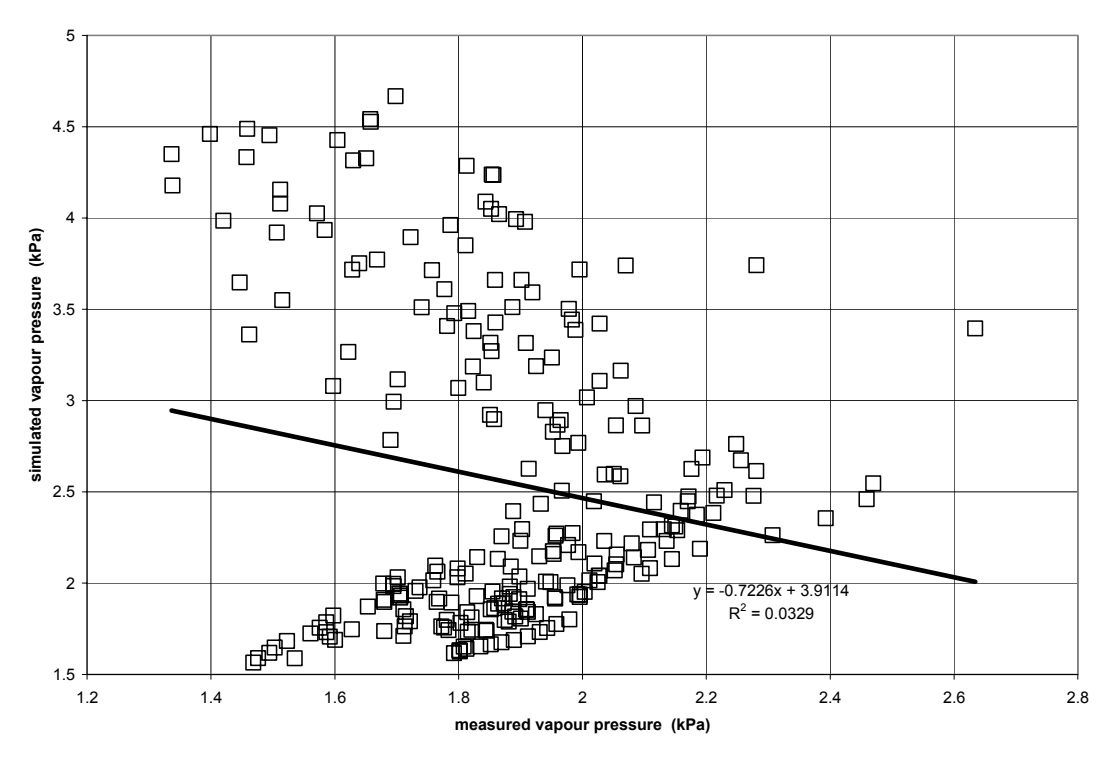


Fig 5.20: Regression analysis for the simulated and measured average vapour pressure inside the greenhouse on DOY 331 to DOY 335

Table 5.5: Root mean square errors of the simulation of the greenhouse vapour pressure using the Gembloux Dynamic Greenhouse Climate Model for DOY 331 to DOY 335

DOY		RMS
	Daytime (kPa)	Nighttime (kPa)
331	0.781	0.143
332	0.575	0.069
333	0.805	0.065
334	1.052	0.080
335	0.936	0.095

The simulated humidity differed significantly form the measured average humidity as shown in Figures 5.18 and 5.19. This is similar to the trend exhibited during the calibration period. The maximum differences between the simulated and measured average relative humidity obtained for the validation were around 43% to 64%. The validation showed overall lower RSME values for both the daytime and nighttime in comparison to the calibration period. DOY 332 and DOY 333 had better simulations of the daytime and nighttime vapour pressure inside the greenhouse respectively compared to the other days whilst the worst simulations were obtained on DOY 334 and Day 331 for the daytime and nighttime respectively.

The regression analysis for the validation period still showed little relationship between the simulated and measured vapour pressure. The validation period had a lower correlation compared to that during the calibration period ( $r^2$ =0.03 and  $r^2$ =0.06 respectively).

The lack of consistence in the model performance during the calibration and validation periods (for both the air temperature and vapour pressure) indicate some errors in the deck file which could not be detected automatically by the in-built control procedures (Pieters, 2002). The two modelling periods should have produced identical differences since there were no changes that had been made after the calibration run.

# **CHAPTER 6**

### **DISCUSSION**

### **6.1** Transmission Coefficients

The transmission values in the greenhouse characteristics file, CHARACT.DAT, of the Gembloux Dynamic Greenhouse Climate Model had to be adjusted in line with those of the greenhouse structure used at Floraline Pvt Ltd. This was done by calculating the ratio of the photosynthetically active radiation (PAR) or total solar radiation inside the greenhouse to that outside the greenhouse. Knowledge of the transmission of the greenhouse structure can be used to determine the amount of total solar radiation available inside. This is of importance because the latter influences the heat balances of the greenhouse layers (air, crop, soil). Total solar radiation transmittance values are also of importance, during the summer period where there is increased radiation intensity. This can assist in the correct precautions to take in mitigating the effects of the increased radiation load during this period. The increased radiation load causes extremely high temperatures (>35 °C), which can negatively impact on crop. Generally the transmission coefficient of the greenhouse structure is not a critical factor for the photosynthetic process in Zimbabwe because light is not a limiting factor in crop production rather the process is usually light saturated.

The average transmittances for PAR and total solar radiation ranged from  $69.3 \pm 7.2$  % to  $74.9 \pm 6.4$ % and  $60.7 \pm 8.3$ % to  $71.7 \pm 7.0$ % respectively for the period under analysis. The transmittance for PAR did not vary much under the different cloud conditions compared to that for total solar radiation. Maximum differences in transmission to the PAR and total solar radiation of 5.6% and 11% respectively were produced for the different cloud conditions. Although Day 311 was a partly cloudy day, it had the lowest transmittances for both PAR and total solar radiation ( $69.3 \pm 7.2$  and  $68.2 \pm 8.6$  respectively), because of the increased cloud cover between 1030 and 1330 (refer to Appendix C). The results show that the transmission of PAR and total solar radiation is dependent on the solar elevation, which affects the angle of incidence. At low solar elevation (in the early hours of the day or late afternoon), where the angle of incidence will be high, the transmittance to PAR and total solar radiation was lower because of increased reflectance and absorptance of both the sky and cover. The reverse was observed with an increase in the solar elevation, which reduced the angle of incidence. The transmittance of both PAR and total solar radiation on cloudy days did not show much variation since diffuse solar radiation does not have a varying angle of incidence (refer to

Figures 5.1). The transmission value for the PAR waveband under new polythene plastic was given as 76% at normal incidence (Pollet, 2002). This compares well with the results obtained in the study since the greenhouse cover has been used for the two years.

# 6.2 Temperature and Vapour Pressure Variations within the Greenhouse

The results showed that there were spatial variations of temperature and vapour pressure within the greenhouse. Sensors placed further (Positions 1 and 4) from the central sensor (Position 3) deviated more than those that were closer (Positions 2 and 5, refer to Figure 4.3). The average temperature and vapour pressure differences from the central sensor ranged from 0.2 °C to 2.7 °C and 0.03 kPa and 0.32 kPa respectively. The daytime period (0630 to 1800) had greater deviations from the central sensor than the nighttime (0030 to 0600 and 1830 to 2400). The high temperature and vapour pressure differences were due to the radiation input, which increased the available energy for heating up the air. This resulted in the greater daytime differences from the central sensor. A statistical analysis of the daytime and nighttime differences showed that the sensors on Positions 1, 2 and 4 differed significantly from the central sensor. The spatial variations of temperature and vapour pressure within the greenhouse was also attributed to the greenhouse rose crop which was at different developmental stage. The crop affected the airflow within the greenhouse thereby creating temperature and vapour pressure differences. Secondly, its transpiration process had an influence on the greenhouse heat and mass balances, which determine its air temperature and humidity levels respectively (Boulard et al., 1999). The lower air temperature and vapour pressure for the sensors on Positions 2, 3 and 5 compared to those on Position 1 and 4 was due to the opening of the side ventilator, which was positioned near the first three. The side ventilator introduced cool, dry air which caused the temperature and vapour pressure of the sensors on Positions 2, 3 and 5 to drop in comparison to those sensors on Position 1 and 4, which were further away.

However, the spatial variations of temperature and vapour pressure within the greenhouse could not be confirmed by a comparison of all the sensors on the Position 3 on DOY 39 (8 February 2005). This was because only three of the sensors that had been used in the earlier part of the experiment were still functional. These were the sensors that had been on Positions 3, 4 and 5. However, since a calibration of all the sensors had been done before they were placed in the greenhouse, it was assumed that they would have shown good agreement when put at position 3.

It was therefore concluded that the greenhouse air was not homogenous. This means that the placement of the sensors in the greenhouse structure is important because it would affect management decisions, which are based on the temperature and vapour pressure measurements obtained.

The temperature and vapour pressure measurements were averaged for the model analysis.

# 6.3 Comparison of the Greenhouse Microclimate with the Outside Measurements

The greenhouse structure was generally warmer than outside with temperature differences between the greenhouse air and outside ranging between 0.9 °C to 6.7 °C (daytime) and 0.05 °C to 3.4 °C (nighttime). Temperatures in the greenhouse fell below those outside on the clear day (DOY 334) for the period 1930 to 2400 as a result of the radiative losses. The greenhouse cover was cooler than the greenhouse air because of increased thermal (infrared) radiation losses under a clear sky. This then leads to heat exchange firstly between the warmer greenhouse air and the cooler greenhouse cover and then the cover and the outside air. The maximum and minimum temperatures obtained in the greenhouse were 33.8 °C and 14.4 °C (DOY 334) on a clear day and 28.8 °C and 16.8 °C on a cloudy day (DOY 340) respectively and for the outside 28.3 °C and 13.4 °C (DOY 334) and 22.5 °C and 16.0 °C (DOY 340). Generally the differences in the radiation input between the clear day and cloudy day will govern the temperature variations obtained between these days as well as between the inside and outside air temperatures. Because of the increased absorption and reflection on the cloudy day, there was a reduction in the radiation received in the greenhouse such that the greenhouse air was not warmed much because of the limited available energy. This resulted in a relatively low maximum temperatures achieved that day (Monteith and Unsworth, 1990). This can be observed by its small temperature range of 12 °C between the maximum and minimum air temperature inside the greenhouse compared to 19.4 °C for the clear day (DOY 340).

The greenhouse temperatures were maintained in the range 14-34 °C. In the study air temperatures inside the greenhouse were below 35°C and this could be attributable to the effectiveness of the climate control system at Floraline Pvt Ltd in preventing the occurrence of extremely high temperatures that would have negatively affected crop productivity. However the nighttime temperatures of below 15 °C is of concern as these could adversely affect crop quality because of the increased incidences of flower deformities (§2.3). It is for

this reason that Floraline Pvt Ltd has installed a heating system, which can be used during winter, where there are increased nighttime periods with temperatures below 15 °C.

Similarly, the greenhouse structure was also humid in comparison to the outside with maximum vapour pressures of 2.3 kPa (inside) for both days and 1.7 kPa (clear day) and 1.9 kPa (cloudy day) for the outside respectively. The two days had the vapour pressure ranges of 1.0 kPa (clear day) and 0.5 kPa (cloudy day) respectively.

The higher air temperature and vapour pressure inside the greenhouse is as a result of two factors: reduced turbulence and the "greenhouse effect". The convective currents within the greenhouse are reduced thereby limiting the exchange of heat between the greenhouse air and the outside such that there is build up of the heat within the greenhouse increasing the latter's air temperature. The "greenhouse effect" also causes a build up in the air temperature because of the trapping of the longwave (thermal) radiation (Monteith and Unsworth, 1992). The high vapour pressure inside the greenhouse may be also be caused by the irrigation system and periodical wetting of the paths as a means of lowering the air temperatures.

### 6.4 Leaf Temperature

Temperature variations were observed between the two leaf surfaces with maximum differences of 4.2 °C and 2.6 °C for the cloudy day and clear day respectively. These variations occurred because of the differences in the radiation received between the upper and lower leaf surfaces. Generally the upper leaf surfaces were found to be warmer than the lower leaf surfaces during the daytime and vice versa at nighttime. The upper leaf surfaces therefore receive more of the radiation compared to the lower leaf surfaces, which are shaded. Furthermore factors such as that a closed canopy and increased leaf area index will contribute in increasing the temperatures differences between the two leaf surfaces due to increased shading. Since roses are hypostomatous, the lower daytime temperatures of the lower leaf surface could be due to the transpiration process since most of the water vapour is lost through the lower surface thereby lowering its temperatures (Bot, 1983). At nighttime, the lower surfaces were warmer because of the reduced thermal radiation exchange with the greenhouse air compared to the upper canopy. Secondly the lower leaf surfaces also received more of the radiant heat flux from the soil compared to the upper leaf surfaces (Bot, 1983).

Temperature variations within a crop canopy have been observed to be negligible such that the vegetation temperature is usually given as an average without the introduction of significant errors (Stanghellini, 1987).

This study did not include a comparison of the simulated and measured leaf temperatures because the stomatal resistance values (1800 s m<sup>-1</sup> and 200 sm<sup>1</sup>) used did not give good simulations of the leaf temperature as with the air temperature. It was thus decided that the performance of the model in the simulation of the leaf temperatures can then be analyzed with further calibration of the transpiration sub-model in future work.

### 6.5 Model Results

The simulation of the greenhouse air temperature by the Gembloux Dynamic Greenhouse Climate Model was generally lower than the actual temperature with maximum differences of up to - 6.3 °C. Overall the model deviated more from the measured average air temperature during the daytime than nighttime. RMSE values were in the range 1.0 - 2.0 °C and 0.2 - 0.8°C on average. The model performance could have been influenced by the high daytime temperature differences between the inside and outside making it impossible for the model to register these variations. The small nighttime differences were thus due to the smaller temperature variations, which the model could simulate. Furthermore the nighttime period was characterized by simple heat and mass budgets because of the absence of the total solar radiation as well as reduced ventilation, which strengthened the performance of the GDGCM (Zhang et al., 1997). Generally the validation period showed a better nighttime simulation of the greenhouse air temperature compared to the calibration. The differences in the simulations for the validation period (DOY 331 to DOY 335) and the calibration period (DOY 308 to DOY 311) indicate some errors in the deck file, which could not be picked up during the runs. This is because the two simulation periods should have given identical results since there were no further adjustments after the initial calibrations of the model which included adjustment of the transpiration sub-model, forcing functions, climate data and the greenhouse and soil characteristics data. It was observed that clear days DOY 310 and DOY 331 produced higher simulation errors, as was shown by their daytime RMSE of 2.0 °C. An exception to this was DOY 335, which also had a high RMSE of 2.0 °C although it was a cloudy day. The average RMSE values for the air temperature for the calibration and validation were 1.48 °C (daytime) and 0.50 °C (nighttime) and 1.78 °C (daytime) and 0.49 °C (nighttime) respectively. Wang and Boulard (2000) who also used the GDGCM obtained a RMSE of 0.8 °C whilst Zhang et al. (1997) who adapted that of Avissar and Mahrer (1982) for use in an unheated commercial greenhouse had 1.2 °C (refer to §2.4). The regression analysis showed that the model simulated the air temperature well with the calibration having a better fit of the actual air temperature compared to the validation. The two simulation periods had correlation values ( $r^2$ ) of 0.95 and 0.96 respectively.

The Gembloux Dynamic Greenhouse Climate Model overestimated the vapour pressure in the greenhouse with a maximum difference of 3.0 kPa being recorded between the simulated and measured average vapour pressure whilst this was around 60% for the relative humidity. The model produced better nighttime simulations similarly to that for the air temperature. The diurnal variation of the simulated humidity was very minimal (refer to Figures 5.16 and 5.18).

There was no relationship between the simulated and measured average vapour pressure (r<sup>2</sup> < 0.1). This indicated that the calibration of the GDGCM carried out during the study was insufficient to produce a relatively close simulation of the greenhouse moisture content. The stomatal resistance values of 1800 s m<sup>-1</sup> (maximum) and 200 s m<sup>-1</sup> (minimum) used in the calibration could have been lower than actual thereby increasing the exchange of mass between the crop and air. This subsequently led to a build up of the moisture content within the greenhouse during the simulation compared to the actual measurements. Secondly the vapour pressure was more sensitive to the partial calibration of some of the model parameters (where changes in the deck file were not carried forward to other relevant files such as the character files or vice versa) to enable to model to run. The current version of the model at times did not run after adjustments to some of the model parameters although there were no indications of programming errors. In the study, the ventilation sub-model (Types 70 and 72) was not calibrated because the mechanism of the computerized ventilation system at Floraline Pvt Ltd was not well understood by the people interviewed.

# **CHAPTER 7**

### **CONCLUSION AND RECOMMENDATIONS**

In the study the greenhouse air was found to be inhomogeneous because of the observed spatial variations of temperature and vapour pressure within the greenhouse. This showed that point measurements of the air temperature and relative humidity (vapor pressure) within the greenhouse cannot be representative of the whole greenhouse. Secondly, the placement of the air temperature and humidity sensors within the greenhouse was important for both accurate measurements and management operations. A comparison of the spatial variations of temperature and vapour pressure with measurements of these sensors on the same mast was not carried out because two of the five sensors developed technical faults. It is proposed that this can be carried out in future work on greenhouse microclimate modelling.

The transmission of the greenhouse to PAR (photosynthetically active radiation) and total solar radiation was found to have average values of  $69.3\pm7.2$  % to  $74.9\pm6.4$ % and  $60.7\pm8.3$ % to  $71.7\pm7.0$ % respectively for the period under analysis. The transmission of the PAR and total solar radiation was influenced by cloud cover, greenhouse construction parts and solar elevation. High cloud cover showed little influence on the transmission of PAR and total solar radiation because of the increase in the diffuse solar radiation component, which does not have a varying angle of incidence. Secondly, the greenhouse construction parts reduced the transmission to PAR and total solar radiation by obstruction of the radiation beam.

The greenhouse air temperature and vapour pressure were significantly different from the outside under cloudy conditions. Temperature differences between the inside and outside were 7.0 °C (clear day) and 5.2 °C (cloudy day) whilst vapour pressure differences were 1.1 kPa (clear day) and 0.4 kPa (cloudy day) respectively. The maximum temperatures inside the greenhouse were generally maintained below 35°C although the minimum temperatures fell below 15 °C on the clear day during the nighttime (1830 to 2400). The climate control system at Floraline Pvt Ltd was therefore effective in regulating the greenhouse daytime air temperatures, which were kept within the recommended limits for the rose crop being grown.

Temperature variations were evident between the two leaf surfaces because of the differences in radiation incident on them whilst at nighttime it was due to increased thermal radiation loss from the upper leaf surface. The lower leaf surface in turn received thermal radiation from the

soil. A temperature difference of 5 °C was obtained between the upper and lower leaf surfaces for the rose canopy at Floraline Pvt. Ltd. Generally the measurements of the leaf temperatures had a lot of inconsistencies because the sensors tended to be out of focus. The displacement of the sensors was caused by management practices such as pruning. In future work leaf measurements should be done using sensors that should be attached to specific leaves to minimize measurement errors. Thermocouples may be used in place of the radiation thermometers as they do not interfere much with daily operations within the greenhouse.

The Gembloux Dynamic Greenhouse Climate Model generally underestimated the air temperature (with a maximum of ~6 °C). The RMSE values were below 2.0 °C for both the calibration and validation periods. The performance of the model was evaluated by considering the differences between the simulated and actual greenhouse air temperature and that outside, the greater these differences, the higher are the simulation errors and vice versa. Subsequently this resulted in better nighttime simulations compared to the daytime. The model was also affected by cloud cover because of its influence on the radiation input. Generally clear days had higher daytime simulation errors compared to the cloudy days with the exception of DOY 335. Overall DOY 311 and DOY 308 had better daytime and nighttime simulations of the greenhouse air temperature, with RMSE of 0.98 °C and 0.29 °C respectively compared to the other days used during the calibration period.

The simulation of the relative humidity by the Gembloux Dynamic Greenhouse Climate Model produced an overestimation with differences of +50% and +20% between the simulated and actual humidities for the daytime and nighttime respectively. The RMSE produced for the vapour pressure were below 1.1 kPa. Similarly to the air temperature simulations, it was observed that daytime differences were greater and secondly the validation showed improved nighttime simulations but increased errors in the daytime. The regression analysis ( $r^2 < 0.1$ ) showed that the GDGCM did not produce any relationship between the simulated and measured vapour pressure. This was attributed to the calibration done during the study not be sufficient to relate to the actual measurements of the vapour pressure within the greenhouse.

The air temperature results showed that the GDGCM has the possibility of providing the floricultural farmers with an affordable method of microclimate control. This was supported by the higher accuracy of the nighttime simulated air temperature, which can be used in decision making to ensure that the correct operations are carried out in maintaining these temperatures above 15 °C. However, the high errors in the simulation of the humidity were of concern since the component is a critical microclimate variable in disease forecasting

particularly at nighttime. Therefore the Gembloux Dynamic Greenhouse Climate Model could not be relied upon in its present form to be effective in achieving optimal climate control within greenhouse since the simulation of the humidity component still requires major improvements. It is hoped that with further calibration to the model parameters, the errors associated particularly with the overall simulation of the humidity can be reduced. The calibration should focus mainly on the ventilation, soil and transpiration sub-models, which were not well accomplished in the study and thus did not relate to the greenhouse at Floraline Pvt. Ltd.

The failure of the version of the model used in the study to run after calibration restricted the evaluation of the model performance particularly the sensitivity analysis of some of the model parameters on the microclimate variables. It is proposed that another version of the model will be used in future research, which can be easily calibrated without the complexities found in the current version. Further work should also be carried out in validating the model under different greenhouse designs as well as different climatic conditions. This study was carried out during the summer period under a greenhouse with automated climate control and future work can be carried out in simple greenhouse structures with manual control in the different agro ecological zones in Zimbabwe or during the winter season.

#### REFERENCES

- Allen, R.G., Perreira, L.S., Raes, D. and Smith, M. (1998): Crop Evapotranspiration Guidelines for Computing Crop Water Requirements. FAO Irrigation and Drainage Paper 56. Food and Agricultural Organisation of the United Nations-Rome.
- Avissar, R. and Mahrer, Y. (1982): Verification study of a numerical greenhouse climate model. Quoted by: Zhang, Y., Mahrer, Y., and Margolin, M. (1997): Predicting the microclimate inside a greenhouse: an application of a one-dimensional numerical model in an unheated greenhouse. *Agricultural and Forest Meteorology*, **86**, 291-297.
- Bafana, B. (2003): Zimbabwe's farmers show a flair for flowers. World Radio for the Environment.
- Bakker, J.C. (1991<sup>a</sup>): Analysis of Humidity Effects on Growth and Production of Glasshouse Fruit Vegetables. Quoted by: Bakker, J.C. *et al.* (eds): Greenhouse climate control an integrated approach. Wageningen Pers.
- Bakker, J.C. (1991<sup>b</sup>): Leaf Conductance of Four Glasshouse Vegetable Crops as affected by Air Humidity. Quoted by: Bakker, J.C. *et al.* (eds): Greenhouse Climate Control an Integrated Approach. Wageningen Pers.
- Bakker, N.J. and Challa, H. (1995): Introduction. In: Bakker, J.C. *et al.* (eds): Greenhouse Climate Control an Integrated Approach. Wageningen Pers. pp 1-3.
- Bontsema, J. (1995): Control Principles. In: Bakker, J.C. *et al.* (eds): Greenhouse Climate Control an Integrated Approach. Wageningen Pers. pp 225.
- Bot, G.P.A. (1995): Greenhouse Climate Control. In: Bakker, J.C. *et al.* (eds): Greenhouse Climate Control an Integrated Approach. Wageningen Pers. pp 211.
- Bot, G.P.A. (1983): Greenhouse climate: from physical processes to a dynamic model. PH. D. Dissertation, Landbouwhogeschool, Wageningen, Netherlands.
- Bot, G.P.A. and van de Braak, N.J. (1995): Physics of Greenhouse Microclimate. In: Bakker, J.C. *et al.* (eds): Greenhouse Climate Control an Integrated Approach. Wageningen Pers.
- Boulard, T. and Baille, A. (1995): Modelling of air exchange in a greenhouse equipped with continuous roof vents. Quoted by: Boulard, T. and Wang, S. (2000): Greenhouse crop transpiration simulation from external climate conditions. *Agricultural and Forest Meteorology*, **100**, 25-34.
- Boulard, T., Haxaire, R., Lamrani, M.A., Roy, J.C. and Jaffrin, A. (1999): Characterization and modelling of the air fluxes induced by natural ventilation in a greenhouse. *Journal of Agricultural Engineering Research*, **74**, 135-144.
- Boulard, T. and Wang, S. (2000): Greenhouse crop transpiration simulation from external climate conditions. *Agricultural and Forest Meteorology*, **100**, 25-34.
- Breuer, J.J. and Knies, P. (1995): Ventilation and Cooling. In: Bakker, J.C. *et al.* (eds): Greenhouse Climate Control an Integrated Approach. Wageningen Pers.

- Businger, J.A. (1963): The glasshouse (greenhouse) climate. Quoted by: Bot, G.P.A. (1983): Greenhouse climate: from physical processes to a dynamic model. PhD. Dissertation, Landbouwhogeschool, Wageningen, Netherlands.
- Challa, H. (2002): Crop models for greenhouse production systems in production systems. Proceedings 4<sup>th</sup> IS on Crop models. Acta Hort. 593, ISHS 2002.
- Challa, H., Heuvelink, E. and van Meeteren, U. (1995): Crop Growth and Development. Quoted by: Bakker, J.C. *et al.* (eds): Greenhouse Climate Control an Integrated Approach. Wageningen Pers.
- Critten, D.L. and Bailey, B.J. (2002): A review of greenhouse engineering development during the 1990s. *Agricultural and Forest Meteorology*, **112**, 1-22.
- Davies, R. (2000): The impact of globalization on local communities: a case study of cut-flower industry in Zimbabwe. International Labour Organisation Southern Africa Multidisciplinary Advisory Team (ILO/SAMAT) Discussion Paper No.13, Harare, Zimbabwe. <a href="http://www.ilo.org/public">http://www.ilo.org/public</a>.
- Delta-T Devices Ltd. (1996): Soil temperature probe (Type ST1-UM-3) User Manual. 128 Low Road, Burwell, Cambridge, CB5 OEJ, England.
- Deltour, J., de Halleux, D., Nijskens, J.Coutisse, S. And Nisen, A. (1985) Dynamic modelling of heat and mass transfer in greenhouses. Quoted by: Wang, S. and Boulard, T. (2000): Predicting the microclimate in a naturally ventilated plastic house in a Mediterranean climate. *Journal of Agricultural Engineering Research*, **75**, 27-38.
- Export Flower Growers Association of Zimbabwe (EFGAZ). (1998): <a href="http://www.samara.co.zw/agro/florigrown.html">http://www.samara.co.zw/agro/florigrown.html</a>.
- Fernandez, J.E. and Bailey, B.J. (1994): The influence of fans on environmental conditions in greenhouses. *Journal of Agricultural Engineering Research*, **58**, 201-210.
- Food and Agricultural Organisation of the United Nations (FAO). (1990): Protected cultivation in the Mediterranean climate. Plant Protection Paper 90.
- Gates, D.M. and Papain, L.E. (1971): Altas of energy budgets of plant leaves. Quoted by: Jones, H.G. (1992): Plants and microclimate: a quantitative approach to environmental plant physiology. Cambridge University Press.
- Gijzen, H. (1995): CO<sub>2</sub> Uptake by the Crop..In: Bakker, J.C. *et al.* (eds), 1995. Greenhouse Climate Control an Integrated Approach. Wageningen Pers. Pp 16-34
- Gijzen, H. (1995): Interaction between CO<sub>2</sub> and Water Loss. In: Bakker, J.C. *et al.* (eds): Greenhouse climate control an integrated approach. Wageningen Pers. Pp 51-62.
- Hall, D.O. and Rao, K.K. (1999): Photosynthesis. 6<sup>th</sup> Edition. Cambridge University Press.
- Jolliet, O. (1994). HORTITRANS, a model for predicting and optimizing humidity and transpiration in greenhouses. *Journal of Agricultural Engineering Research*, **57**, 23-37.
- Jolliet, O. and Bailey, B.J. (1992): The effect of climate on tomato transpiration in greenhouses: measurements and models comparison. *Agricultural and Forest*

- Meteorology, **58**: 43-62.
- Jones, H.G. (1992): Plants and microclimate: a quantitative approach to environmental plant physiology. Cambridge University Press.
- Kostyuk, V.L., Koval skaya, I.M. and Garan'ko, L.B. (1990): Quoted by: Critten, D.L. and Bailey, B.J. (2002): A review of greenhouse engineering development during the 1990s. *Agricultural and Forest Meteorology*, **112**, 1-22.
- Kozai, T., Goudriaan, J. and Kiruma, M. (1978): Light transmission and photosynthesis in greenhouse. Quoted by: Pollet, I. (2002): Radiation transmission through dry and condensate covered greenhouse cladding materials. PhD. Dissertation, Facultiet Landbouwkundige en Toegepaste, Biologische Werenschappen, Universitiet Gent.
- Kozai, T. and Kiruma, M. (1977): Direct solar light transmission into multi-span greenhouses. Quoted by: Pollet, I. (2002): Radiation transmission through dry and condensate covered greenhouse cladding materials. Ph. D. Dissertation, Facultiet Landbouwkundige en Toegepaste, Biologische Werenschappen, Universitiet Gent.
- Larson, R.A. (1980): Introduction to Floriculture. Academic Press, Inc, New York.
- Lee, R (1973): Quoted by: Mhizha, T. (2003): Influence of Ageing of Plastic Greenhouse Covering Materials on Some Aspects of the Greenhouse Microclimate. MSc. Thesis. Agricultural Meteorology, University of Zimbabwe.
- Madakadze, R. (2000): Rose Production. In: Masimbe, S. and Madakadze, R. Horticulture 2. University College of Distance Education. University of Zimbabwe.
- Marcelis, L.F.M. and de Koning, A.N.M. (1995): Biomass Partitioning in Plants. In: Bakker, J.C. *et al.* (eds): Greenhouse Climate Control an Integrated Approach. Wageningen Pers.
- Mashonjowa, E. (2001): The Effect of Covering Material on Plant Microclimate. MSc. Thesis. Agricultural Meteorology, University of Zimbabwe.
- Mastalerz, J.W. (1977): The Greenhouse Environment: the effect of environmental factors on the growth and development of flower crops. John Wiley and Sons Inc.
- Mattson and Widner, (1971): Quoted by: Masimbe, S. and Madakadze, R. 2000: Horticulture 2. University College of Distance Education. University of Zimbabwe.
- Mhizha, T. (2003): Influence of Ageing of Plastic Greenhouse Covering Materials on Some Aspects of the Greenhouse Microclimate. MSc. Thesis. Agricultural Meteorology, University of Zimbabwe.
- Monteith, J.L. and Unsworth, M.H. (1990): Principles of Environmental Physics, 2<sup>nd</sup> Edition. Edward Arnold, London.
- Nederhoff, E.M. and De Graaf. (1983): Effects of CO<sub>2</sub> on Leaf Conductance and Canopy Transpiration Rate of Greenhouse Grown Cucumber and Tomato. Quoted by: Bakker, J.C. *et al.* (eds): Greenhouse Climate Control an Integrated Approach. Wageningen Pers
- Nelson, P.V. (1991): Greenhouse Operation and Management. Prentice Hall. London

- Omniflora. (2005): The cut -flower production in Zimbabwe. http://www.omniflora.com/e-zim.htm. 01 November 2005
- Pieters, J. (2002): Greenhouse Climate Modelling: from fundamental thermodynamics to a detailed climate mechanism. Unpublished.
- Politiv Ltd. (1999). Manufacture and Marketing. Polyethylene for Industry and Agriculture.
- Pollet, I. (2002): Radiation Transmission through Dry and Condensate Covered Greenhouse Cladding Materials. PhD. Dissertation, Facultiet Landbouwkundige en Toegepaste, Biologische Werenschappen, Universitiet Gent.
- Popovski, K. (1996): Greenhouse Climate Factors. Quoted by: Mashonjowa, E. (200): The Effect of Covering Material on Plant Microclimate. MSc. Thesis. Agricultural Meteorology, University of Zimbabwe.
- Rosenberg, N., Blad, B.L. and Verma, S.B. (1983): Microclimate: The biological environment. Quoted by: Mhizha, T., 2003. Influence of Ageing of Plastic Greenhouse Covering Materials on Some Aspects of the Greenhouse Microclimate. MSc. Thesis. Agricultural Meteorology, University of Zimbabwe.
- Seginer, I. (1997): Alternative design formulae for the ventilation rate of the greenhouses. Quoted by: Wang, S. and Boulard, T. (2000): Predicting the microclimate in a naturally ventilated plastic house in a Mediterranean climate. *Journal of Agricultural Engineering Research*, **75**, 27-38.
- Seginer, I., Boulard, T. and Bailey, B.J. (1994): Neural network models of the greenhouse climate. *Journal of Agricultural Engineering Research*, **59**, 203-216.
- Seginer, I. (1984): Quoted by: Stanghellini, C. (1987): Transpiration of greenhouse crops: an aid to climate management. PhD. Dissertation, Instituut voor Mechanisatae, Arbeid en Gebouwen, Wageningen, 150pp.
- Sguazzin, A. (2001): Zimbabwe as a rose is nipped in the bud. http://www.zimbabwesituation.com./feb16.html.
- Stanghellini, C. (1987): Transpiration of greenhouse crops: an aid to climate management. PhD. Dissertation, Instituut voor Mechanisatae, Arbeid en Gebouwen, Wageningen, 150pp.
- Swinbank, W.G. (1963): Long-wave radiation from clear skies. In: Pieters, J., 2002. Greenhouse Climate Modelling: From fundamental thermodynamics to a detailed climate mechanism. Unpublished.
- Tibbitts, T.W. and Langhans, R.W., 1993. Controlled-environment studies. Quoted by: Mashonjowa, E., 2001. The Effect of Covering Material on Plant Microclimate. MSc. Thesis. Agricultural Meteorology, University of Zimbabwe.
- Wang, S. and Boulard, T. (2000): Predicting the microclimate in a naturally ventilated plastic house in a Mediterranean climate. *Journal of Agricultural Engineering Research*, **75**, 27-38.

- Wartena, L., Palland, C.L. and Vossen, G.H.L. 1973: Checking of some formulae for the calculation of long wave radiation from skies. Quoted by: Bakker, J.C. *et al.* (eds): Greenhouse climate control an integrated approach. Wageningen Pers. Pp137.
- von Noodegraaf, C. And Welles, G.W.H. (1995): Product quality. In: Bakker, J.C. *et al.* (eds), Greenhouse climate control an integrated approach. Wageningen Pers.
- Yang, X., Short, T.H., Fox, F.D. and Bauerle, W.L. (1990): Transpiration, leaf temperature and stomatal resistance of a greenhouse cucumber crop. *Agricultural and Forest Meteorology*, **51**, 197-209.
- Zhang, L. and Lemeur, R. (1992): Effect of aerodynamic resistance on energy balance and Penman-Monteith estimates of evapotranspiration in greenhouse conditions. *Agricultural and Forest Meteorology*, **58**, 209-228.
- Zhang, Y., Mahrer, Y., and Margolin, M. (1997): Predicting the microclimate inside a greenhouse: an application of a one-dimensional numerical model in an unheated greenhouse. *Agricultural and Forest Meteorology*, **86**, 291-297.
- Zhang, Y., Teitel, M. and Barak, M. (2001): Vertical temperature and humidity gradients in a naturally ventilated greenhouse. *Journal of Agricultural Engineering Research.* **78** (4), 431-436.

Appendix A: Day of the year (Julian) calendar

	1	2	3	4	5	6	7	8	9	10	11	12	13	14	15	16	17	18	19	20	21	22	23	24	25	26	27	28	29	30	31
JAN	1	2	3	4	5	6	7	8	9	10	11	12	13	14	15	16	17	18	19	20	21	22	23	24	25	26	27	28	29	30	31
FEB	32	33	34	35	36	37	38	39	40	41	42	43	44	45	46	47	48	49	50	51	52	53	54	55	56	57	58	59			
MAR	60	61	62	63	64	65	66	67	68	69	70	71	72	73	74	75	76	77	78	79	80	81	82	83	84	85	86	87	88	89	90
APR	91	92	93	94	95	96	97	98	99	100	101	102	103	104	105	106	107	108	109	110	111	112	113	114	115	116	117	118	119	120	
MAY	121	122	123	124	125	126	127	128	129	130	131	132	133	134	135	136	137	138	139	140	141	142	143	144	145	146	147	148	149	150	151
JUN	152	153	154	155	156	157	158	159	160	161	162	163	164	165	166	167	168	169	170	171	172	173	174	175	176	177	178	179	180	181	
JUL	182	183	184	185	186	187	188	189	190	191	192	193	194	195	196	197	198	199	200	201	202	203	204	205	206	207	208	209	210	211	212
AUG	213	214	215	216	217	218	219	220	221	222	223	224	225	226	227	228	229	230	231	232	233	234	235	236	237	238	239	240	241	242	243
SEP	244	245	246	247	248	249	250	251	252	253	254	255	256	257	258	259	260	261	262	263	264	265	266	267	268	269	270	271	272	273	
OCT	274	275	276	277	278	279	280	281	282	283	284	285	286	287	288	289	290	291	292	293	294	295	296	297	298	299	300	301	302	303	304
NOV	305	306	307	308	309	310	311	312	313	314	315	316	317	318	319	320	321	322	323	324	325	326	327	328	329	330	331	332	333	334	
DEC	335	336	337	338	339	340	341	342	343	344	345	346	347	348	349	350	351	352	353	354	355	356	357	358	359	360	361	362	363	364	365

Add 1 to values not in italics during a leap year.

Appendix B: Temperature and relative humidity probes used for the periods: 3 to 7 November 2004 (DOY 308 to DOY 311), 25 to 30 November 2004 (DOY 330 to DOY 335), 1 to 6 December 2004 (DOY 336 to DOY 341) and 6 to 11 February 2005 (DOY 37 to DOY 42) respectively

Month	Day	HMP45AC s/n 393B	HMP45AC s/n 143	CS500	YA100C	RHT2nl-02
NT 1	3	++	++	++	-	++
November	4	++	++	++	-	++
	5	++	++	++	++	++
	6	++	++	++	++	++
	7	++	++	++	++	++

Month	Day	HMP45AC s/n 393B	HMP45AC s/n 143	CS500	YA100C	RHT2nl-02
	25	++	-	++	++	++
November	26	++	-	++	++	++
	27	++	-	++	++	++
	28	++	-	++	++	++
	29	++	-	++	++	++
	30	++	-	++	++	++

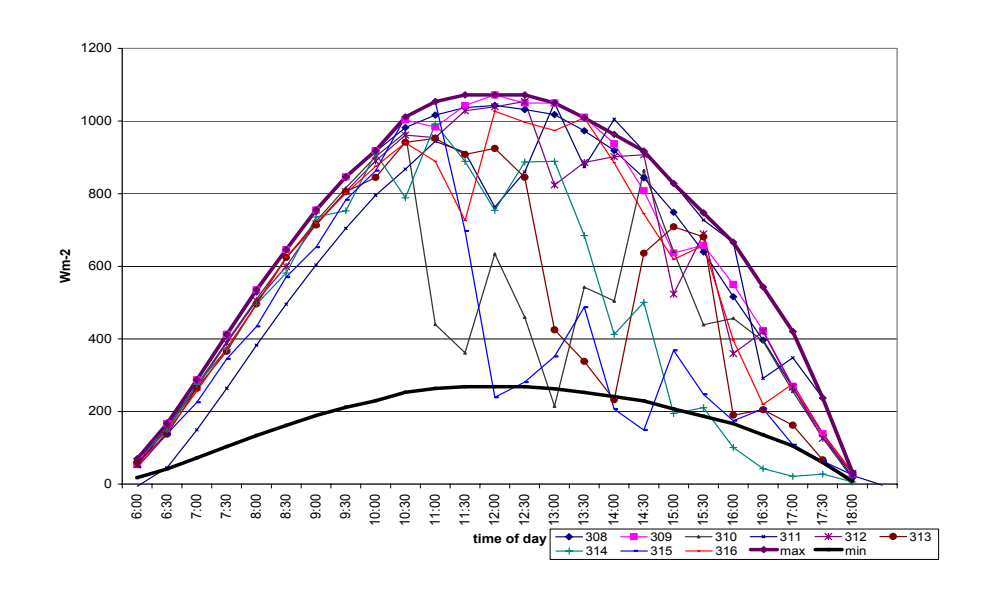
Month	Day	HMP45AC s/n 393B	CS500	YA100C	RHT2nl-02	RHT2nl-01
	1	++	++	++	++	+-
D 1	2	++	++	++	++	+-
December	3	++	++	++	++	+-
	4	++	++	++	++	+-
	5	++	++	++	++	+-
	6	++	++	++	++	+-

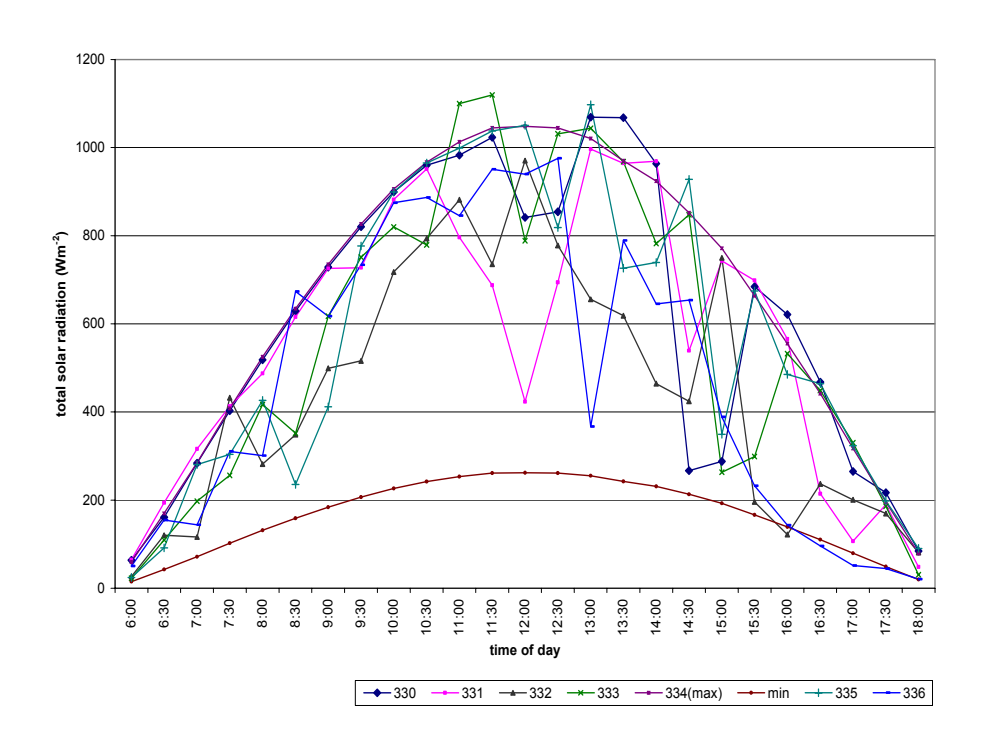
Month	Day	HMP45AC s/n 393B	CS500	YA100C	RHT2nl-02	RHT2nl-01
	6	++	++	++		+-
February	7	++	++	++		+-
	8	++	++	++		+-
	9	++	++	++		+-
	10	++	++	++		+-
	11	++	++	++		+-

# Key

- ++ both temperature and humidity sensors working
- +- only temperature sensor working
- -- both sensors not working

Appendix C: Calculation of cloudiness from the maximum and minimum solar radiation values for DOY 308-316 and DOY 330-336 respectively





Appendix D: Regression analysis for the calibration of the transpiration sub-model of the Gembloux Dynamic Greenhouse Climate Model

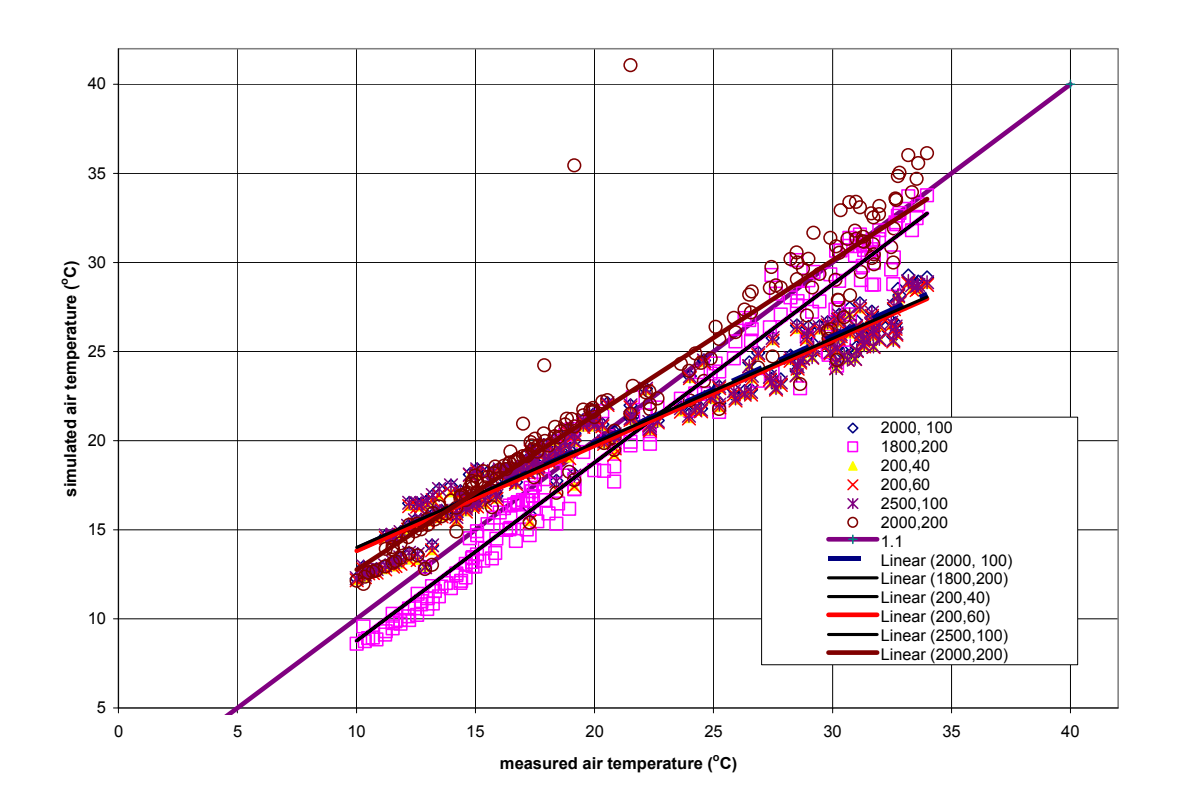
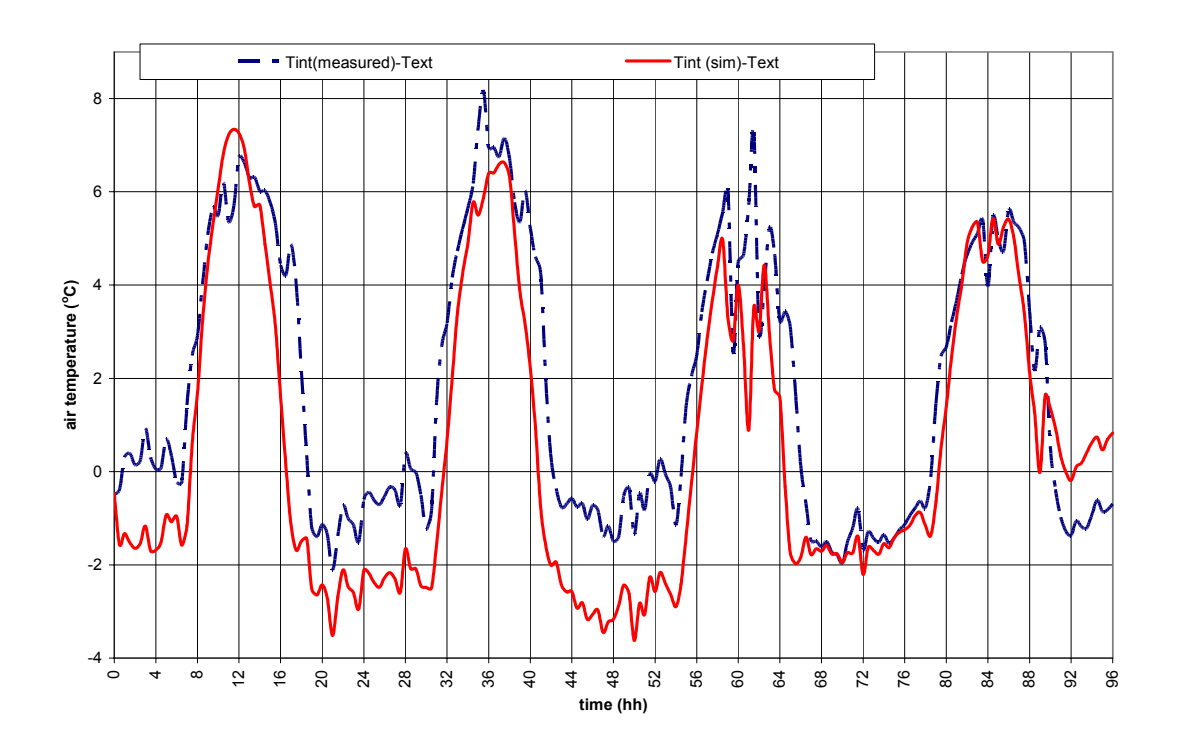
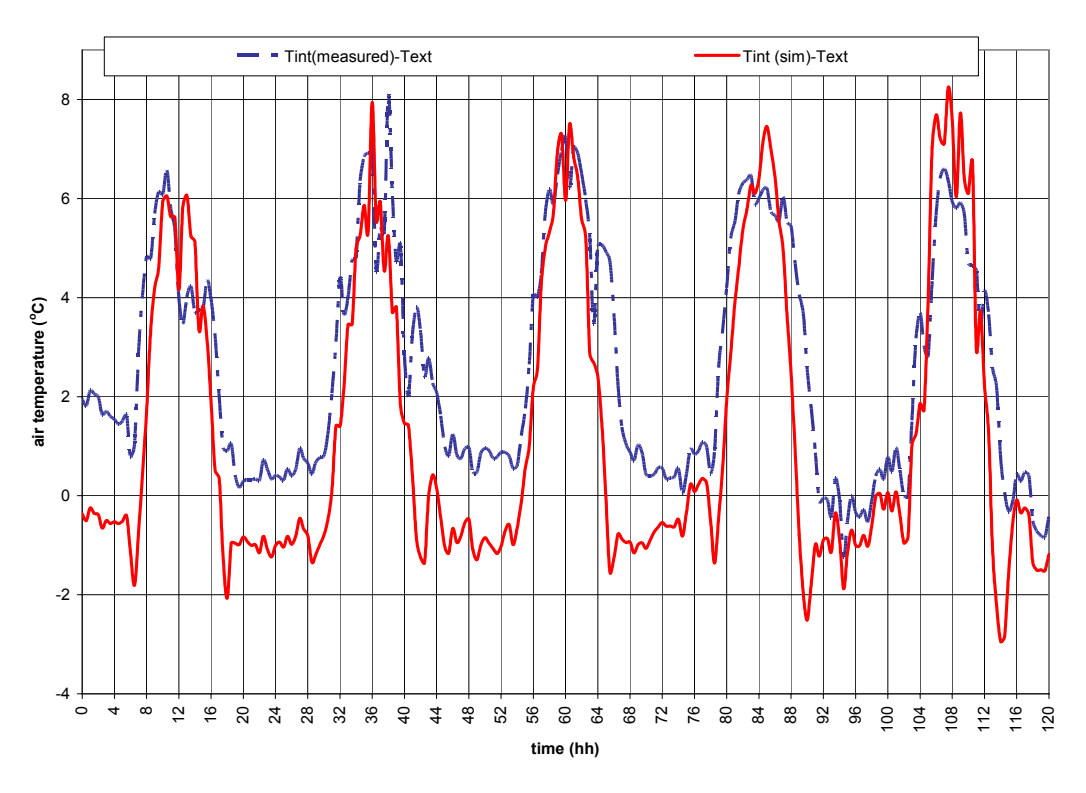


Table showing the regression analysis equations for the stomatal resistance values used in the calibration of the transpiration sub-model of the Gembloux Dynamic Greenhouse Microclimate Model

Stomatal resistance values (maximum and minimum)	Regression analysis equations
2000,100	$y=0.598x +7.972$ $(r^2=0.954)$
1800, 200	$y=1.001x -1.254$ $(r^2=0.963)$
200,40	$y=0.592x +7.877$ $(r^2=0.950)$
200,60	$y = 0.591x + 7.903$ $(r^2 = 0.950)$
2500,100	$y=0.588x +7.877$ $(r^2=0.950)$
2000, 200	$y=0.868x +4.067$ $(r^2=0.881)$

Appendix E: The differences between the simulated and measured air temperature inside the greenhouse and the measured outside air temperature for the calibration (DOY 308 to DOY 311) and validation (DOY 331 to DOY 335) periods respectively





Appendix F: The differences between the simulated and measured vapour pressure inside the greenhouse and the measured outside vapour pressure for the calibration (DOY 308 to DOY 311) and validation (DOY 331 to DOY 335) periods respectively

